Institute of Sound and Vibration Research

Collected Presentations from a Workshop on the Acoustics of Fan-Gust Interaction

M.C.M. Wright

ISVR Technical Memorandum No 897

October 2002

University of Southampton

SCIENTIFIC PUBLICATIONS BY THE ISVR

Technical Reports are published to promote timely dissemination of research results by ISVR personnel. This medium permits more detailed presentation than is usually acceptable for scientific journals. Responsibility for both the content and any opinions expressed rests entirely with the author(s).

Technical Memoranda are produced to enable the early or preliminary release of information by ISVR personnel where such release is deemed to the appropriate. Information contained in these memoranda may be incomplete, or form part of a continuing programme; this should be borne in mind when using or quoting from these documents.

Contract Reports are produced to record the results of scientific work carried out for sponsors, under contract. The ISVR treats these reports as confidential to sponsors and does not make them available for general circulation. Individual sponsors may, however, authorize subsequent release of the material.

UNIVERSITY OF SOUTHAMPTON

INSTITUTE OF SOUND AND VIBRATION RESEARCH

FLUID DYNAMICS AND ACOUSTICS GROUP

Collected Presentations from a Workshop on the Acoustics of Fan-Gust Interaction

by

M C M Wright

ISVR Technical Memorandum No. 897

October 2002

Authorized for issue by
Professor C L Morfey, Group Chairman

Introduction and acknowledgements

This technical memorandum contains the collected presentations from a workshop held at the ISVR on August 22^{nd} and 23^{rd} 2002 on the acoustics of fan – gust interaction. The workshop was funded by the UK Engineering and Physical Sciences Research Council (EPSRC). These presentations are also available at full size and in colour on the ISVR web site at http://www.isvr.soton.ac.uk/FDAG/fangust and it is recommended that these be used in practice; this document allows those who would prefer to cite a physical document to do so.

The workshop was proposed and programmed by Professor C. L. Morfey, Dr P. F. Joseph, Professor R. J. Astley and myself. Thanks are also due to Elizabeth Hylton and Neil Bateman of the EPSRC for facilitating its funding within the short time available, and for their 'Acoustics Theme Day' held during the 2002 Institute of Acoustics conference, which provided the original inspiration for the workshop. Thanks are also due to all the participants, both presenters and non-presenters, for their attendance and contribution. Finally, the assistance of Mrs S. J. Brindle in organising the workshop was, as always, invaluable.

Contents

Airfoil gust interaction - historical survey
Dr Phillip Joseph, ISVR, Southampton

Some benchmark tests for the computational aeroacoustics of leading-edge gust interaction
Dr John Chapman, Department of Mathematics, University of Keele

The gust
Professor Stewart Glegg, Department of Ocean Engineering, Florida Atlantic University

Asymptotic modelling of airfoil-gust interaction
Dr Nigel Peake & Dr Alison Cooper, DAMTP, University of Cambridge

Rotor wake turbulence noise
Dr Ed Envia, NASA

Vane unsteady pressure measurements
Dr Ed Envia, NASA

Fan/gust interaction noise in context
Dr Alec Wilson, Rolls-Royce plc, Derby

Supersonic leading-edge noise
Mr Chris Powles, Department of Mathematics, University of Keele

Application of a linearized Euler analysis to fan noise prediction
Dr Ed Envia, NASA

Aerodynamics and acoustics of cascades in nonuniform flows
Professor Hafiz Atassi, Aerospace & Mechanical Engineering, University of Notre Dame

Aerodynamic and acoustic response of an annular cascade in swirling flows
Mr Basman Elhadidi, Aerospace & Mechanical Engineering, University of Notre Dame

Feasibility of direct simulation of model blade/gust interaction problems
Professor Neil Sandham, School of Engineering Sciences, University of Southampton

Airfoil – Gust Interaction Historical Survey

Dr Phillip Joseph
ISVR
University of Southampton

Airfoil - Gust Interaction Historical Survey

P. Joseph

Two classical problems

- Wagner problem - Airfoil undergoing step change in angle of attack
- Sears problem - Airfoil encountering a gust

Flat-plate airfoil theory Hierarchy of problems

Increasing complexity

$$\left.\begin{matrix} 2D\,\text{gust} \\ 3D\,\text{gust} \end{matrix}\right\}\ \text{Incompressible Flow}$$

$$\left.\begin{matrix} 2D\,\text{gust} \\ 3D\,\text{gust} \end{matrix}\right\}\ \text{Compressible Flow}$$

1938 - 1952

Incompressible flow over a two-dimensional flat-plate airfoil.

von Karman (1938) Sears (1939), Kemp (1952)

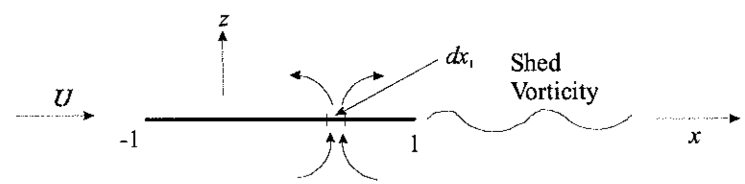

Assumptions

- Small perturbations. Boundary condition of zero normal velocity applied at the boundary $z = 0$
- Kutta condition. Pressure jump across the airfoil set equal to zero at the trailing edge (TE)
- Vortices shed from the TE because of the application of the Kutta condition are assumed to lie in the plane $z = 0$ and move downstream from the TE with velocity U.

Solution and its interpretation

Pressure on the airfoil at x due to upwash at element dx_1 may be expressed in the form

$$\boxed{dp = dp_{ap} + dp_{qs} + dp_w}$$

$$dp_{ap} = \pm\frac{\rho_0}{2\pi} bL(x, x_1)\frac{\partial w(x_1, t)}{\partial t} dx_1$$ Apparent mass

$$dp_{qs} = \pm\frac{\rho_0 dx_1}{\pi} U\sqrt{\frac{1-x}{1+x}}\sqrt{\frac{1+x_1}{1-x_1}}\frac{w(x_1,t)}{x_1 - x} dx_1$$ Quasi-steady

$$dp_w = \pm\frac{\rho_0 U dx_1}{\pi b}\sqrt{\frac{1-x}{1+x}}\sqrt{\frac{1+x_1}{1-x_1}}(C(k)-1)w(x_1)e^{i\omega t}$$ Shed vorticity (harmonic result)

where

$$L(x, x_1) = \ln\left[\frac{(x-x_1)^2 + \left(\sqrt{1-x^2} - \sqrt{1-x_1^2}\right)^2}{(x-x_1)^2 + \left(\sqrt{1-x^2} + \sqrt{1-x_1^2}\right)^2}\right]$$

and

$$C(k) = \frac{H_1^{(1)}(k)}{H_1^{(2)}(k) + iH_0^{(2)}(k)}$$ The Theodorsen function

$$k = \frac{\omega b}{U}$$ Reduced frequency

The Sears Problem
Gust moving at free stream velocity

Assume harmonic gust being convected with the free stream

$$w_g(x_1, t) = w_0\, e^{i(\omega t - kx)}$$

$$w(x_1, t) = -w_0\, e^{i(\omega t - kx_1)}$$ Zero normal-velocity b.c.

Substituting for w into the expression for $dp(x_1)$ and integrating over x_1

$$p = \mp\rho_0 U w_0\sqrt{\frac{1-x}{1+x}} S(k) e^{i\omega t}$$ S is the Sears function given by

(Incompressible) Sears function

$$S(k) = C(k)[J_0(k) - iJ_1(k)] + iJ_1(k)$$

$$S(k) = \frac{2}{\pi k}\frac{1}{H_0^{(2)}(k) - iH_1^{(2)}(k)}$$

(Incompressible) Sears function

$S(k)$

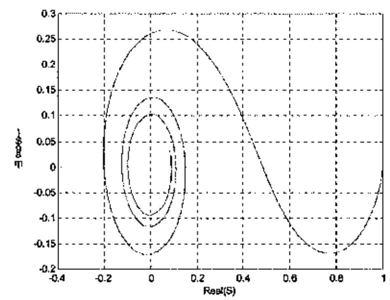

Response relative to centre

$S(k)e^{ik}$

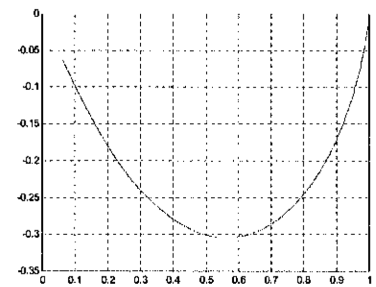

Response relative to LE

Comments

- Pressure variation with x, $\sqrt{(1-x)/(1+x)}$ independent of k. 2D incompressible linear airfoil theory predicts that the pressure on an airfoil passing through any form of 2D gust moving with the free stream is distributed proportional to $\sqrt{(1-x)/(1+x)}$
- Contribution of shed vorticity will always give the pressure distribution $\sqrt{(1-x)/(1+x)}$ whereas the quasi-steady and inertial contributions will not

Total lift $L(t)$ and moment $M(t)$

$$L(t) = -2b\int_{-1}^{1} p(x,t)\,dx \qquad M(t) = -2b^2\int_{-1}^{1} x\,p(x,t)\,dx$$

$$L(t) = 2\pi\rho_0 bUw_0S(k)e^{i\omega t} \qquad M(t) = -\frac{b}{2}L(t)$$

Centre of lift acts through quarter chord point

Limiting high and low (reduced) frequency behaviour

$$S(k) \to 1, \qquad k \to 0$$

- $L(t)$ reduces to quasi-steady (qs) approximation. Difference between general result and qs result is the lift due to lift-force required to accelerate the surrounding fluid plus the lift generated by vorticity generated in the wake acting back on the airfoil

$$S(k) \to \frac{\exp[-i(k-\pi/4)]}{\sqrt{2\pi k}}, \qquad k \to \infty$$

- Airfoil relatively unaffected by gusts of high (reduced) frequency

1968

Two-dimensional incompressible theory Horizontal gust

In a typical airfoil - gust interaction, both vertical and horizontal velocity components are present.

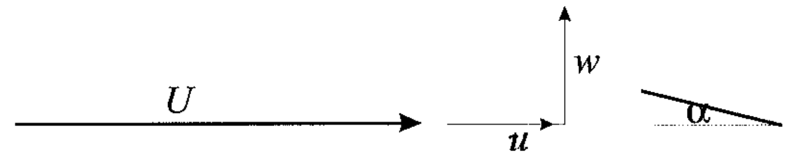

Horizontal gust

The horizontal-gust problem has been studied by Horlock (1968)

$$u_g = u_0\, e^{i(\omega t - kx)}$$

Horizontal gust resolved in vertical direction

$$L_u(t) = 2\pi\rho_0 b U (u_0\alpha) T(k) e^{i\omega t}$$

$$T(k) = S(k) + J_0(k) + J_1(k)$$

$$\boxed{\frac{L_u}{L_w} = \frac{u_0}{w_0}\alpha \frac{T(k)}{\underbrace{S(k)}_{\approx 2}}}$$

For $u_0 \approx w_0$ horizontal gust contribution significant for $\alpha > 10^\circ$

1969 - 1971

Three - dimensional incompressible theories

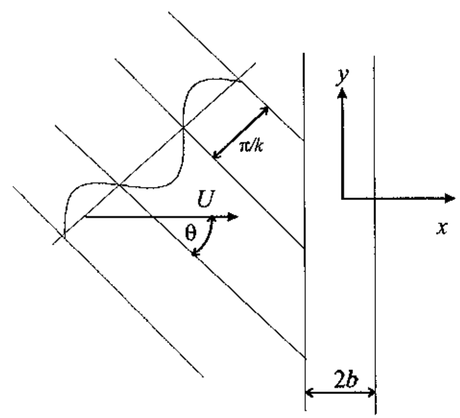

Three - dimensional incompressible theories

- Problem solved exactly by Graham (1970) for an airfoil of infinite span. Solution in the form of infinite series
- Approximate analytical solution obtained by Filotas (1969)
- Solutions reduce to 2D result for $\theta = \pi/2$
- Mugridge (1971) derived an approximate muliplicative factor for the 2D strip theory approximation

Approach by Filotas

$$w_g(x, y) = w_0\, \mathrm{e}^{ik(x\cos\theta + y\sin\theta)}$$

Seek solution of the form $\Delta p = g(x)\mathrm{e}^{ik(x\cos\theta + y\sin\theta)}$.

Filotas solves for the limiting cases $k \to 0, \infty$. A function is then postulated that predicts the correct limiting behaviour, with the assumption that it gives reasonable predictions for intermediate k-values.

Solution for large k

$$p \to \pm \frac{\rho_0 U w_0}{\sqrt{2\pi k}} \sqrt{\frac{1+x}{1-x}}\, \mathrm{e}^{-i\theta/2} \mathrm{e}^{ikx - k_y(x+1+iy)}, \qquad k \to \infty$$

- For $k_y \neq 0$ the pressure decays exponentially with distance from the LE. Loading should behave as a delta function for $k\cos\theta >> 1$
- Shape of the loading distribution depends on k_y but not on k_x
- k_x affects the amplitude of the distribution but not its shape
- Centre of lift is not fixed at quarter-chord point but approaches the LE as frequency increases

Solution of Mugridge

$$C_L^2 = 4\pi^2 \frac{w_0^2}{U^2} \frac{1}{1+2\pi k_x} \frac{k_x^2 + 2/\pi^2}{k_x^2 + k_y^2 + 2/\pi^2}$$

Good agreement with the exact solution of Graham for $k_x < 1$, but breaks down rapidly at frequencies above this.

Unlike the Filotas solution, the Mugridge results does not have the correct $k \to \infty$ asymptote.

The Mugridge prediction for the pressure distribution similar to $\sqrt{(1-x)/(1+x)}$ but Filotas has shown that this behaviour breaks down for large k_y.

1970 - 1971

Two - dimensional compressible theories

Fluid incompressibility implies that disturbances at TE are felt at the LE with no time delay. For this to be a good approximation,

$$\frac{2b}{c-U}<\frac{2\pi}{\omega}$$

Assuming $\max\frac{\Delta t}{T}=\frac{1}{\pi}$ incompressible unsteady theory limited to

$$\frac{kM}{1-M}<1 \qquad (k=\omega/c)$$

1970 - 1971

Numerical solutions of Graham and Adamczyk

Graham (1970) and Adamczyk (1971) have obtained numerical solutions for the unsteady lift in a two-dimensional compressible flow.

Their analyses differ but their solutions are exact within the limitations of small perturbation theory.

Graham presents Sears-type lift coefficients for $0\le k\le 6$

Adamczyk analysis is applicable to any Mach number, reduced frequency and gust convection speed

Analytic solutions of Sears (1971) and Osborne (1973)

Ignoring terms of order $\left(Mk\beta^2\right)^2$

$$p=\mp\rho_0\frac{U}{\beta}w_0\sqrt{\frac{1-x}{1+x}}S(k')\mathrm{e}^{i\left(\omega t+k'M^2x\right)},\quad k'=k/\beta^2,\qquad \beta^2=1-M^2$$

$$L(t)=2\pi\rho_0\frac{bU}{\beta}w_0K(k',M)\mathrm{e}^{i\omega t}$$

Modified Sears function which accounts for the first order effects of finite chord/wavelength ratio. Valid at low k

$$K(k',M)=S(k')\left[J_0\left(M^2k'\right)-iJ_1\left(M^2k'\right)\right]$$

Amiet correction to the Osborne-Sears formulation (1971)

The Osborne-Sears formulation implies exactness to order $\varepsilon = Mk/\beta$. This assumes that the exact solution may be expressed as a series expansion in ε. The validity of this assertion has been questioned by Amiet for two-dimensional problems with an infinite wake. By direct expansion of the exact integral equation, the following corrections to the Osborne-Sears results are obtained:

$$\left.\begin{aligned}p_{Am}(x,t)&=p_{Os}(x,t)\\ L_{Am}(t)&=L_{Os}(t)\end{aligned}\right\}\mathrm{e}^{ikf(M)/\beta^2},\quad f(M)=(1-\beta)\ln M+\beta\ln(1+\beta)-\ln 2$$

Discrepancy is of $O(k)$

Adamczyk solution for large kM

In general the compressible gust problem must be solved numerically. Adamczyk (1971) has obtained an exact solution in the limit of high frequency k.

At sufficiently high k at finite Mach number the gust and acoustic wavelength become much smaller than the chord. The airfoil may therefore be modelled as a *semi-infinite plate*. With the LE at $x = 0$

$$p_1 = \mp \frac{\rho_0 U w_0}{\sqrt{(1+M)\pi k x}} e^{i\left(\omega t - \frac{Mkx}{1+M} - \pi/4\right)}, \qquad kM \to \infty$$

This solution does not satisfy the Kutta condition at $x = 2$

Adamczyk solution *cont*

Total lift is calculated from

$$L_1(t) = 2\pi\rho_0 b U w_0 \frac{1}{\beta} S_1(k,M) e^{i\omega t}$$

where

$$S_1(k,M) = \frac{\sqrt{2}\beta}{\pi k\sqrt{M}}\left[C\left(\sqrt{\frac{2kM}{1+M}}\right) - iS\left(\sqrt{\frac{2kM}{1+M}}\right)\right] e^{i(k-\pi/4)}$$

Note that:

Setting $M = 1$ in this expression reduces to the lift expression for transonic unsteady flow derived by Landahl **(1961)**. In the high reduced frequency limit,

$$S_1(t) \to \frac{\beta}{\pi k\sqrt{M}} e^{i(k-\pi/2)}, \qquad k \to \infty$$

cf $k^{-1/2}$ and $e^{i\pi/4}$ for asymptotic Sears function

The Landahl (1972) iterative correction procedure

The previous solution violates the TE boundary condition. Landhal proposed a procedure which corrects the downstream b.c. but violates the upstream b.c. Applying this procedure iteratively generates an infinite series in powers of $k^{-1/2}$ that converges for all k.

Adamczyk (1972) has calculated the second term in the series that sets $p_1 + p_2 =$ 0 at the TE.

$$S_2(t) = \frac{\beta\sqrt{1+M}}{iM(\pi k)^{3/2}}\left[E^*\left(\frac{2}{\beta}\sqrt{kM}\right) - \frac{1-i}{2} + \left[\frac{1-i}{2} - \sqrt{\frac{2}{1+M}}E^*\left(\sqrt{\frac{2kM}{1-M}}\right)\right] e^{-i\frac{2kM}{1+M}}\right] e^{ik}$$

S_2 is a generally small term at practical frequencies and Mach numbers can be neglected

1970 - 1971

Three - dimensional compressible theories Graham's Similarity Principle

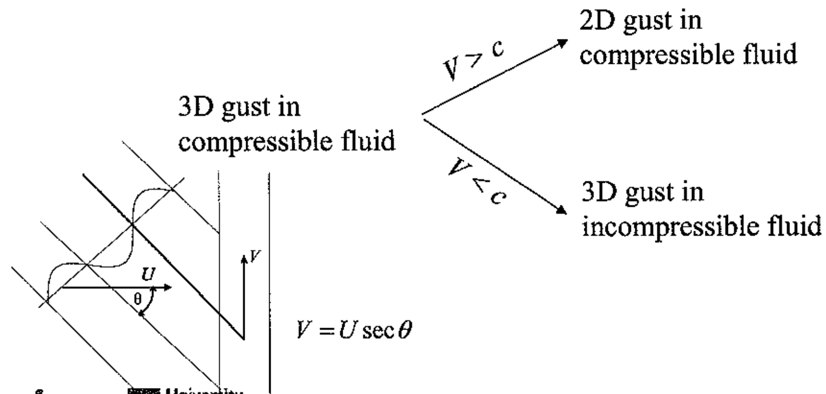

$V = U \sec\theta$

Subsonic trace velocity
$V < c$

Application of the Prandtl-Glauert transform the governing equations to an incompressible problem. Graham shows that the boundary condition on the airfoil and the wake transform properly. The case $V < c$ is therefore equivalent to the 3D incompressible problem discussed previously.

$$\tilde{k}_x = k_x / \beta^2, \quad \tilde{k}_y = k_y\left(1-\sigma^2\right)/\beta, \quad \sigma = Mk_x / \beta k_y, \quad \tilde{M} = 0$$

$$C_p\left(M, k_x, k_y, x\right) = \frac{1}{\beta}\tilde{C}_p\left(0, \tilde{k}_x, \tilde{k}_y, x\right)e^{i\left[M^2\tilde{k}_x x + \left(\tilde{k}_y - k_y\right)y\right]}$$

Actual flow   Transformed flow

Supersonic trace velocity
$V > c\ (\sigma > 1)$

The transformation for this case is less well known to convert the 3D problem to an equivalent 2D problem

$$\overline{M} = M\sqrt{1 - 1/\sigma^2}, \quad \bar{k}_x = k_x\left(1 + k_y^2 / k_x^2\right) = k_x\overline{\beta}^2 / \beta^2,$$

$$\overline{\beta} = \sqrt{1 - \overline{M}^2}, \quad \bar{k}_y = 0, \quad \sigma = Mk_x / \beta k_y$$

$$C_p\left(M, k_x, k_y, x\right) = \sqrt{1 + k_x^2 / k_y^2}\ .\overline{C}_p\left(\overline{M}, \bar{k}_x, 0, x\right)e^{i\left[xk_x / k_y - y\right]}$$

Note, putting $V = c\ (\sigma = 1)$ in either similarity relation recovers the Osborne result

Some benchmark tests for the computational aeroacoustics of leading-edge gust interaction

Dr John Chapman

Department of Mathematics

University of Keele

SOME BENCHMARK TESTS FOR THE COMPUTATIONAL AEROACOUSTICS OF LEADING-EDGE GUST INTERACTION

C. J. CHAPMAN
DEPARTMENT OF MATHEMATICS
UNIVERSITY OF KEELE
ENGLAND

22 AUGUST 2002
SOUTHAMPTON

1

AEROENGINE NOISE REAL-LIF

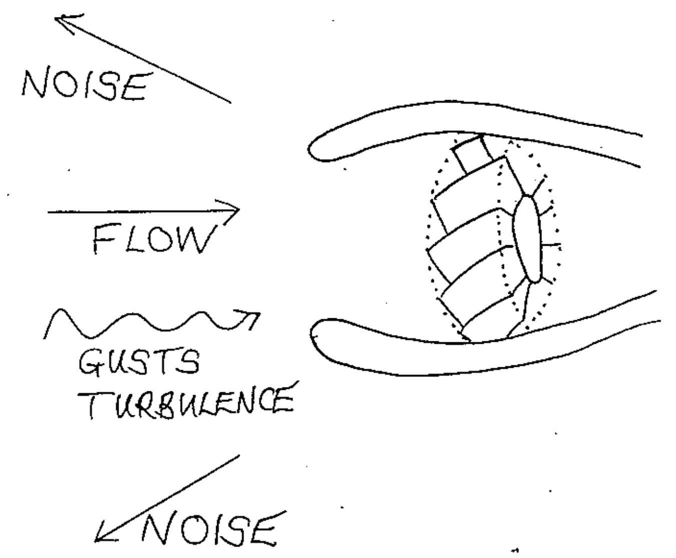

Much of the noise is produced at the

leading edge of the fan blade

2

N IMPORTANT LIMIT

ET r_{LE} = RADIUS OF CURVATURE OF LEADING EDGE

c = CHORD

λ = WAVELENGTH OF SOUND

SSUME

$$\underbrace{r_{LE} \ll \lambda}_{\text{REPLACE LE BY A LINE}} \underbrace{\ll c}_{\text{\& REPLACE BLADE BY A HALF-PLANE}}$$

OBTAIN A HALF-PLANE DIFFRACTION PROBLEM

3

HALF-PLANE BLADE-VORTEX INTERACTION

A CLASSICAL PROBLEM !

IMPORTANT CONTRIBUTIONS BY

R. AMIET (1975 - ...)
S. E. WIDNALL (1980 - ...)
Y. P. GUO (1989 - ...)

PRESENT INVESTIGATION

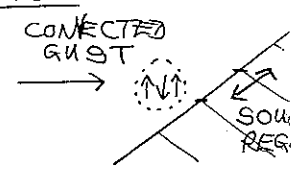

(1) TO FIND THE 3-DIMENSIONAL ACOUSTIC DIRECTIVITY PATTE PRODUCED BY A LOCALISED GU

(2) INCLUDING THE NEAR FIE

RESENT INVESTIGATION

3) ... AND INCLUDING THE ACOUSTIC FIELD PROPAGATING ALONG THE LEADING EDGE ('THE EDGE WAVE')

4) ... AND TO ANSWER A FUNDAMENTAL QUESTION

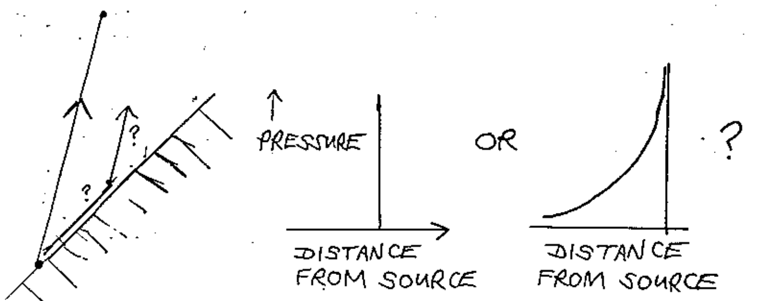

NO TAIL
3D – NO EDGE
2D – EDGE

TAIL
2D – NO EDGE

ES THE BASIC SOLUTION HAVE A 'TAIL'?
IOT OBVIOUS, BECAUSE THERE COULD BE A RAY PATH VIA LEADING EDGE.)

AEROENGINE NOISE SIMPLIFIED

THE BLADE-VORTEX INTERACTION PROBLE

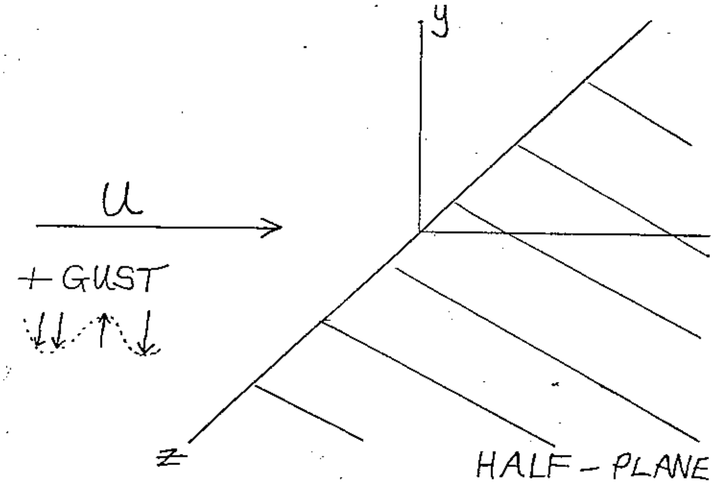

HALF-PLANE
$y = 0, \quad x \geq C$
all z

CONVECTED GUST :

VERTICAL COMPONENT OF VELOCITY $= f\left(t - \frac{x}{U}, z\right.$

BOUNDARY-VALUE PROBLEM

$$\left\{ \frac{1}{c_0^2}\left(\frac{\partial}{\partial t} + U\frac{\partial}{\partial x}\right)^2 - \left(\frac{\partial^2}{\partial x^2} + \frac{\partial^2}{\partial y^2} + \frac{\partial^2}{\partial z^2}\right)\right\}\phi = 0$$

ϕ = velocity potential for acoustic field

$\underset{\sim}{u}$ = acoustic velocity $= \nabla\phi$

p = acoustic pressure $= -\rho_0\left(\frac{\partial}{\partial t} + U\frac{\partial}{\partial x}\right)\phi$

$$C: \quad \frac{\partial\phi}{\partial y} = -f\left(t - \frac{x}{U}, z\right) \quad \left(\begin{matrix} y = 0^{\pm} \\ x > 0 \end{matrix}\right)$$

$\partial\phi \qquad (y = 0)$

AEROACOUSTIC COORDINATES

MACH NO.: $M = \frac{U}{c_0} < 1$

$$(\bar{x}, \bar{y}, \bar{z}) = \left(\frac{x}{1-M^2}, \frac{y}{(1-M^2)^{\frac{1}{2}}}, \frac{z}{(1-M^2)^{\frac{1}{2}}}\right.$$

AEROACOUSTIC POLAR COORDINATES

AXIS OF POLAR COORDS: $\bar{z}$-AXIS (L.E.)

ANGLE AROUND $\bar{z}$-AXIS: $\bar{\phi}$

ANGLE FROM $\bar{z}$-AXIS: $\bar{\theta}$

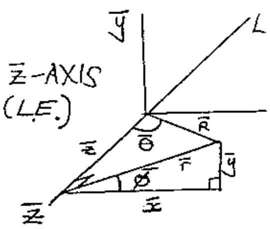

CYLINDRICAL POLARS : $(\bar{r}, \bar{\phi}, \bar{z})$

SPHERICAL POLARS : $(\bar{R}, \bar{\theta}, \bar{\phi})$

$(\bar{x}, \bar{y}, \bar{z}) = (\bar{r}\cos\bar{\phi}, \bar{r}\sin\bar{\phi}, \bar{z})$

VINE GUST SHAPES (WITHOUT DELTA-FUNCTIONS)

ET $\quad \text{GUST} = \underbrace{f_0\left(t - \frac{x}{u}\right)}_{\text{LONGITUDINAL SHAPE}} \underbrace{g(z)}_{\text{TRANSVERSE SHAPE}}$

VHERE

$$f_0\left(t-\frac{x}{u}\right) = \begin{cases} v_0\, e^{-i\omega_0 (t - \frac{x}{u})} & \text{SINGLE-FREQUENCY} \\ v_0\, e^{-\frac{1}{2}\left\{\frac{t - x/u}{\tau}\right\}^2} & \text{GAUSSIAN} \\ v_0\, H\left(\frac{t - x/u}{\tau}, -1, 1\right) & \text{TOP-HAT} \end{cases}$$

$$g(z) = \begin{cases} e^{-\frac{1}{2}\left(\frac{z}{a}\right)^2} & \text{GAUSSIAN} \\ H\left(\frac{z}{a}, -1, 1\right) & \text{TOP-HAT} \\ 1 & \text{UNIFORM} \end{cases}$$

AMES: SINGLE-FREQUENCY × GAUSSIAN etc.

TOP VIEW OF GUST SHAPES

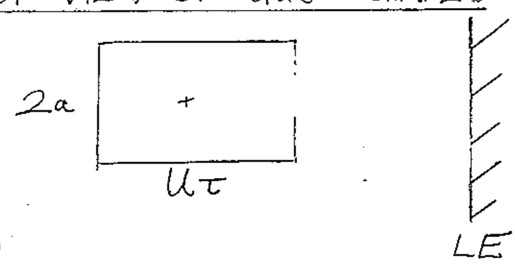

TOP-HAT × TOP-HAT

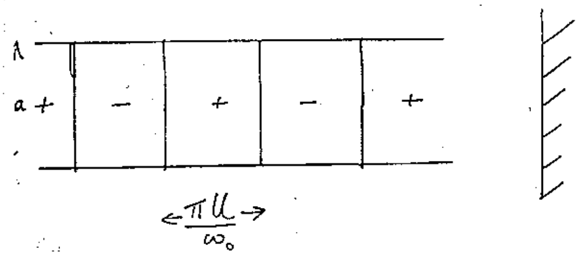

SINGLE-FREQUENC × TOP-HAT

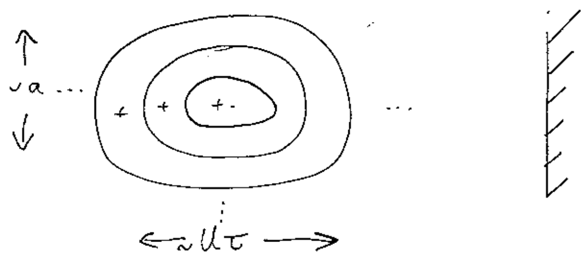

GAUSSIAN × GAUSSIAN

etc.

GUST PARAMETERS

frequency $\quad \omega_0$

rise-time $\quad \tau$

width $\quad a$

aspect ratio $\quad \frac{a}{U\tau}$

Mach number $\quad M$

non-dimensional groups $\quad \frac{\bar{a}}{c_0\tau}, \ \frac{\omega_0 \bar{a}}{c_0},$

$\frac{\bar{R}}{c_0\tau}, \ \frac{\bar{r}}{c_0\tau}, \ \frac{\omega_0\bar{R}}{c_0}, \ \frac{\omega_0\bar{r}}{c_0}$

CODE PARAMETERS

time-step

grid size

artificial viscosity

⋮

SINGLE-FREQUENCY × UNIFORM $\quad$ 2D

GUST: $\quad V_0\, e^{-i\omega_0 (t - x/U)}$

ACOUSTIC FIELD:

EVERYWHERE! FAR-FIELD APPROXIMAT. NOT USED.

$$p = -\frac{e^{\frac{1}{4}\pi i}}{\sqrt{\pi}} \frac{\rho_0 c_0 \bar{v}_0 M^{\frac{3}{2}}}{(1+M)^{\frac{1}{2}}} \cos\tfrac{1}{2}\bar{\phi} \left(\frac{c_0}{\omega_0 \bar{r}}\right)^{\frac{1}{2}} e^{-i\omega_0\left(t + \frac{M\bar{x}}{c_0} - \frac{\bar{r}}{c_0}\right)}$$

WELL-KNOWN

GAUSSIAN × UNIFORM

GUST: $$V_0 \, e^{-\frac{1}{2}\left(\frac{t-x/U}{\tau}\right)^2}$$

ACOUSTIC FIELD:

EVERYWHERE! NO NEED FOR FAR-FIELD APPROXIMATION

$$p = -\frac{1}{2}\frac{\rho_0 c_0 \bar{V}_0 M^{\frac{3}{2}}}{(1+M)^{\frac{1}{2}}} \cos\tfrac{1}{2}\bar{\phi} \left(\frac{c_0\tau}{\bar{r}}\right)^{\frac{1}{2}} h(T)$$

$$T = \frac{1}{\tau}\left(t + \frac{M\bar{x}}{c_0} - \frac{\bar{r}}{c_0}\right)$$

$$h(T) \equiv |T|^{\frac{1}{2}} e^{-\frac{1}{4}T^2}\left\{I_{-\frac{1}{4}}\left(\tfrac{1}{4}T^2\right) + \mathrm{sgn}(T)\, I_{\frac{1}{4}}\left(\tfrac{1}{4}T^2\right)\right\}$$

TAIL: $$h(T) \sim \frac{2\sqrt{2}}{\sqrt{\pi T}} \qquad (T \to \infty)$$

PRE-CURSOR: $$h(T) \sim \frac{2}{\sqrt{\pi |T|}} e^{-\frac{1}{2}T^2} \qquad (T \to -\infty)$$

C.J. CHAPMAN KEELE 14 AUG 02

TOP-HAT × UNIFORM

GUST: $$V_0 \, H\left(\frac{t-x/U}{\tau}, -1, 1\right)$$

ACOUSTIC FIELD:

EVERYWHERE NO NEED FOR FAR-FIELD APPROX.

$$p = -\frac{2}{\pi}\frac{\rho_0 c_0 \bar{V}_0 M^{\frac{3}{2}}}{(1+M)^{\frac{1}{2}}} \cos\tfrac{1}{2}\bar{\phi} \left(\frac{c_0\tau}{\bar{r}}\right)^{\frac{1}{2}} \tilde{h}(T)$$

$$T = \frac{1}{\tau}\left(t + \frac{M\bar{x}}{c_0} - \frac{\bar{r}}{c_0}\right)$$

$$\tilde{h}(T) \equiv H_0(T+1)\,|T+1|^{\frac{1}{2}} - H_0(T-1)\,|T-1|^{\frac{1}{2}}$$

$$\therefore \quad \tilde{h}(T) = \begin{cases} 0 & (T < - \\ \dfrac{1}{\sqrt{T}} + \dfrac{1}{8T^2\sqrt{T}} + \cdots & (T \gg \end{cases}$$

C.J. CHAPMAN KEELE 14 AUG (

FAR-FIELD SHAPE FACTOR

FAR-FIELD: $$p \sim \rho_0 c_0 \bar{V}_0 M^{\frac{3}{2}} \frac{\cos\frac{1}{2}\bar{\phi}\, \sin^{\frac{1}{2}}\bar{\theta}}{(1+M\sin\bar{\theta})^{\frac{1}{2}}} \frac{\bar{a}}{\bar{R}} S$$

$S \equiv$ FAR-FIELD SHAPE FACTOR

SINGLE-FREQUENCY × GAUSSIAN

GUST: $$v_0 e^{-i\omega_0(t-x/U)} \, e^{-\frac{1}{2}\left(\frac{z}{a}\right)^2}$$

FAR-FIELD:

$$S = -\frac{1}{\sqrt{\pi}} e^{-\frac{1}{2}\left(\frac{\omega_0\bar{a}}{c_0}\right)^2 \cos^2\bar{\theta}} \; e^{-i\omega_0\left(t+\frac{M\bar{x}}{c_0}-\frac{\bar{R}}{c_0}\right)}$$

$\frac{\omega_0\bar{a}}{c_0} \gg 1$: 'super-directive'

SINGLE-FREQUENCY × TOP-HAT

GUST: $V_0 e^{-i\omega_0(t - x/U)} H(\frac{z}{a}, -1, 1)$

FAR-FIELD:

$$S = -\frac{\sqrt{2}}{\pi}\frac{\sin((\omega\bar{a}/c_0)\cos\bar{\theta})}{(\omega\bar{a}/c_0)\cos\bar{\theta}} e^{-i\omega_0(t + \frac{M\bar{x}}{c_0} - \frac{\bar{R}}{c_0})}$$

$\frac{\omega\bar{a}}{c_0} \gg 1$: multi-lobed

GAUSSIAN × GAUSSIAN

GUST: $V_0 e^{-\frac{1}{2}\left(\frac{t - x/U}{\tau}\right)^2} e^{-\frac{1}{2}\left(\frac{z}{a}\right)^2}$

FAR-FIELD

$$S = -\frac{e^{-\frac{1}{2}\frac{\{(t + M\bar{x}/c_0 - \bar{R}/c_0)/\tau\}^2}{1 + (\bar{a}/(c_0\tau))^2\cos^2\bar{\theta}}}}{\pi^{\frac{1}{2}}\{1 + (\bar{a}/(c_0\tau))^2\cos^2\bar{\theta}\}^{\frac{1}{2}}}$$

NB:
VERY DIFFERENT FAR-FIELDS FOR

$\frac{\bar{a}}{c_0\tau} \ll 1$, $\frac{\bar{a}}{c_0\tau} \gg 1$

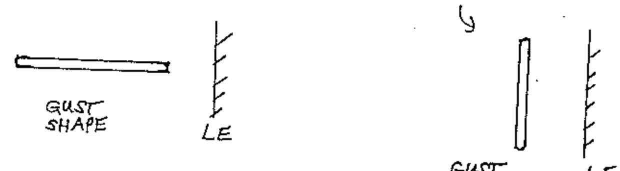

GAUSSIAN × TOP-HAT

GUST: $V_0 e^{-\frac{1}{2}\left(\frac{t - x/U}{\tau}\right)^2} H(\frac{z}{a}, -1, 1)$

FAR-FIELD:

$$S = -\frac{\Phi(T_+) - \Phi(T_-)}{(\bar{a}/(c_0\tau))\cos\bar{\theta}}$$

$$T_\pm = \frac{1}{\tau}\left(t + \frac{M\bar{x}}{c_0} - \frac{\bar{R}}{c_0}\right) \pm \frac{\bar{a}}{c_0\tau}\cos\bar{\theta}$$

$$\Phi(\xi) \equiv \frac{1}{\sqrt{2\pi}}\int_{-\infty}^{\xi} e^{-\frac{1}{2}s^2}\,ds = \frac{1}{2}\left(1 + \operatorname{erf}\left(\frac{\xi}{\sqrt{2}}\right)\right)$$

TOP-HAT × GAUSSIAN

GUST: $V_0 H\left(\frac{t - x/U}{\tau}, -1, 1\right) e^{-\frac{1}{2}\left(\frac{z}{a}\right)^2}$

FAR-FIELD:

$$S = -\frac{1}{\sqrt{\pi}}\{\Phi(\tilde{T}_+) - \Phi(\tilde{T}_-)\}$$

$$\tilde{T}_\pm = \frac{\frac{1}{\tau}(t + M\bar{x}/c_0 - \bar{R}/c_0) \pm 1}{(\bar{a}/(c_0\tau))|\cos\bar{\theta}|}$$

TOP-HAT × TOP-HAT

GUST: $$V_0\, H\left(\frac{t - x/U}{\tau}, -1, 1\right) H\left(\frac{z}{a}, -1, 1\right)$$

FAR-FIELD:

$$S = -\frac{1}{\sqrt{2}\,\pi}\,\frac{H_0(T_{++})T_{++} - H_0(T_{+-})T_{+-} - H_0(T_{-+})T_{-+} + H_0(T_{--})T_{--}}{(\bar{a}/(c_0\tau))\cos\bar{\theta}}$$

$$T_{\pm\pm} = \frac{t + M\bar{x}/c_0 - \bar{R}/c_0}{\tau} \pm 1 \pm \left(\frac{\bar{a}}{c_0\tau}\right)\cos\bar{\theta}$$

H_0 = Heaviside step function

NB $S = 0$ WHEN $T_{\pm\pm}$ ALL POSITIVE or ALL NEGATIVE

∴ SOUND FIELD BEGINS & ENDS SUDDENLY (i.e. NO 'TAIL')

USE OF ABOVE RESULTS FOR BENCHMARK TESTS

(i) PARAMETRIC STUDY

FOR GIVEN GRID SIZE, TIME STEP, ARTIFICIAL VISCOSITY, ...

DETERMINE ACCURACY OF CODE FOR GIVEN FREQUENCY, RISE-TIME, WIDTH, OBSERVER POSITION, MACH NUMBER, ...

e.g. DETERMINE HOW ACCURATELY A CODE CAN CALCULATE AN IMPULSIVE SOUND FIELD PRODUCED BY A GUST WITH SHARP EDGES.

(ii) CALCULATION OF FAR ACOUSTIC FIELD FROM NEAR-FIELD DATA

DETERMINE SENSITIVITY TO POSITION OF NEAR-FIELD CONTROL SURFACE,

e.g. ITS DISTANCE FROM LEADING EDGE.

The gust

Professor Stewart Glegg
Department of Ocean Engineering
Florida Atlantic University

"The Gust"

Stewart Glegg
Florida Atlantic University
and
William Devenport
Virginia Polytechnic

Presented at the Workshop on the Acoustics of Fan Gust Interaction, Southampton, UK, August 2002

Rotor/Stator Interaction Noise

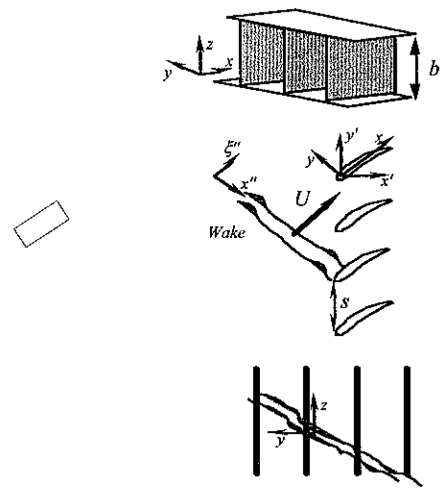

Classical Approach

- Frequency domain analysis is used
- Gust is decomposed into its Fourier components
- Response to a harmonic gust is calculated

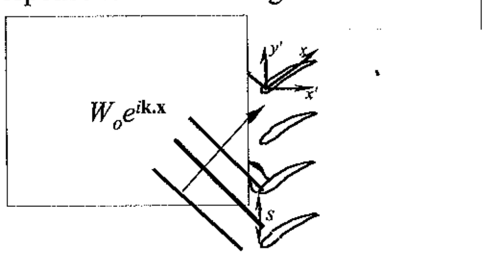

Questions

- *Can we model the gust in more detail?*
- *Is the classical approach optimal?*
- *Can we define a gust in the time domain for CFD calculations of the blade response?*

The Optimal Gust

Proper Orthogonal Decomposition(Lumley)

The unsteady part of the flow is decomposed into a set of uncorrelated modes

$$u_i(\mathbf{x},t)=\sum_n b_n(t_R)\phi_i^{(n)}(\mathbf{x},t)$$

Mode amplitudes are uncorrelated stochastic random variables

Proper Orthogonal Modes

$$R_{ij}(\mathbf{y},\mathbf{y}',t,t')=\sum_n \lambda_t^{(n)}\phi_i^{(n)}(\mathbf{y},t)\phi_j^{(n)}(\mathbf{y}',t')$$

Eigenvalues $\quad \lambda_t^{(n)}=Ex\left[b_n^2\right]$

Modes are obtained by solving the eigen value problem

$$\boxed{\frac{1}{2TV}\int_{-T}^{T}\int_{V} R_{ij}(\mathbf{y},\mathbf{y}',t,t')\phi_j^{(n)}(\mathbf{y}',t')d\mathbf{y}'dt=\lambda_t^{(n)}\phi_i^{(n)}(\mathbf{y},t)}$$

$$Ex[u_i(\mathbf{x},t)u_j(\mathbf{x}',t')]=R_{ij}(\mathbf{x},\mathbf{x}',t,t')$$

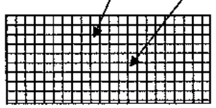

Note: for homogeneous flows the modes are harmonic so the approach reduces to Fourier decomposition

Proper Orthogonal Decomposition of a Wake Flow

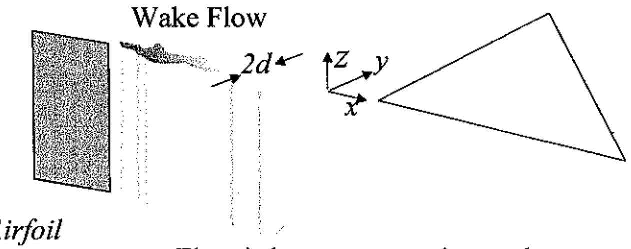

Flow is homogeneous in z and t
Approximately homogeneous in x
Decomposition applied in y direction only

$$u_i(\mathbf{x})=\sum_n b_n(x_R,z_R)\phi_i^{(n)}(y)$$

Proper Orthogonal Decomposition of an Airfoil wake

Eigenvalues

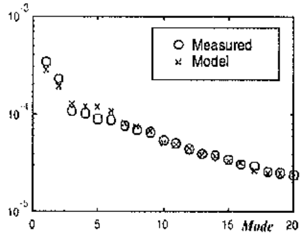

Figure 2. Eigenvalue spectra from the one-dimensional proper orthogonal decomposition in the y direction.

Modes

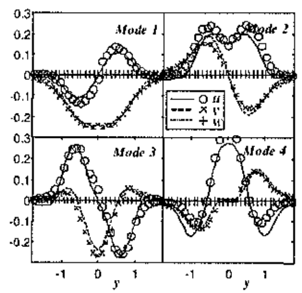

Proper Orthogonal Modes of the Wake: These results show the upwash component of typical POMs of the wake. Note the periodicity in the direction along the wake, as expected. Each of these POMs can be treated as being statistically independent.

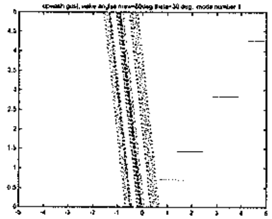

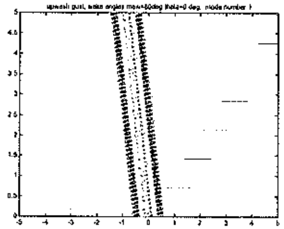

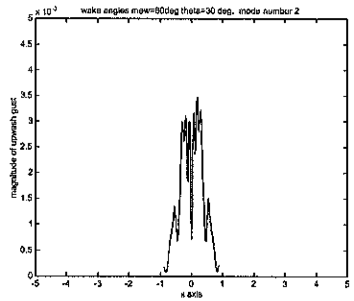

Time History of Gust: This shows a typical upwash gust associated with each POM. Note the high frequency oscillations within the wake, and the envelope of the gust.

The Gust Response

Time Domain Calculations

The acoustic response to each velocity mode $\phi_i^{(n)}(\mathbf{y},t)$ is calculated directly giving the response $P^{(n)}(\mathbf{x},t)$ for the n^{th} mode. For linear systems the total response is then

$$\boxed{P(\mathbf{x},t)=\sum_n b_n(t_R)P^{(n)}(\mathbf{x},t)}$$

Giving the cross spectrum

$$\boxed{C_{PP}(\mathbf{x},\mathbf{x}',\omega)=\sum_n \lambda_t^{(n)}P^{(n)}(\mathbf{x},\omega)P^{(n)}(\mathbf{x}',\omega)}$$

Frequency Domain Calculations

$$w_i^{(n)}(\mathbf{k},\omega)=\int_{-T}^{T}\int_V \phi_i^{(n)}(\mathbf{y},t)e^{i\mathbf{k}.\mathbf{y}+i\omega t}\frac{dVdt}{(2\pi)^4}$$

$$\boxed{P(\mathbf{x},\omega)=\sum_n b_nP^{(n)}(\mathbf{x},\omega)=\sum_n b_n\int w_i^{(n)}(\mathbf{k},\omega)g_i(\mathbf{x},\mathbf{k},\omega)d\mathbf{k}}$$

Giving the cross spectrum

$$\boxed{C_{PP}(\mathbf{x},\mathbf{x}',\omega)=\sum_n \lambda_t^{(n)}P^{(n)}(\mathbf{x},\omega)P^{(n)}(\mathbf{x}',\omega)}$$

Compact Eddy Structures

Proper Orthogonal Modes with one homogeneous direction

- Modes are harmonic in homogeneous directions.
- A complete analysis based on POMs would require 10^4 modes to be considered. It is not clear that only a few modes are dominant in many situations.
- *Is there an alternative?*

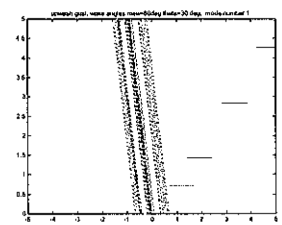

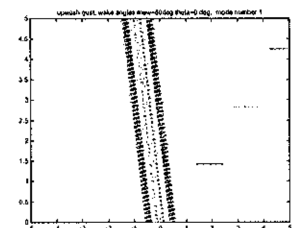

Linear Stochastic Estimates

Modes are obtained by minimizing the error function

$$E = Ex\left[\left(u_i(x,y,z) - \sum_n b_n(x_R,z_R)\kappa_i^{(n)}(x-x_R,y,z-z_R)\right)^2\right]$$

Linear Stochastic Estimator

Provide the best estimator of the flow in a time average sense

Combining LSE and POD

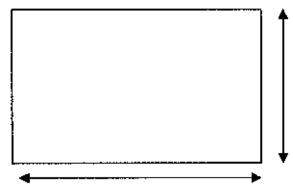

Devenport et al (1999)

Compact Eddy Structures(1)

The 3D Compact Eddy Structure is the projection of the 1D POM onto the Correlation function

$$\kappa_j^{(n)}(\Delta x, y', \Delta z) = \frac{1}{L\lambda_o^{(n)}}\int R_{ij}(y,y',\Delta x,\Delta y)\phi_i^{(n)}(y)dy$$

Compact Eddy Structures

Complementary 1D POM eigenvalues

Complementary 1D POMs

Compact Eddy Structures(2)

This result can be inverted to provide the correlation function

$$R_{ij}(\mathbf{y},\mathbf{y}') = \sum_n \lambda_o^{(n)}\phi_i^{(n)}(y)\kappa_j^{(n)}(\Delta x, y', \Delta z)$$

One dimensional modes

Compact Eddy Structure

Compact Eddies Structures in Airfoil wake

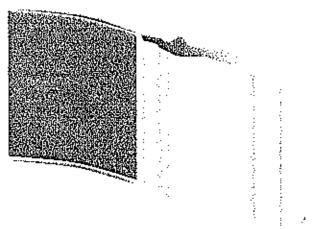

Devenport et al (1999)

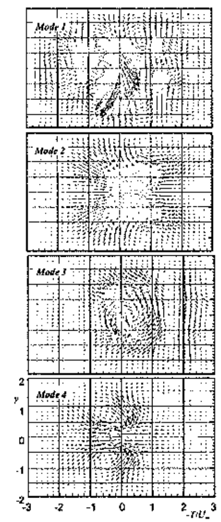

Figure 4. Characteristic eddy structures corresponding to the first 4 modes deduced from the measured two-point correlation tensor. Distances in inches, l=0.686".

CES Structures:
CES are an alternative to POMs as shown here. The CES mode has a complementary POM illustrated in the lower figure which has no variation along the wake. Note the vortical nature of the CES.

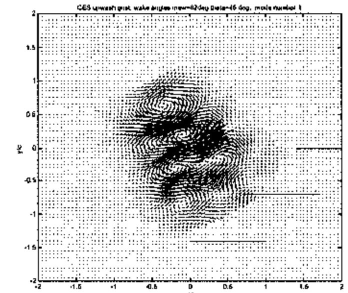

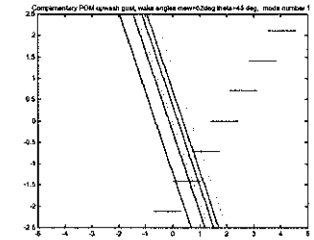

CES in y-z Plane:
Shows the spanwise structure of the CES and it's complimentary POM

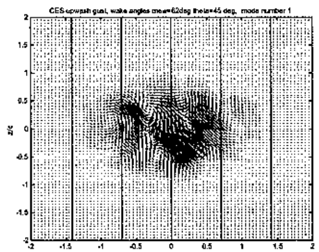

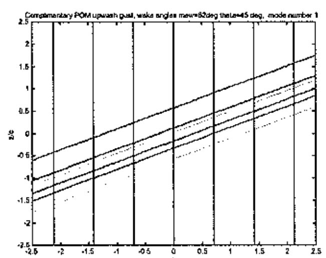

Calculating the Blade Response Using CES(1)

$$P(\mathbf{x},\omega) = \int u_i(\mathbf{k},\omega) g_i(\mathbf{x},\mathbf{k},\omega) d\mathbf{k}$$

$$C_{PP}(\mathbf{x},\mathbf{x}',\omega) = \int \int g_i(\mathbf{x},\mathbf{k},\omega) g_j^*(\mathbf{x}',\mathbf{k}'\omega) \Phi_{ij}(\mathbf{k},\mathbf{k}') d\mathbf{k} d\mathbf{k}'$$

$$\Phi_{ij}(\mathbf{k},\mathbf{k}') = \frac{1}{(2\pi)^6} \int \int R_{ij}(y,y',\Delta x,\Delta z) e^{i\mathbf{k}.\mathbf{y}-i\mathbf{k}'.\mathbf{y}'} dV dV'$$

$$= \sum_n \lambda_o^{(n)} \frac{1}{(2\pi)^6} \int \int \phi_i^{(n)}(y) \kappa_j^{(n)}(\Delta x, y', \Delta z) e^{i\mathbf{k}.\mathbf{y}-i\mathbf{k}'.\mathbf{y}'} dV dV'$$

$$= \sum_n \lambda_o^{(n)} \hat{\phi}_i^{(n)}(k_y) \left(\hat{\kappa}_j^{(n)}(\mathbf{k}')\right)^* \delta(k_x - k_x') \delta(k_z - k_z')$$

Calculating the Blade Response Using CES(2)

$$C_{PP}(\mathbf{x},\mathbf{x}',\omega) = \sum_n \lambda_o^{(n)} \int \left\{ \int g_i(\mathbf{x},\mathbf{k},\omega)\hat{\phi}_i^{(n)}(k_y)dk_y \right\} \left\{ g_j(\mathbf{x}',\mathbf{k}'\omega)\hat{\kappa}_j(\mathbf{k}') \right\}^* d\mathbf{k}'$$

$$\mathbf{k} = (k_x', k_y, k_z')$$

Prediction Approach

To predict rotor noise from the CES structures of a generic wake we estimate the wake angles and wake width from RANS calculations and scale the wind tunnel measurements on flow speed and wake width.

We then calculate the wavenumber spectra for each CES and complementary POM.

Plots of the upwash component in X_Y plane for first 3 modes

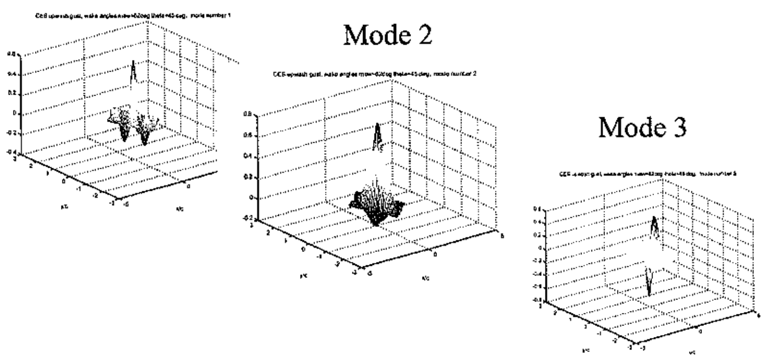

Noise Calculations: Typical noise spectra for Boeing Fan

note:
1) Levels are of correct magnitude
2) Mode 1 through 4 dominate
3) spectral peak at 14 kHz for lower order modes

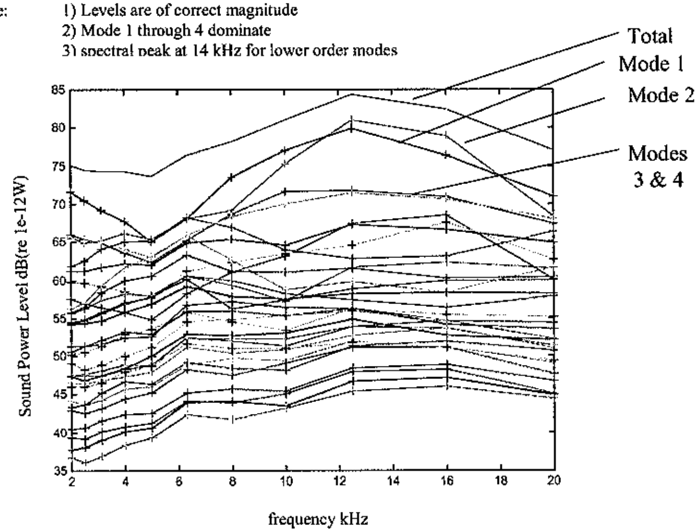

Comparison with Boeing Measurements POD Turbulence Model of Wake 55% Condition Wake angle $\mu=62°$

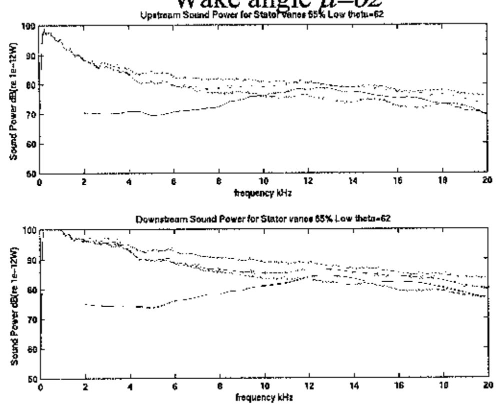

Details of the Flow

The Blade Wakes

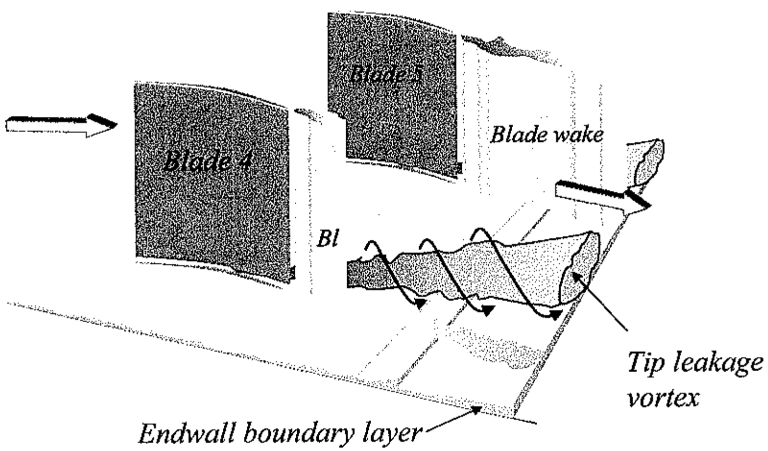

Statistical Description of the Flow

$$Ex[u_i(\mathbf{x},t)u_j(\mathbf{x'},t')]=R_{ij}(\mathbf{x},\mathbf{x'},t,t')$$

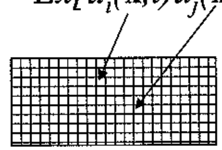

Note: for homogeneous stationary flows the correlation function is only dependent on *t-t'* and **x-x'**

Velocity Spectra in the Wake

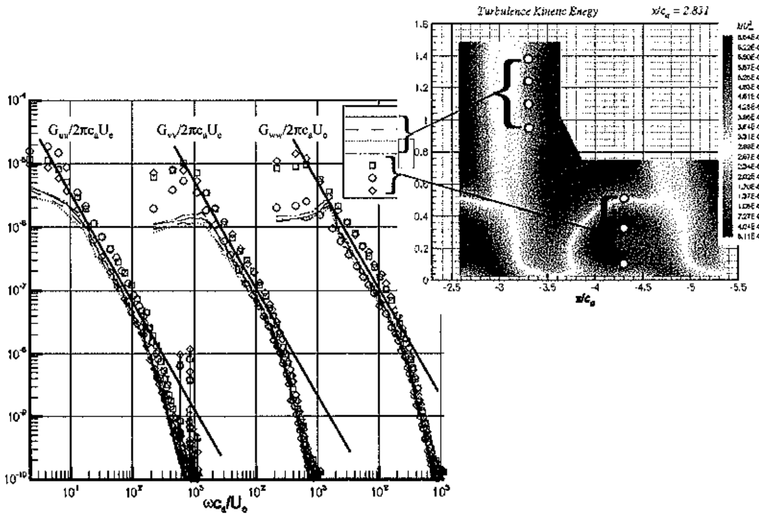

Estimating $R_{ij}(\mathbf{x},\mathbf{x}')$ from single point statistics

•Incompressible flow

$$R_{ij}(\mathbf{x},\mathbf{x}') = \varepsilon_{ikn}\varepsilon_{jml}\frac{\partial^2 q_{nl}(\mathbf{x},\mathbf{x}')}{\partial x'_m \partial x_k}$$

•Single Point Statistics

$$\lim_{\mathbf{x}'\to\mathbf{x}} R_{ij}(\mathbf{x},\mathbf{x}') = Ex\left[u_i(\mathbf{x})u_j(\mathbf{x})\right]$$

A suitable form for the tensor is given by

$$q_{nl}(\mathbf{x},\mathbf{x}') = [\ \alpha_{no}(\mathbf{x})\alpha_{ol}(\mathbf{x}') - \frac{1}{2}\delta_{nl}\alpha_{po}(\mathbf{x})\alpha_{op}(\mathbf{x}')\ ]h(|\mathbf{x}-\mathbf{x}'|)$$

where

$$\left(\alpha_{ij}(\mathbf{x})\right)^2 = Ex\left[u_i(\mathbf{x})u_j(\mathbf{x})\right]$$

and

$$h(s) = s^2 + \sum_{n=1}^{\infty}\frac{a_n s^{n+2}}{(n+1)(n+2)}$$

Cross Correlation Functions of a Wake Flow $R_{ij}(y,y')$

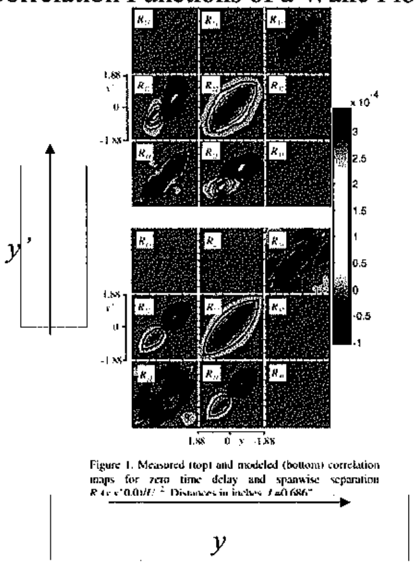

Figure 1. Measured (top) and modeled (bottom) correlation maps for zero time delay and spanwise separation

Proper Orthogonal Decomposition of an Airfoil wake

Eigenvalues

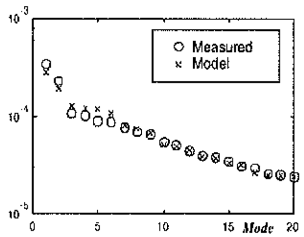

Figure 2. Eigenvalue spectra from the one-dimensional proper orthogonal decomposition in the y direction.

Modes

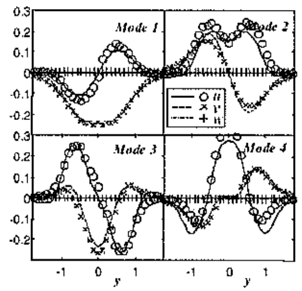

Conclusions

- POD analysis provides a method for modeling inhomogeneous turbulent flows
- CES provide insight into flow structures supported in the homogeneous directions of a 2D flow
- POD/CES analysis give high frequency noise levels comparable with existing methods.
- Methods are available for estimating the two point correlation tensor from single point statistics

Asymptotic modelling of airfoil – gust interaction

Dr Nigel Peake &

Dr Alison Cooper

Department of Applied Maths and Theoretical Physics

University of Cambridge

Asymptotic Modelling of Airfoil-Gust Interaction

Nigel Peake & Alison Cooper

DAMTP, Cambridge University

August 27, 2002

Ingmar Evers, DAMTP
Ed Kerschen, University of Arizona

- Interaction of unsteady disturbances with an isolated airfoil
  1. Airfoil angle-of-attack and camber (Myers & Kerschen JFM 292,353), thickness (Tsai. PhD thesis, U. Arizona)
  2. Transonic flow (Evers & Peake JFM, 411)
- Cascade Effects
  1. Upstream radiation, tonal (Peake & Kerschen, JFM 347)
  2. Broadband (Evers & Peake, JFM 463)
  3. Downstream radiation, tonal (Peake & Kerschen, JFM submitted)
- Propagation of rotor wakes through swirling flow.
  1. Modes in slowly-varying duct (Cooper & Peake JFM 445)
  2. Large azimuthal-order asymptotics.

The basic airfoil problem

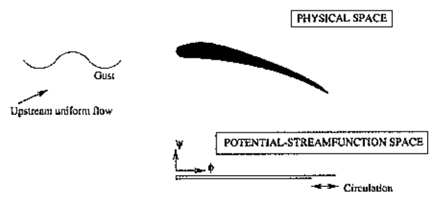

Far upstream gust velocity is $\mathbf{A}\exp(\mathrm{i}k\phi + \mathrm{i}kk_n\psi + \mathrm{i}kk_3z)$. k is the reduced frequency. Blade camber angle and thickness are $O(\delta)$.

Asymptotics: $\delta \ll 1$, $k \gg 1$, WITH $k\delta = O(1)$.

Unsteady velocity decomposition $\mathbf{u} = \mathbf{v} + \nabla h$. Here $\mathbf{v}$ is the vortical velocity, and equation for unsteady velocity potential, $h(\phi, \psi)$, is

$$(\mathcal{L}_0 + \mathcal{L}_1)(h) = k\delta S(\phi, \psi)\exp(\mathrm{i}k\Omega)$$

plus normal velocity boundary condition on $\psi = 0, 0 < \phi < 2b$.

- $\mathcal{L}_0$ is the uniform-flow Helmholtz operator
- $\mathcal{L}_1$ accounts for propagation through nonuniform mean flow, and is $O(\delta)$.
- $k\delta S(\phi, \psi)\exp(\mathrm{i}k\Omega)$ is the source term, being the interaction between the convected/distorted gust and the mean flow.

Asymptotic matching

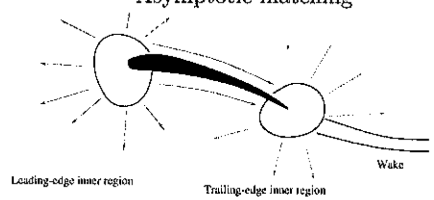

- Leading-edge interaction leads to pressure directivity

$$\frac{\left[D_0(\theta) + \delta\sqrt{k}D_1(\theta)\right]}{\sqrt{r}} \exp(ikwr + ik\delta P_1)$$

- Scattering of leading-edge field by trailing edge gives secondary source, size $O(1/\sqrt{k})$ smaller.

TRANSONIC NONUNIFORM FLOW

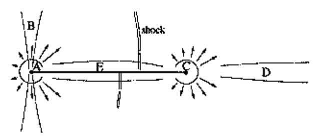

Scalings $1 - M_\infty = O(\delta^{2/3})$, $k\delta^{2/3} = O(1)$. Mean flow solution of TSD equation.

Shock wave weak, but strong beaming in gust direction for loaded blade.

(From Evers & Peake, JFM 411)

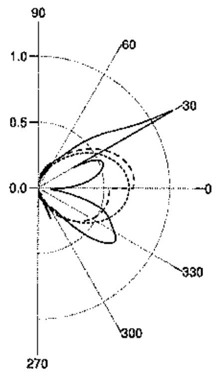

Gust-cascade interaction

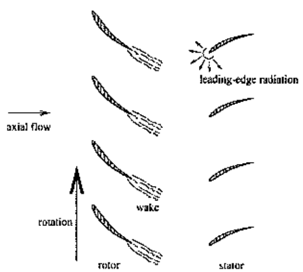

Aim to combine single-airfoil results into a cascade calculation. Study:

- Upstream radiation
- Unsteady pressure in blade passages
- Downstream radiation

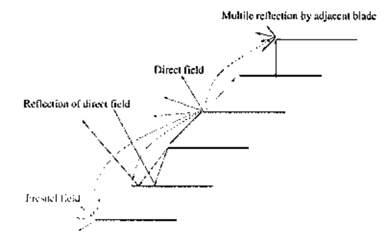

NB. $O(k\delta)$ phase changes due to nonuniform flow

Summation over all cylindrically-decaying contributions:

$$\sum \frac{D(\theta)}{r^{1/2}} \exp(\mathrm{i}kwr + \mathrm{i}k\delta P) = \sum [A_0 + A_1] \exp(\mathrm{i}\sigma x + \mathrm{i}\eta y)$$

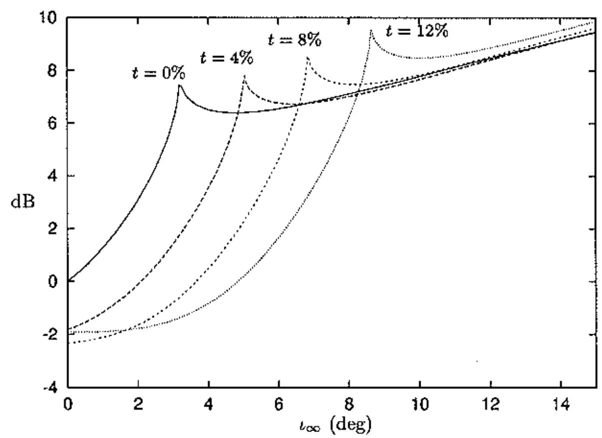

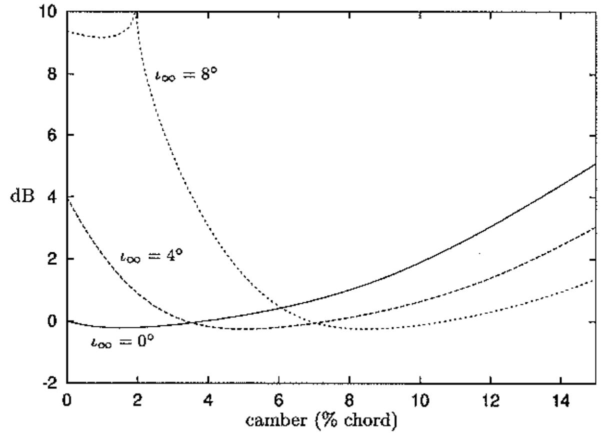

BROADBAND NOISE

Upstream radiation spectrum takes the form

$$\Pi \propto \sum_n \sum_l \int_{k_3} \left[\varphi_{22}|E_n|^2 + \varphi_{11}|E_t|^2 + \varphi_{12}|E_t E_n|\right] \mathrm{d}k_3$$

Summation over azimuthal order, n, radial order, l, integration over spanwise wavenumber k_3. Note contributions from

- blade normal, n, gust component
- blade tangential, ι, gust component
- cross-correlation.

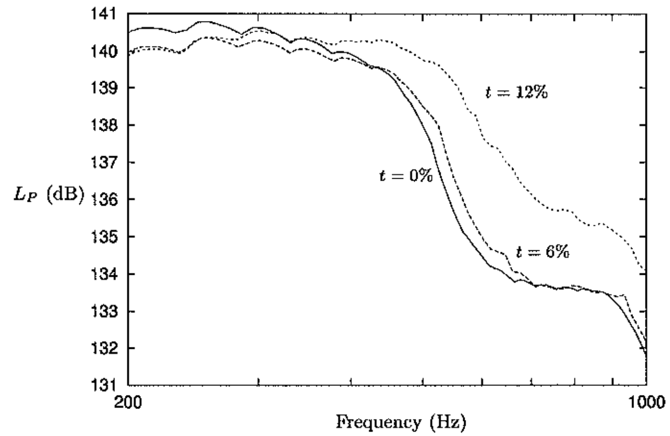

FLOW IN BLADE PASSAGES

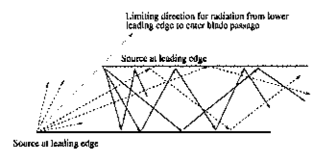

Distorted duct mode $\cos\left[\frac{n\pi\psi}{s} + \Theta^n(\phi,\psi)\right]\exp(-\mathrm{i}k^n\phi + \mathrm{i}\Xi^n(\phi,\psi))$.

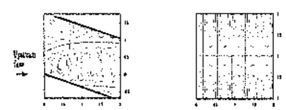

DOWNSTREAM NOISE

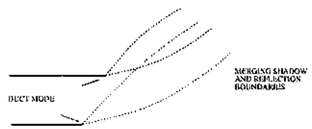

- Scattering of duct modes at trailing edges, plus distortion through downstream flow.
- Beaming along duct-mode angle directions

Directivity from a single blade passage

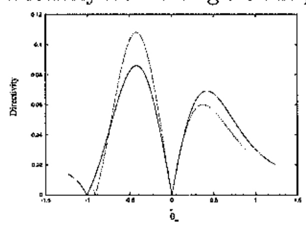

Direction and amplitude of beams modified by nonuniform flow.

Downstream radiation $\sum_n A_n D(\theta_n)\exp(\mathrm{i}\sigma^n x + \mathrm{i}\eta^n y)$, so:

(i) Maximal modal amplitude when mode angle corresponds to beam direction

(ii) Zero modal amplitude when mode propagates parallel to streamline direction (trailing-edge scattering $\sin\theta/2$).

Scattering of $n = 2$ duct mode into radiation modes, for varying inter-blade phase angle.

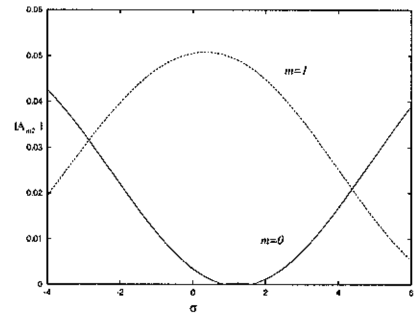

LARGE AZIMUTHAL-ORDER ASYMPTOTICS

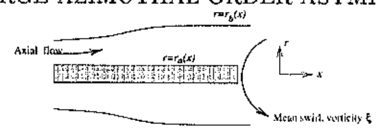

$$\mathbf{u}(\mathbf{x},t) = U(r,x)\mathbf{e}_x + W(r,x)\mathbf{e}_\theta + \epsilon V(r,x)\mathbf{e}_r + \nabla\phi(\mathbf{x},t) + \mathbf{a}(\mathbf{x},t)$$

$$\frac{D\mathbf{a}}{Dt} + (\mathbf{a}.\nabla)\mathbf{U} = -\xi \times \nabla\phi$$

$$\left[\frac{D}{Dt}\frac{1}{C_0^2}\frac{D}{Dt} - \frac{1}{D_0}\nabla.(D_0\nabla)\right]\phi = \frac{1}{D_0}\nabla.(D_0\mathbf{a})$$

Assume all unsteady velocities of form

$$(\mathbf{A}(x,r), \phi(x,r)) \exp\left(\mathrm{i}mK(x,r) + \mathrm{i}m\theta - \mathrm{i}m\Omega t\right)$$

KEY ASSUMPTIONS:

1. Large blade number, $m = NB \gg 1$.
2. Slow axial variations, $\epsilon \ll 1$.

Scaling $|\mathbf{A}| = O(1)$, $|\phi| = O(1/m)$, then at $O(m)$

$$-\omega + \frac{mW}{r} + K_x U = 0$$

At $O(1)$, from vorticity equation,

$$U\frac{\partial A_r}{\partial x} - \frac{2W}{r}A_\theta + \mathrm{i}VK_rA_r = \frac{\mathrm{i}}{r}\Gamma\phi + \mathrm{i}K_x\phi\frac{\partial U}{\partial r}$$
$$U\frac{\partial A_\theta}{\partial x} + \Gamma A_r + \mathrm{i}VK_rA_\theta + A_x\frac{\partial W}{\partial x} = -\mathrm{i}\Gamma K_r\phi - \mathrm{i}K_x\frac{\partial W}{\partial x}\phi$$
$$U\frac{\partial A_x}{\partial x} + \frac{\partial U}{\partial r}A_r + \mathrm{i}VK_rA_x + A_x\frac{\partial U}{\partial x} = -\mathrm{i}K_r\phi\frac{\partial U}{\partial r} + \frac{\mathrm{i}\phi}{r}\frac{\partial W}{\partial x}$$

where $\Gamma = (rW)_r/r$

From the wave equation,

$$\left(K_r^2 + K_x^2 + \frac{1}{r^2}\right)\phi = \mathrm{i}\left(K_rA_r + K_xA_x + \frac{A_\theta}{r}\right)$$

Hydrodynamic boundary-layer, width $O(1/m)$, on walls, including extra exponentially-decaying solution to satisfy boundary conditions. Rescale $R = (r - r_b(x))/m$, and find

$$U\frac{\partial \hat{A}_r}{\partial x} - \frac{2W}{r}\hat{A}_\theta + \mathrm{i}VK_r\hat{A}_r = \frac{\mathrm{i}}{r}\Gamma\hat{\phi} + \mathrm{i}K_x\hat{\phi}\frac{\partial U}{\partial r}$$

$$U\frac{\partial \hat{A}_\theta}{\partial x} + \Gamma\hat{A}_r + \mathrm{i}VK_r\hat{A}_\theta + \hat{A}_x\frac{\partial W}{\partial x} = -\mathrm{i}\Gamma K_r\hat{\phi} - \mathrm{i}K_x\frac{\partial W}{\partial x}\hat{\phi} - \Gamma\frac{\partial \hat{\phi}}{\partial R}$$

$$U\frac{\partial \hat{A}_x}{\partial x} + \frac{\partial U}{\partial r}\hat{A}_r + \mathrm{i}VK_r\hat{A}_x + \frac{\partial U}{\partial x}\hat{A}_x = -\mathrm{i}K_r\hat{\phi}\frac{\partial U}{\partial r} + \frac{\mathrm{i}\hat{\phi}}{r}\frac{\partial W}{\partial x} - \frac{\partial U}{\partial r}\frac{\partial \hat{\phi}}{\partial R}$$

Now steady-flow quantities evaluated on $R = 0$.

Rescaled wave equation is

$$\frac{\partial^2\hat{\phi}}{\partial R^2} + 2\mathrm{i}K_r\frac{\partial\hat{\phi}}{\partial R} - \left(K_r^2 + K_x^2 + \frac{1}{r^2}\right)\hat{\phi} = -\frac{\partial \hat{A}}{\partial R} - \mathrm{i}K_r\hat{A}_r - \mathrm{i}\hat{A}_\theta\left(\frac{1}{r} + K_x\frac{\partial U/\partial r}{\Gamma}\right)$$

Axial wake perturbation.

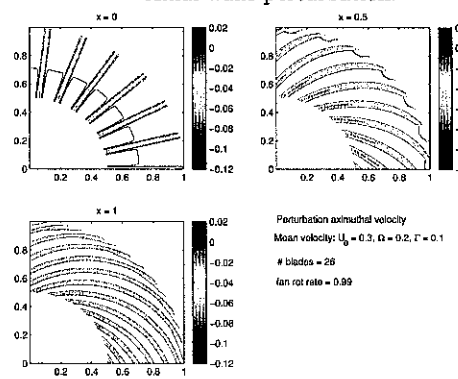

Radial wake perturbation

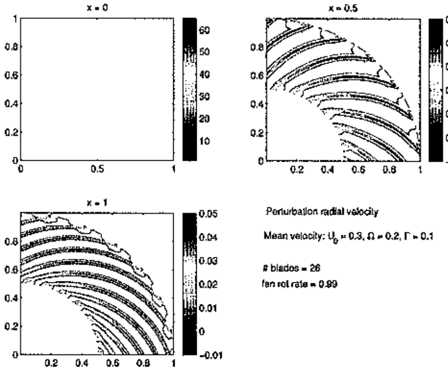

Radial variation at given axial location

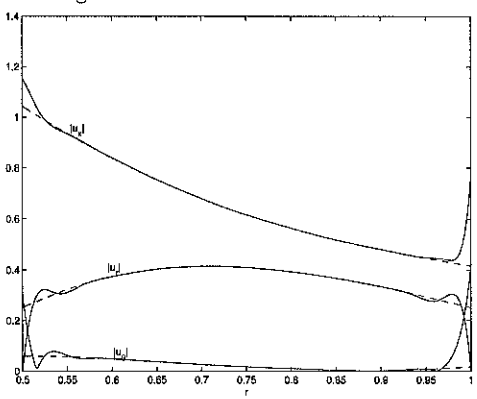

- Take evolved downstream disturbance, and perform local cascade calculation at each radius of stators. Systematic justification via Matched Asymptotic Expansions.
- Note that, at $X = X_s$, phase $\exp(\mathrm{i}k(r)X)$ has axial wavenumber $k(r)$ and radial wavenumber $k'(r)X_s$.
- Cascade output provides unsteady pressure just upstream of stators, in form

$$p(r)\exp(\mathrm{i}\hat{m}\theta + \mathrm{i}\hat{m}\chi(r)) \ ,$$

with scattered mode order $\hat{m} = m - nV$.

- For $\hat{m} = O(1)$ project onto upstream sonic modes. For $\hat{m} \gg 1$, ray tracing back through swirling flow (cf Envia AIAA Paper 98-2318).

Upstream modal amplitudes - no swirl

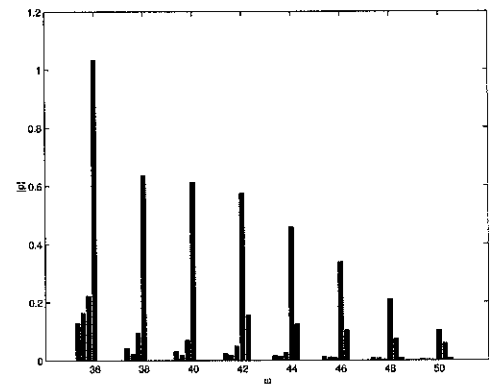

$$\hat{m} = 26 - 1 \times 50 = -24$$

Upstream modal amplitudes - with swirl. $B = 26$, $V = 50$, $\hat{m} = -24$. The amplitudes of the three propagating 'sonic' modes.

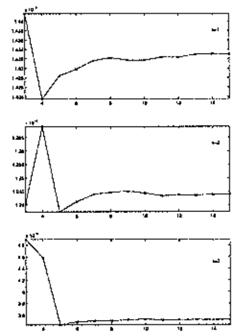

FURTHER DEVELOPMENTS

1. Large $\hat{m}$ asymptotics of nearly sonic components - different scalings on $\mathbf{A}$ and ϕ.
2. Rotor-stator coupling condition.
3. Cascade response for $O(1)$ camber:

- Forward stagnation point close to leading edge, and local angle of attack small, allows use of Kerschen local analysis.
- $O(1)$ mean-flow distortions implies numerical ray tracing.

Rotor wake turbulence noise

Dr Ed Envia
NASA

AIAA-2002-2489

Rotor Wake Turbulence Noise

Ed Envia
NASA Glenn Research Center

❑ Broadband Rotor-Stator Interaction Noise

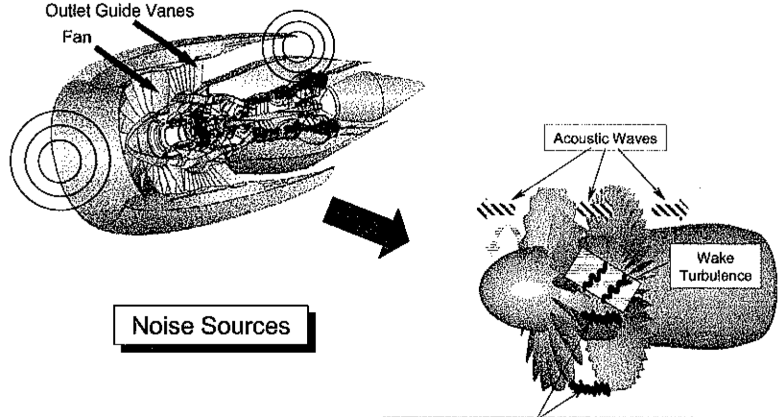

❑ Methodology

- (1) Wake Description: RANS Calculations
  - Meanflow characteristics
  - Turbulence intensity and integral length scales
- (2) Blade-Row Response: <u>Isolated</u> Flat-Plate Annular Cascade
  - Stripwise lift response (2D cascade)
  - Classical duct acoustics (3D)
- (3) Broadband Spectrum: Combine (1) & (2)
  - Modal power description on per frequency basis
  - "<u>Inlet</u>" and "<u>exhaust</u>" spectra of in-duct acoustic power

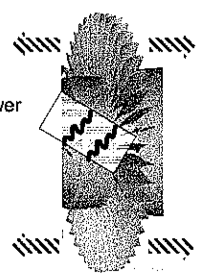

❑ RANS Results (example)

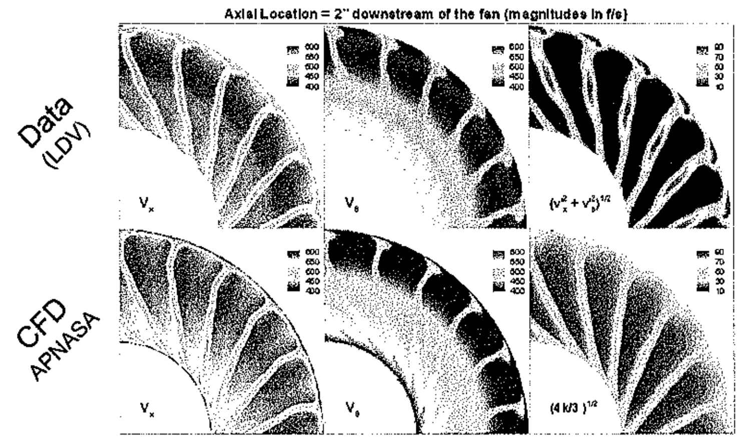

❑ Wake Turbulence Model

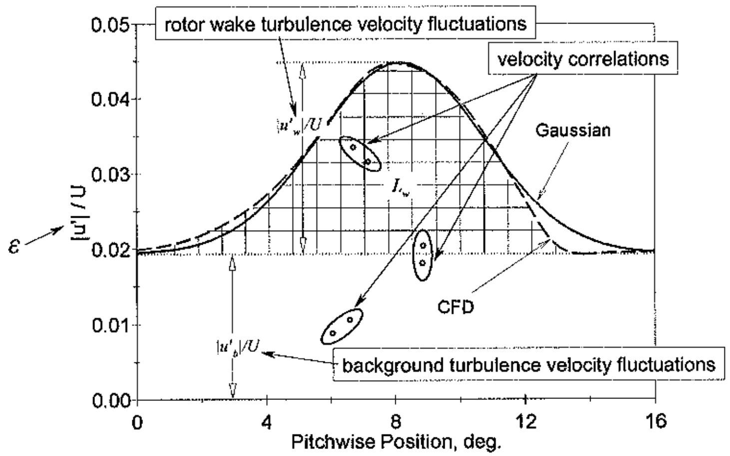

❑ Noise Spectrum (pressure)

chordwise lift integral (2D)

$$\langle p_{mn}(\omega)\, p^*_{mn}(\omega)\rangle = \frac{(\rho_0 N_V)^2}{k^2_{mn}(\omega)} \int_{r_H}^{r_T} \left|C_{mn}(\bar r,\omega)\right|^2 \;\psi^2_m(\kappa_{mn}\bar r)\,\Psi(\bar r)\,d\bar r$$

duct radial mode shapes (3D)

gust velocity correlation function

$$\Psi(\bar r) = U^2 L_w \left\{ \frac{(N_B L_w \varepsilon_w)^2}{(2\pi)^2 \bar r^3} \sum_{m_1=-\infty}^{\infty} \sum_{q_1=-\infty}^{\infty} \left| e^{-\frac{1}{4\pi}\left(\frac{m_1 N_B L_w}{\bar r}\right)^2} \right|^2 \tilde\phi_{1x}(\lambda_{1x}L_x)\,\tilde\phi_{1t}(\lambda_{1t}L_t) + \left(\frac{2N_B L_w \varepsilon_b \varepsilon_w}{2\pi \bar r^2} + \frac{\varepsilon_b^2}{\bar r}\right) \sum_{q_1=-\infty}^{\infty} \tilde\phi_{2x}(\lambda_{2x}L_x)\,\tilde\phi_{2t}(\lambda_{2t}L_t) \right\} d\bar r$$

turbulence intensity

turbulence integral length scales

❑ Testbed: 22-inch Source Diagnostic Test Fan Rig

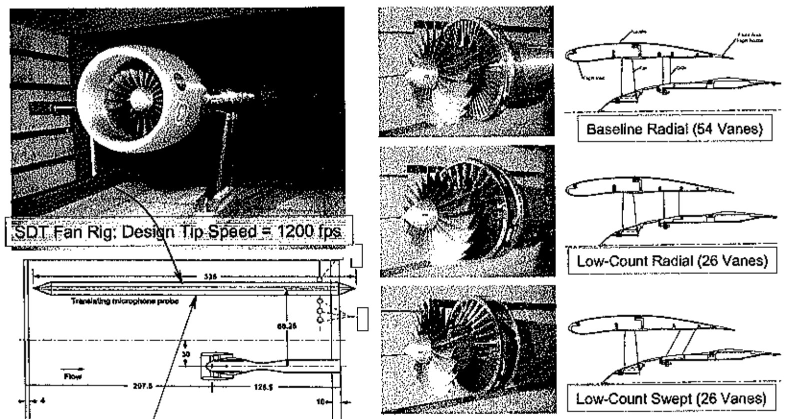

Farfield pressure spectra obtained at many microphone positions for several fan tip speeds.

❑ Noise Source Separation (inlet, exhaust)

inlet + exhaust noise

–

inlet noise

≅

exhaust noise

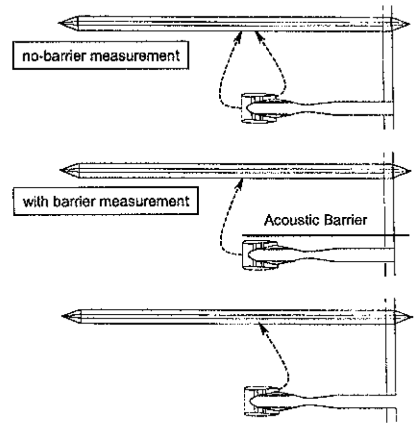

❑ Noise Source Separation (rotor, stator)

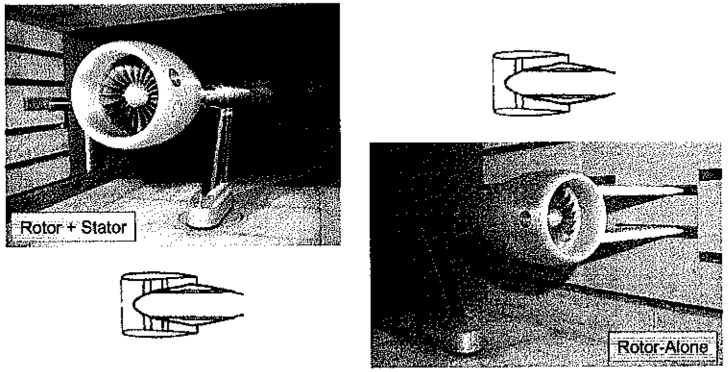

❑ Noise Source Separation (Example: Baseline OGV Data)

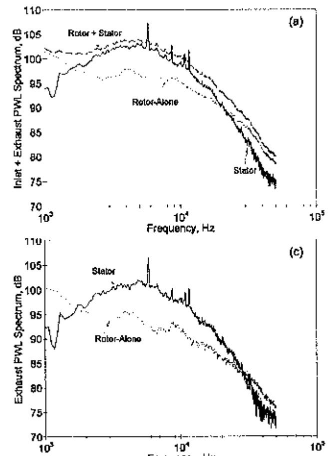

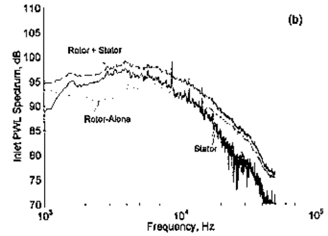

Power level (PWL) spectra obtained by integrating measured pressure directivity at each frequency correcting for propagation distance losses.

❑ Issues and Caveats

- ➢ Spectra Acquired in the Range 50% to 100% of Fan Design Tip Speed
  - Predictions carried out for three speeds:
    - Approach condition (~62% design tip speed)
    - Cutback condition (~88% design tip speed)
    - Takeoff condition (100% design tip speed)
- ➢ Isolating OGV Spectra Was Only Possible at the Approach Condition
  - Rotor-alone noise was found to be greater than rotor + stator combination
- ➢ Tones and Shaft Orders Contribution Not Extracted from Data
  - Measured spectra have some coherence in them
  - Coherence "contamination" increases with tip speed
- ➢ Theory Does Not Account for Unsteady Blade Row Coupling or Rotor Transmission Losses
- ➢ Theoretical Results Are Not Corrected or Adjusted in Any Way

❑ Data-Theory Comparisons

- ➢ Baseline Radial OGV Spectra at Approach Speed

Note the difference in scales

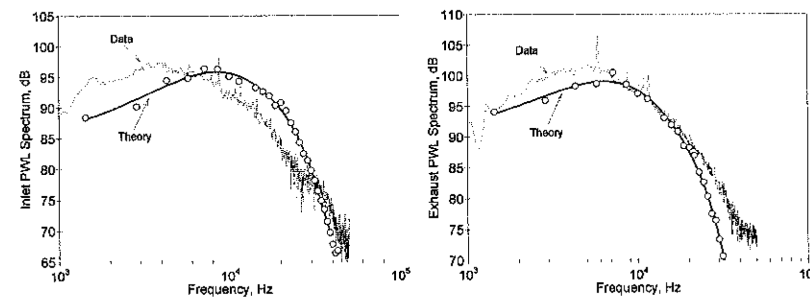

❑ Data-Theory Comparisons

➢ Low-Count Radial OGV Spectra at Approach Speed

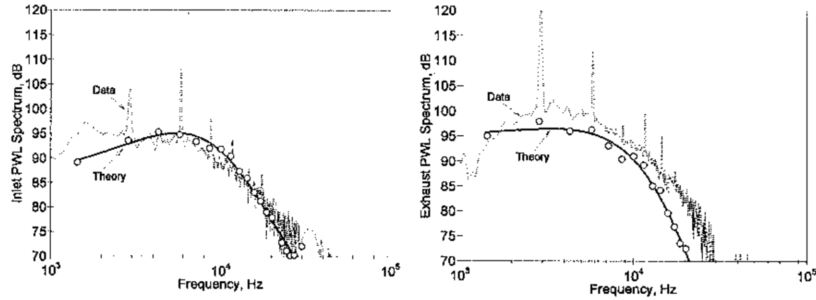

❑ Data-Theory Comparisons

➢ Low-Count Swept OGV Spectra at Approach Speed

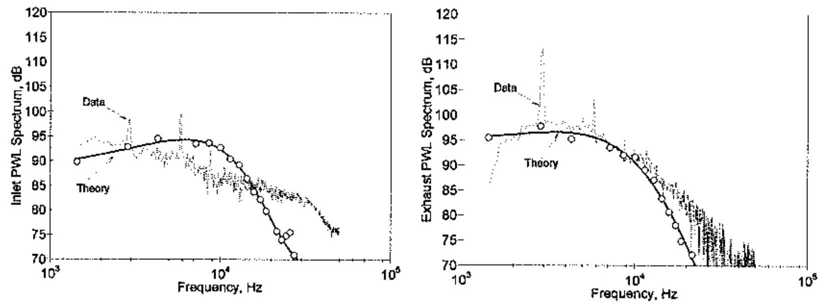

❑ Data-Theory Comparisons

➢ Influence of Vane Count and Sweep on Spectra

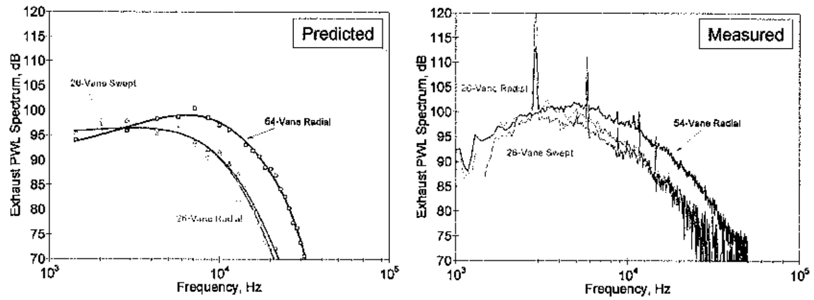

Exhaust Spectra at Approach Speed

❑ Predicted Trend with Fan Tip Speed

➢ Predicted Trends Agree with Measurements

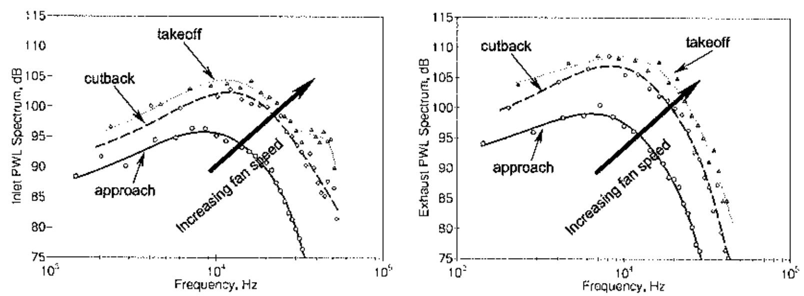

Conclusions

- ❑ Predicted spectra of stator exhaust acoustic power shows reasonable agreement with measurements where comparisons are possible.
- ❑ The theory does not account for unsteady blade row coupling and rotor transmission losses and tends to over-predict the measured inlet spectral levels.
- ❑ Predictions are "as is" with no adjustment to levels or spectral shapes.
- ❑ Predicted spectral trends with tip speed, vane count and vane sweep are consistent with measurements where comparisons are possible.
- ❑ CFD provides acceptable wake turbulence characteristics for use as input to the stator noise model.

Vane unsteady pressure measurements

Dr Ed Envia
NASA

Vane Unsteady Pressure Measurements

Ed Envia
NASA Glenn Research Center

Fan Noise Source Diagnostic Test Summary

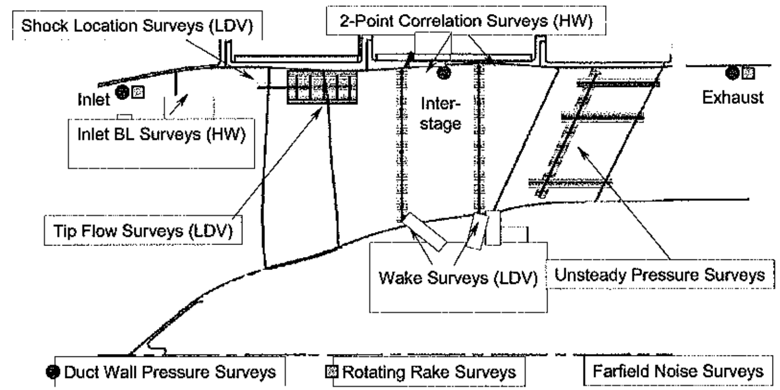

Tested 2 Fans, 3 Outlet Guide Vanes and Rotor-Alone Configurations

Vane Test Matrix

- ❑ 2 Outlet Guide Vane Configurations
- ❑ 7 Fan Tip Speeds → Approach, Cutback and Takeoff

Radial OGV

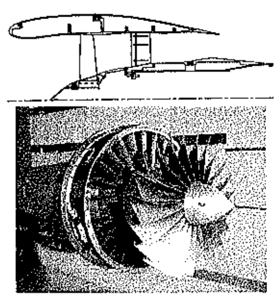

Swept OGV

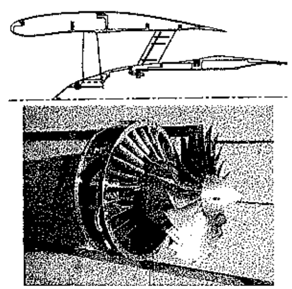

Vane Sensor Layout

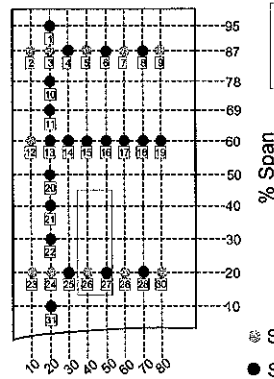

- ❑ Identical Layout on % Basis
- ❑ $\Delta p = p_s - p_p$, p_s, p_p Measurements

Sensor Locations on Vane 1 and Vane 2

● Sensor Locations on Vane 1 Only

31 Transducers on Vane 1
11 Transducers on Vane 2

Vane Pressure Data

- Fixed Sampling Rate (128 kHz)
  - Pressure time series resampled to correct for fan rpm drift
- Time-Domain Averaging $\rightarrow$ Spectral Decomposition
  - Broadband content (random) ◀
  - Shaft order content (coherent)
  - BPF harmonic content (coherent) ◀
- BPF Harmonic and Broadband Results (Δp, p_p)
  - Influence of sweep
  - Dependence on fan tip speed
- Additional Broadband Results
  - Chordwise and spanwise correlations (temporal)
  - Integral length scale of pressure (spatial)

Spectral Decomposition

- Time-Domain Averaging

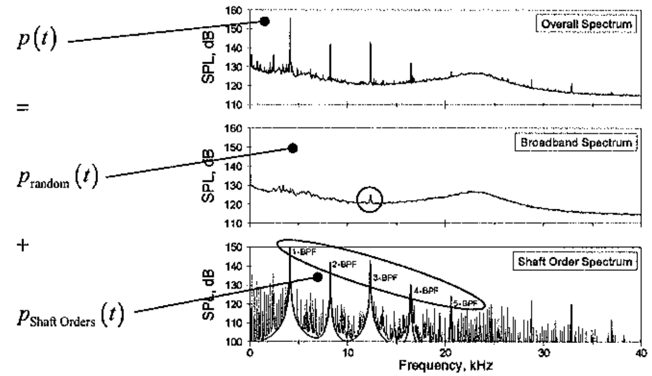

Influence of Vane Sweep

- BPF Harmonic Content

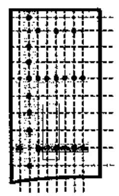

3xBPF: Takeoff Condition

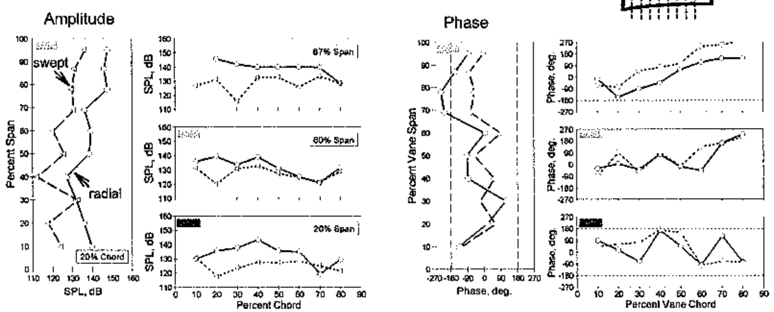

Effect of Fan Tip Speed

- BPF Harmonic Content (SPL)

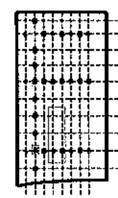

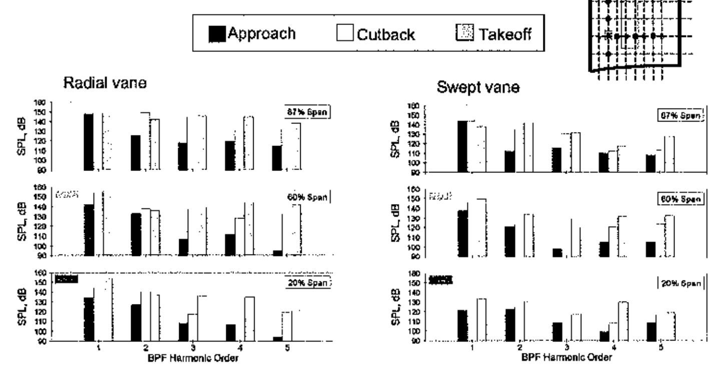

Δp, p_p Levels

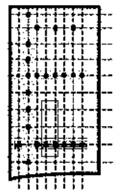

❑ BPF Harmonic Content

2xBPF: Cutback Condition

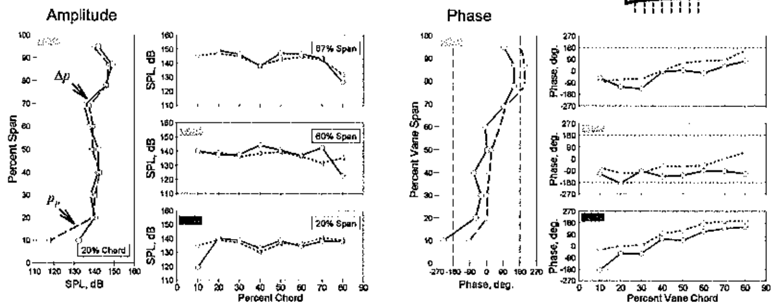

ISVR Workshop, August 22 - 23, 2002

9

Influence of Vane Sweep

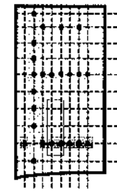

❑ Broadband Content (r.m.s.)

Approach Condition

Takeoff Condition

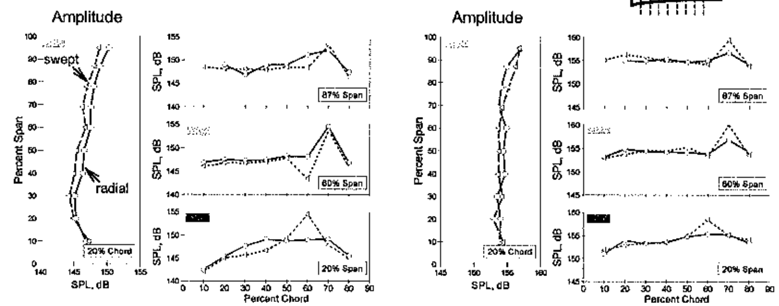

ISVR Workshop, August 22 - 23, 2002

10

Δp, p_p Levels

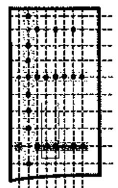

❑ Broadband Content (r.m.s.)

Approach Condition

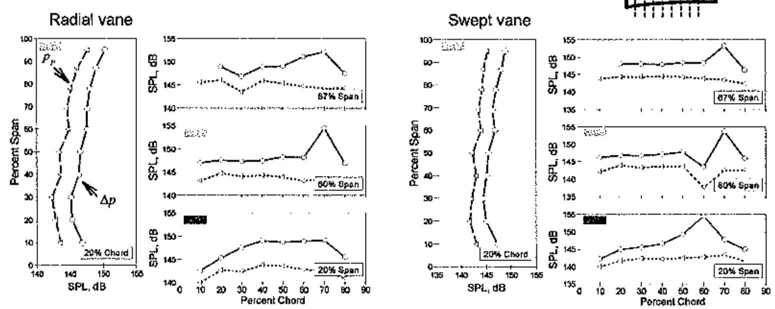

ISVR Workshop, August 22 - 23, 2002

11

Tip Speed Dependence

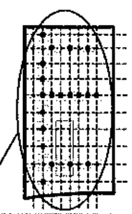

❑ Broadband Content (r.m.s.)

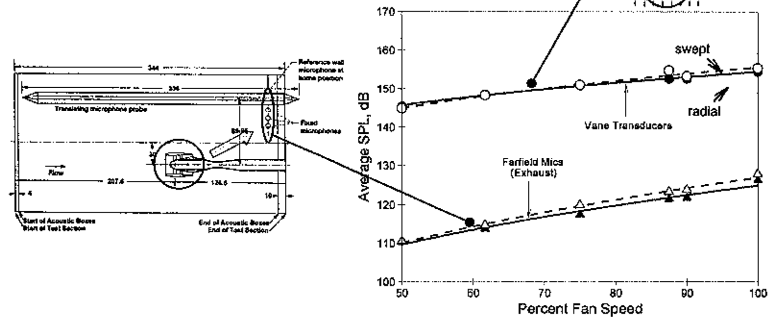

ISVR Workshop, August 22 - 23, 2002

12

Pressure Correlation

- Time-Delay Correlations (Broadband Content)

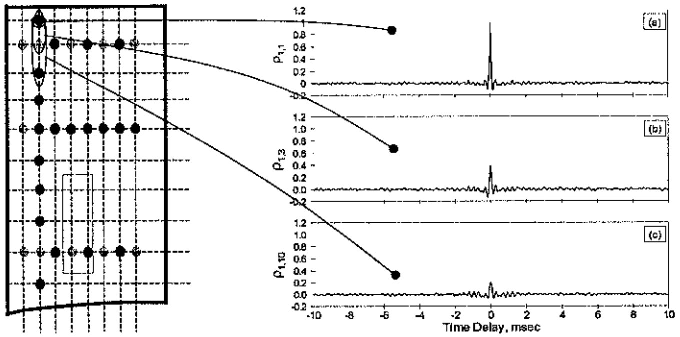

Spatial Coherence

- Zero-Time-Delay Correlations → Spatial Integral Scale

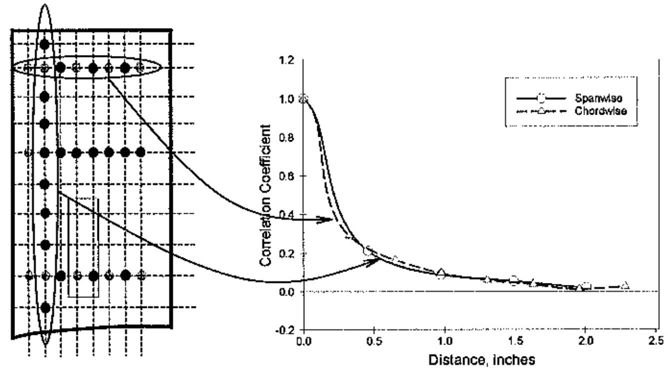

Integral Length Scales of Pressure

- Spanwise Variations of Integral Scale

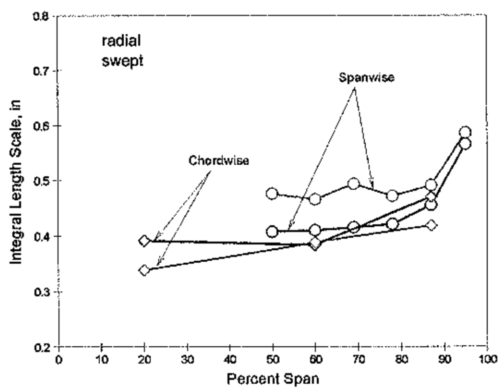

Dependence of Integral Scale on Tip Speed

- Spanwise-Averaged Integral Scale

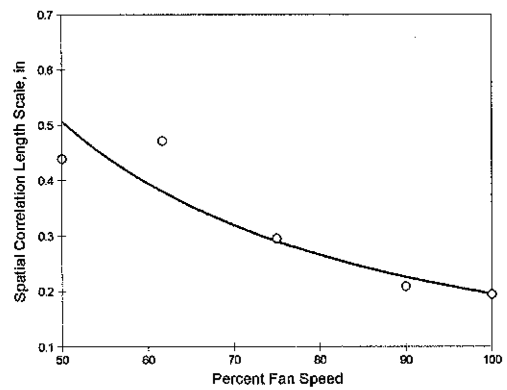

Summary

- ❑ Analysis of data indicates that:
  - vane unsteady pressure levels are sensitive to sweep and fan tip speed.
  - vane average r.m.s random levels (in dB) vary linearly with fan tip speed and track quite well with corresponding average farfield levels.

- ❑ Evidence of strong coherence of broadband pressure on the vane
  - Correlation levels are nearly the same along the span and chord.
  - Vane surface pressure field is approximately homogeneous.
  - Integral length scale of vane pressure decreases monotonically with fan tip speed.

Fan/gust interaction noise in context

Dr Alec Wilson
Rolls-Royce plc
Derby

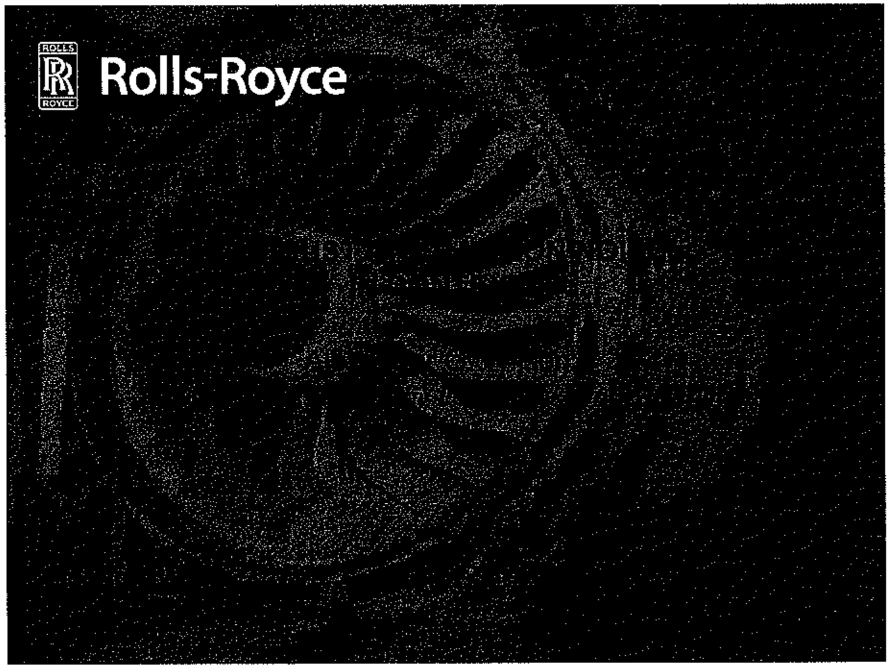

The Context

Fan Stage Gust/Bladerow Interaction

- Fan/OGV Interaction Noise
  - Bladerow Reflection/Transmission
- Inlet Flow Distortion / Fan Interaction Noise
- Broadband Noise

➢ Measurements
➢ Significance
➢ Physical Processes
➢ Calculation Methods

Fan Rig: Farfield Fwd Arc 1BPF Noise vs Speed

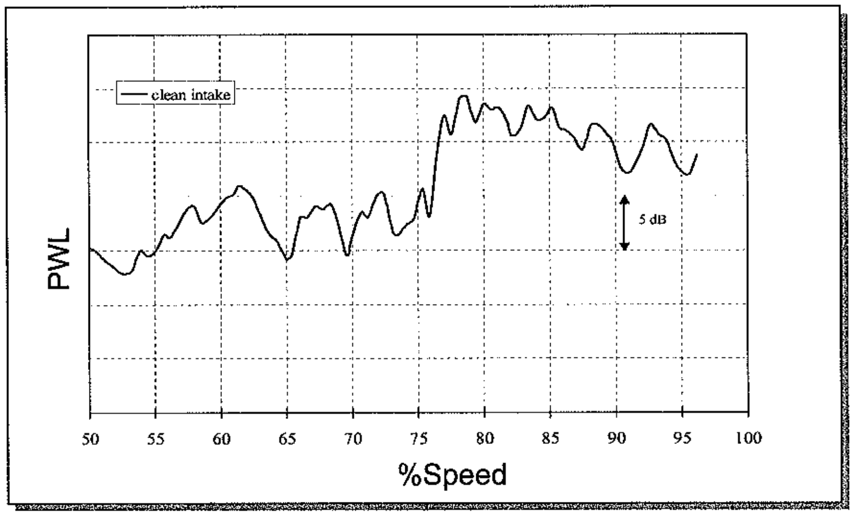

Fan/OGV Interaction Noise

Farfield Fwd Arc Noise vs Engine Order: 60% Spd

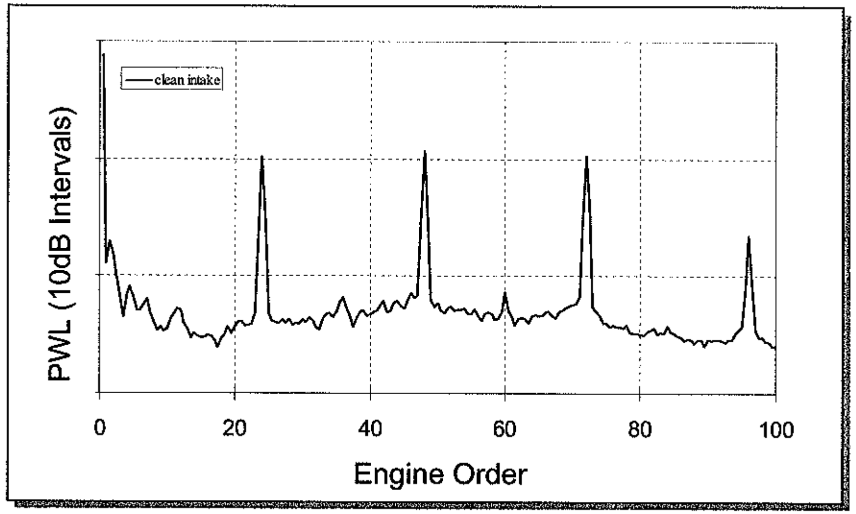

Fan/OGV: Modal Breakdown at 60% Speed

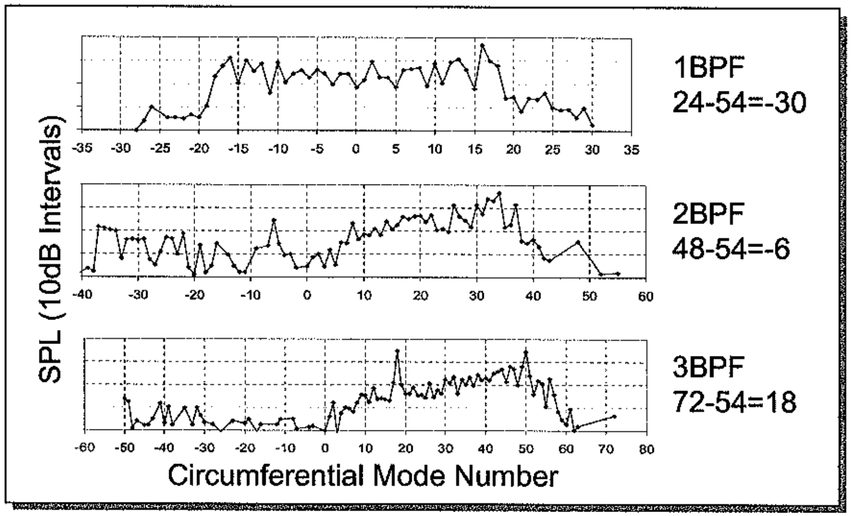

Fan/OGV Interaction Noise: Basic Mechanism

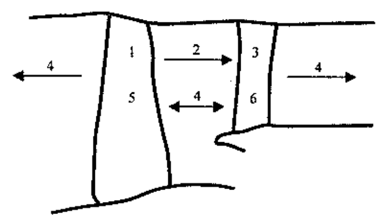

1. Rotor Wake Generation
2. Wake Propagation
3. Wake/Vane Interaction
4. Acoustic Propagation
5. Rotor Reflection / Transmission
6. OGV Reflection / Transmission

Fan/OGV Interaction Noise

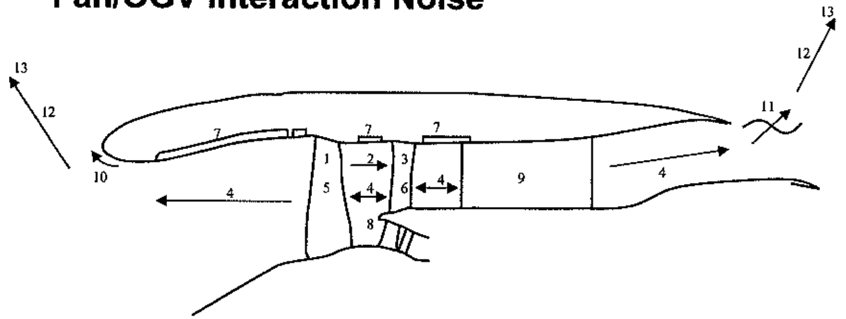

1. Rotor Wake Generation
2. Wake Propagation
3. Wake/Vane Interaction
4. Acoustic Propagation
5. Rotor Refl/Transm
6. OGV Refl/Transm
7. Liner Attenuation
8. Core Interaction
9. Pylon etc. Refl/Transm
10. Refraction
11. Propn Thru Shear Layer
12. Propn to Farfield
13. Weighting to EPNL

Fan/OGV Interaction Noise: Methods

- Physically based correlation
- Analytic 'steady' flow + semi-analytic linearised response
  - Wake propagation model
  - Twisted flat plates (unloaded)
  - Multiple fan/ogv interactions
- CFD 'steady' flow + numerical linearised blade response + analytic green's function
- CFD 'steady' flow + numerical linearised response
- Unsteady non-linear CFD

CFD for Fan/OGV Interaction (Schematic)

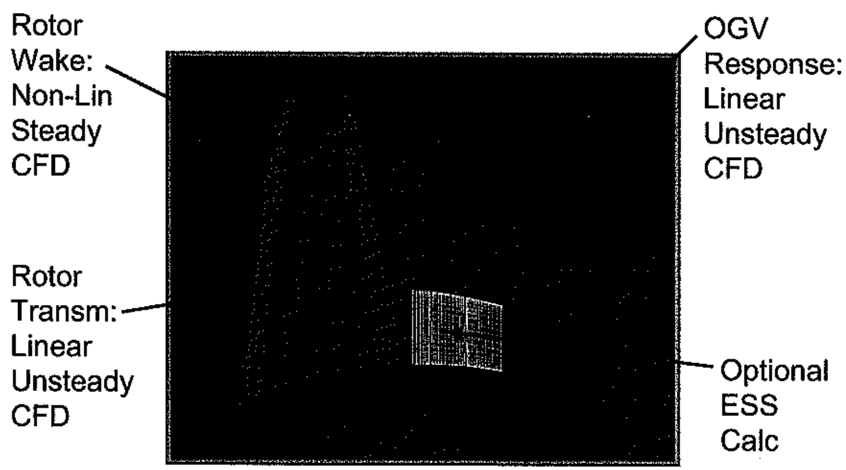

Flat Plate Validation Case

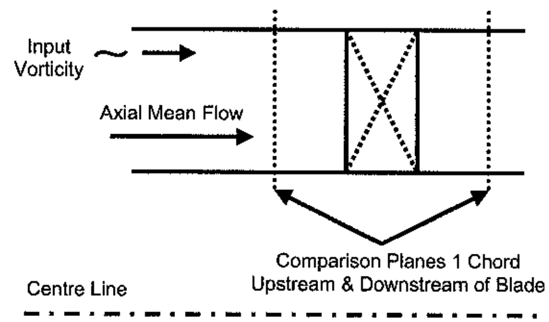

[Cat. 4 Problem from 3rd CAA Wkshp on Benchmark Problems, Cleveland '99]

Flat Plate Validation Case

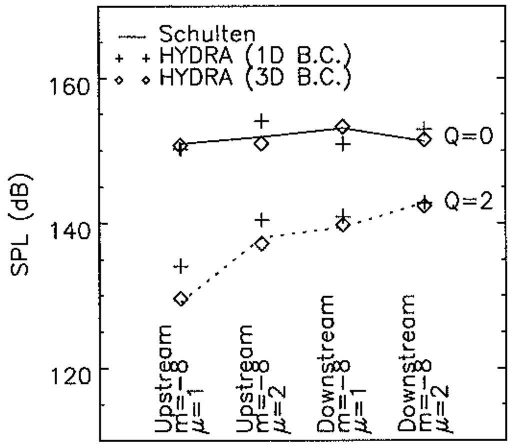

More info: AIAA-2001-2135

Fan / Inlet Flow Distortion Interaction Noise

- Steady distortion (eg 'droop')
- Unsteady distortion (eg crosswind)

"Simple Droop" (Schematic)

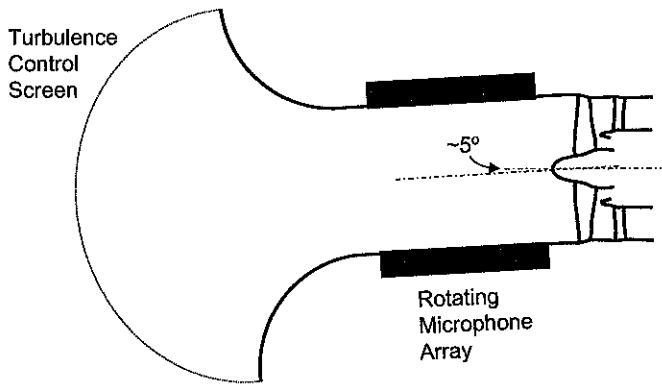

Simple Droop: Farfield Fwd Arc 1BPF Noise vs Spd

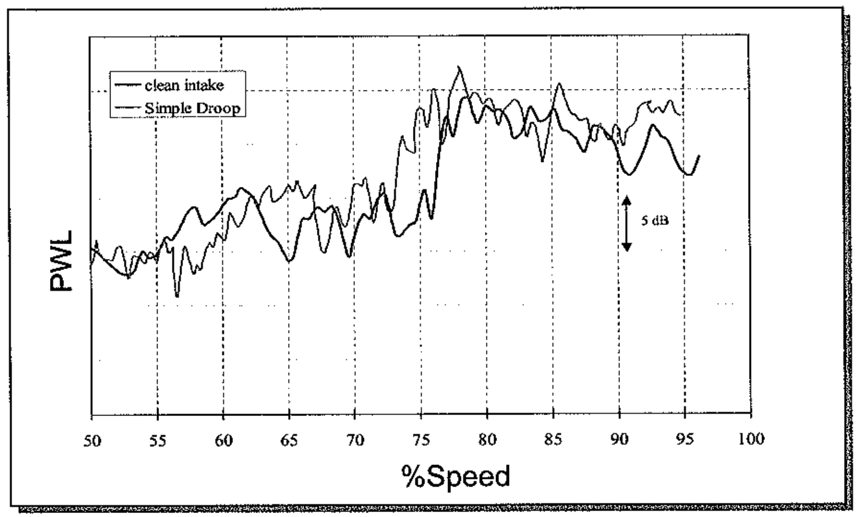

Simple Droop: Modal Breakdown at 75% Spd, 1BPF

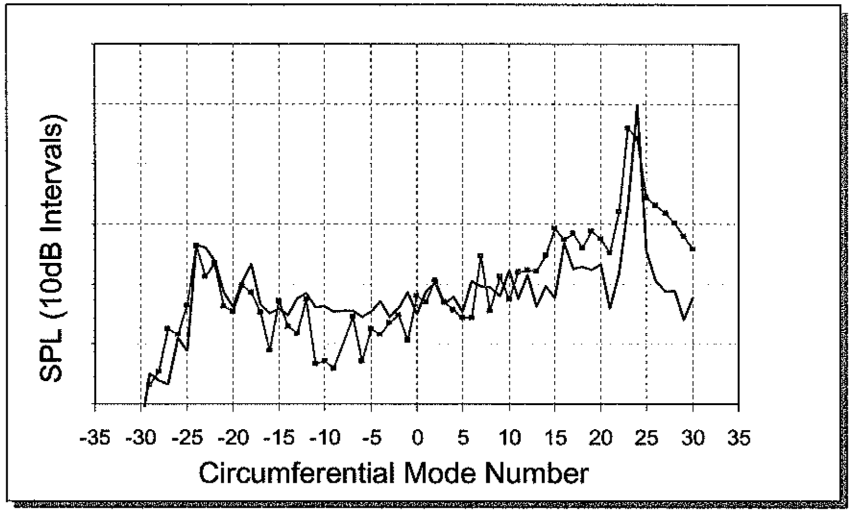

Fan / Inlet Flow Distortion Interaction Noise

- Physically based correlation
- Analytic ‘distortion’ flow + semi-analytic linearised response
- CFD ‘steady’ flow + numerical linearised blade response + analytic green’s function
- CFD ‘steady’ flow + numerical linearised response
- Unsteady non-linear CFD

Broadband Noise

Farfield Fwd Arc 1BPF Noise vs Engine Order

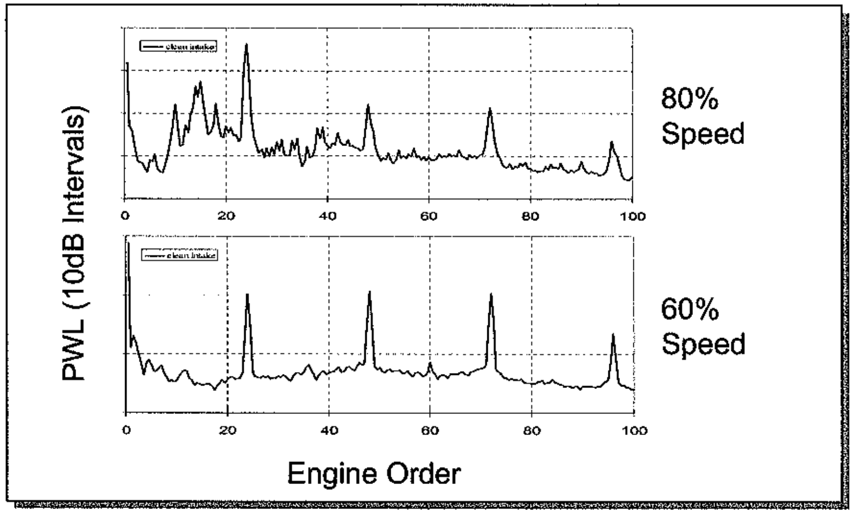

Broadband Noise

- Physically based correlation for multiple sources
- Analytic turbulence + analytic linearised response + radiation calculation
- Analytic turbulence + linearised CFD blade response + radiation calculation
- RANS CFD turbulence + linearised CFD blade response + radiation calculation
- LES/DES turbulence +

Turbulent Spectral Amplitude

Fan Wake Turbulence / OGV Interaction, 70% Spd

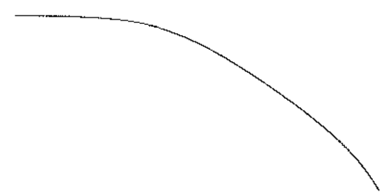

Broadband Computational Requirement

Fan Wake Turbulence / OGV Interaction, 70% Speed

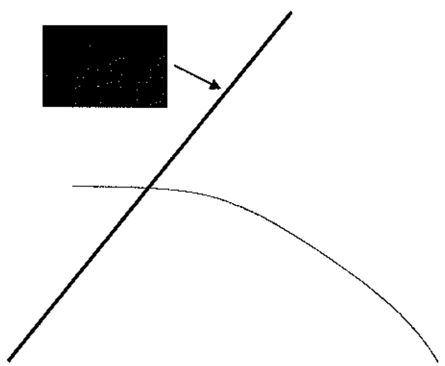

Conclusions

- Fan/OGV interaction noise
  - Bladerow transmission/reflection important
- Inlet flow distortion interaction noise
  - Important at all speeds, especially just below cut-on
- Broadband
  - Dominant engine source at low speed
  - Important source at high speed also
  - Source split less clear
- General
  - High frequencies not yet amenable to CFD/CAA methods
  - Need modal content to assess liner effectiveness

Research Priorities

- Application of CFD/CAA to specific problems at low-mid frequencies
- Semi-analytical methods for
  - Mid-high frequencies
  - Fast design methods
  - Understanding
- Broadband noise:
  - What measurements needed?
  - How to characterise turbulence?
  - CFD/CAA: RANS for low frequency BB?
    Turbulence info from RANS?
    LES and DES?
  - Improving correlation / semi-analytic methods

Supersonic leading-edge noise

Mr Chris Powles

Department of Mathematics

University of Keele

Supersonic Leading-Edge Noise

C.J. Powles
Department of Mathematics,
University of Keele,
Staffordshire

22nd August 2002

Overview

1. Background to problem
2. Physical system - Boundary value problem
3. Solution procedure
4. Solution: double integral formula
5. Simplifications:
   - The two-dimensional case
   - Asymptotic solution for localised gusts
6. Examples of specific gusts
7. Summary and conclusions

History Of Problem

Flat plate approach common: Miles, Amiet, Cannell, Martinez and Widnall, Ffowcs Williams and Guo, Peake, etc.

Half plane:

- Amiet (1975, 1976, 1986)

- Martinez and Widnall (1980, 1983)

- Ffowcs Williams and Guo (1988)

- Guo (1989, 1990, 1991)

Extensions: Quarter plane, Mean loading, Finite wings, Cascades, Etc

Physical system

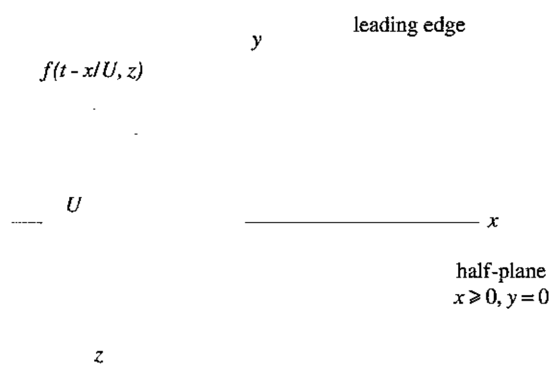

Half plane: $y = 0, \quad x \geq 0$

Mean flow: $U\underline{e}_x = Mc_0\underline{e}_x$

Boundary value problem

Disturbances small - LINEAR INVISCID THEORY.

Gust-plate interaction through y-component of gust velocity in plane $y = 0$, $x > 0$.

This is convected, so has form $f(t - x/U, z)$

Define acoustic velocity potential:

$$\underline{u} = \nabla\varphi \qquad p = -\rho_0 \left(\frac{\partial}{\partial t} + U\frac{\partial}{\partial x}\right)\varphi$$

$\underline{u} =$ acoustic particle velocity,
$p =$ acoustic pressure perturbation,
$\rho_0 =$ undisturbed density of fluid.

Potential must obey convected wave equation:

$$\frac{1}{c_0^2}\left(\frac{\partial}{\partial t} + U\frac{\partial}{\partial x}\right)^2 \varphi - \nabla^2\varphi = 0$$

Boundary Conditions:

Rigid plate gives:

$$\frac{\partial\varphi}{\partial y} = -f(t - x/U, z) \qquad y = 0^{\pm}, x > 0.$$

Supersonic flow gives:

$$\frac{\partial\varphi}{\partial y} = 0 \qquad y = 0^{\pm}, x < 0.$$

Combining these:

$$\frac{\partial\varphi}{\partial y} = -f(t - x/U, z)\mathrm{H}(x) \qquad y = 0^{\pm}.$$

Solutions must obey radiation/causality conditions.

Solution

Define Fourier Transforms:

$$\Phi(k, y, m, \omega) = \iiint_{-\infty}^{\infty} \varphi(x, y, z, t) e^{i(\omega t - kx - mz)} dx dz dt$$

$$\varphi(x, y, z, t) = \frac{1}{(2\pi)^3} \iiint_{-\infty}^{\infty} \Phi(k, y, m, w) e^{-i(\omega t - kx - mz)} dk dm d\omega$$

Transform wave equation:

$$\frac{\partial^2\Phi}{\partial y^2} - \left\{k^2 + m^2 - \frac{(\omega - Uk)^2}{c_0^2}\right\}\Phi = 0.$$

Define function $\gamma(k, m, \omega)$:

$$\gamma(k, m, \omega) = \left\{k^2 + m^2 - \frac{(\omega - Uk)^2}{c_0^2}\right\}^{1/2},$$

$$\mathrm{Re}(\gamma(k, m, \omega)) \geq 0.$$

By symmetry Φ must be odd in y, so radiation condition dictates solution:

$$\Phi(k, y, m, \omega) = A(k, m, w)\mathrm{sgn}(y) e^{-\gamma(k,m,\omega)|y|}.$$

Transforming boundary condition:

$$\frac{\partial\Phi}{\partial y} = \iiint_{-\infty}^{\infty} -f(t - x/U, z)\mathrm{H}(x) e^{i(\omega t - kx - mz)} dx dz dt$$

Let $t' = t - x/U$, and define the gust transform:

$$\mathrm{F}(\omega, m) = \iint_{-\infty}^{\infty} f(t', z) e^{i(\omega t' - mz)} dt' dz.$$

Evaluating transformed B.C:

$$\frac{\partial\Phi}{\partial y} = \frac{-iU\mathrm{F}(\omega, m)}{\omega - Uk} \qquad y = 0^{\pm}.$$

From our solution:

$$\frac{\partial\Phi}{\partial y} = -A(k, m, \omega)\gamma(k, m, \omega) \qquad y = 0^{\pm}.$$

Therefore the inversion integral gives:

$$\varphi(x,y,z,t) = \frac{1}{(2\pi)^3}\iiint_{-\infty}^{\infty} \frac{iU\mathrm{sgn}(y)\mathsf{F}(\omega,m)}{(\omega-Uk)\gamma(k,m,\omega)} e^{-i(\omega t-kx-mz)} e^{-\gamma(k,m,\omega)|y|} dk dm$$

Our interest is the pressure. Transforming operators:

$$p(x,y,z,t) = \frac{-\rho_0 M c_0 \mathrm{sgn}(y)}{(2\pi)^3}\iiint_{-\infty}^{\infty} \frac{\mathsf{F}(\omega,m)}{\gamma(k,m,\omega)} e^{-i(\omega t-kx-mz)} e^{-\gamma(k,m,\omega)|y|} dk dm.$$

Isolating the k integral:

$$K = \int_{-\infty}^{\infty} \frac{e^{ikx-\gamma(k,m,\omega)|y|}}{\gamma(k,m,\omega)} dk$$

Branch points:

$$k_{\pm} = \frac{M\omega/c_0}{M^2-1} \pm \frac{(\omega^2/c_0^2 + m^2(M^2-1))^{1/2}}{M^2-1}$$

Recalling $\mathrm{Re}(\gamma(k,m,\omega)) \geq 0$, we factorise γ:

$$\gamma(k,m,\omega) = +i(M^2-1)^{1/2}(k-k_+)^{1/2}(k-k_-)^{1/2}.$$

Complex k plane:

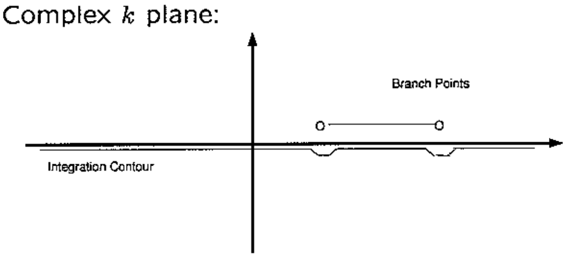

For $x < (M^2-1)^{1/2}|y|$ (ie $\overline{x} < |\overline{y}|$) we close contour in lower half plane to give 0.

For $\overline{x} > |\overline{y}|$: Make substitution:

$$k = k_c + (k_+ - k_c)\cos(\chi) \quad ; \quad k_c = \frac{1}{2}(k_+ + k_-)$$

Then we have a standard integral, and:

$$K = \frac{2\pi}{(M^2-1)^{1/2}} e^{i\omega M\overline{x}/c} \mathsf{J}_0(\{\omega^2/c^2 + m^2(M^2-1)\}^{1/2}(\overline{x}^2-\overline{y}^2)^{1/}$$

Then the general pressure integral is:

$$p(x,y,z,t) = \frac{-\rho_0 M c_0 \mathrm{sgn}(y)}{(2\pi)^2(M^2-1)^{1/2}} \iint_{-\infty}^{\infty} \mathsf{F}(m,\omega) e^{-i\omega(t-M\overline{x}/c)} e^{imz}$$
$$\times \mathsf{J}_0\left(\{\omega^2/c^2 + m^2(M^2-1)\}^{1/2}(\overline{x}^2-\overline{y}^2)^{1/2}\right)$$
$$dm dw$$

Simplifications and asymptotics

If gust velocity function $f(t-x/U,z)$ has no z dependence, the general m integral may be evaluated, giving single integral in terms of a transform $\mathsf{F}(\omega)$.

$$p(x,y,t) = \frac{-\rho_0 M c_0 \mathrm{sgn}(y)}{2\pi(M^2-1)^{1/2}} \int_{-\infty}^{\infty} \mathsf{F}(\omega) e^{-i\omega(t-M\overline{x}/c)}$$
$$\times \mathsf{J}_0\left(\omega/c(\overline{x}^2-\overline{y}^2)^{1/2}\right) dw$$

If gust velocity profile is instead localised in z, consider Mach cone: $\overline{x}^2 > \overline{y}^2 + \overline{z}^2$

Substitution:

$$m = \frac{\omega}{c_0}(M^2-1)^{-1/2}\sinh(\chi)$$

Hankel approximation:

$$\mathsf{J}_0(\alpha) \simeq \left(\frac{2}{\pi\alpha}\right)^{1/2}\cos(\alpha - \pi/4)$$

Then:

$$p(x,y,z,t) \simeq \frac{-\rho_0 M c_0 \mathsf{sgn}(y)}{(2\pi)^2(M^2-1)}\left(\frac{2}{\pi}\right)^{1/2}\int_{-\infty}^{\infty}\left(\frac{\omega}{c_0}\right)^{1/2} e^{-i\omega(t-M\overline{x}/c)}$$
$$\int_{-\infty}^{\infty}\mathsf{F}\left(\frac{\omega}{c_0}(M^2-1)^{-1/2}\sinh(\chi),\omega\right)e^{i\omega\overline{z}\sinh(\chi)/c_0}$$
$$\cos\left(\frac{\omega}{c_0}(\overline{x}^2-\overline{y}^2)^{1/2}\cosh(\chi)\right)\cosh^{1/2}(\chi)\,d\chi\, d\omega$$

Then we get 2 integrals:

$$I_{1,2} = \int_{-\infty}^{\infty}\mathsf{F}\left(\frac{\omega}{c_0}(M^2-1)^{-1/2}\sinh(\chi),\omega\right)$$
$$\cosh^{1/2}(\chi)\,e^{\pm i\frac{\omega\overline{R}_h}{c_0}\cosh(\chi-\mathrm{arcsinh}(-\overline{z}/\overline{R}_h))}d\chi.$$

Applying stationary phase:

$$p(x,y,z,t) \simeq p_1(x,y,z,t)+p_2(x,y,z,t);$$

where

$$p_{1,2}(x,y,z,t) = \frac{-\rho_0 M c_0 \mathsf{sgn}(y)}{(2\pi)^2(M^2-1)}\frac{1}{\overline{R}_h}\int_{-\infty}^{\infty} e^{-i\omega(t-M\overline{x}/c\mp\overline{R}_h/c)}$$
$$\times\mathsf{F}\left(\frac{\omega}{c_0}(M^2-1)^{-1/2}\tan\overline{\theta}_h,\omega\right)d\omega.$$

and we have defined:

$$\overline{R}_h = (\overline{x}^2-\overline{y}^2-\overline{z}^2)^{1/2},$$
$$\tan\overline{\theta}_h = (-\overline{z}/\overline{R}_h).$$

Three-dimensional examples

SINUSOIDAL GUSTS

Dual influences:

Rectilinear normal:

$$f(t-x/U,z) = v_0 e^{i\omega_0(t-x/U)}.$$

Exact pressure:

$$p(x,y,t) = \frac{-\rho_0 M c_0 v_0 \mathsf{sgn}(y)}{(M^2-1)^{1/2}}e^{i\omega_0(t-x/U)}\mathsf{J}_0\left(\frac{\omega_0}{c_0}(\overline{x}^2-\overline{y}^2)^{1/2}\right)$$

Seperable normal delta:

$$f(t-x/U,z) = v_0 e^{i\omega_0(t-x/U)}\delta(z/a)$$

Exact pressure:

$$p(x,y,t) = \frac{-\rho_0 M c_0 v_0 a \mathsf{sgn}(y)}{\pi(M^2-1)}e^{i\omega_0(t-x/U)}\frac{1}{\overline{R}_h}\cos\left(\frac{\omega_0}{c_0}\overline{R}_h\right)$$

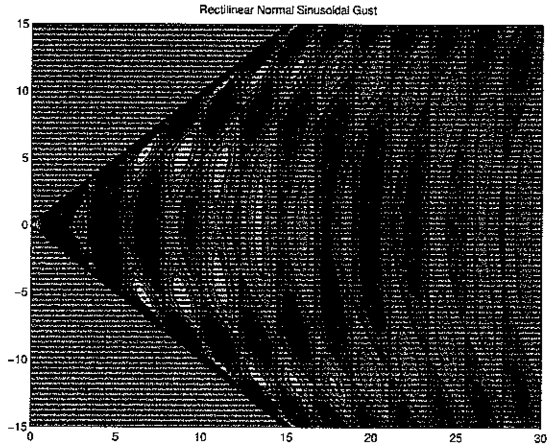

Rectilinear Normal Sinusoidal Gust

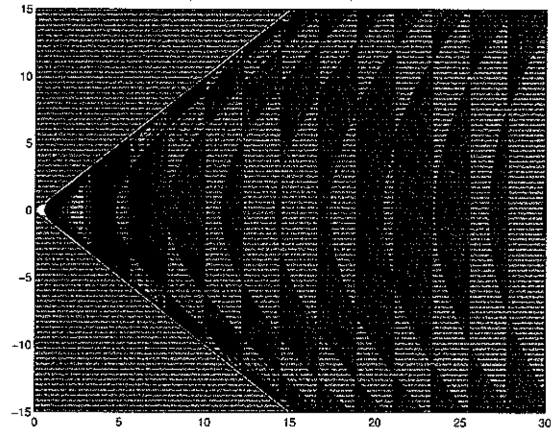

Seperable Normal Sine X Delta in plane Z = 0

8

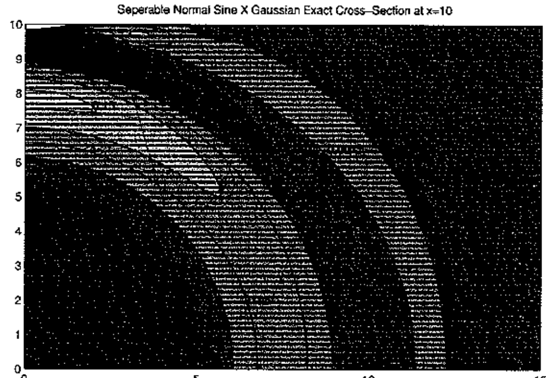

Seperable Normal Sine X Gaussian Exact Cross–Section at x=10

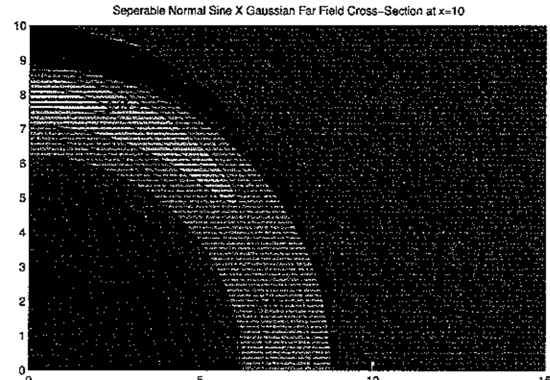

Seperable Normal Sine X Gaussian Far Field Cross–Section at x=10

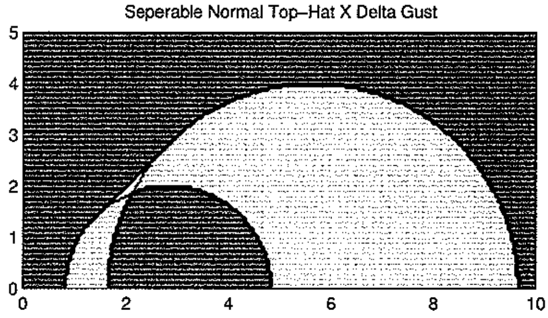
Seperable Normal Top–Hat X Delta Gust
0
1
2
3
4
5
0
2
4
6
8
10

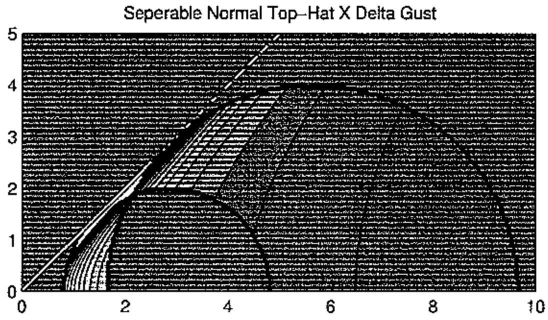
Seperable Normal Top–Hat X Delta Gust
0
1
2
3
4
5
0
2
4
6
8
10

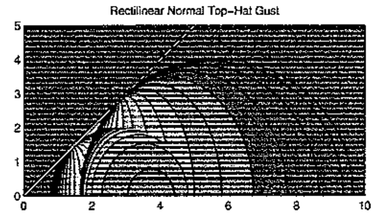
Rectilinear Normal Top–Hat Gust
0
1
2
3
4
5
0
2
4
6
8
10

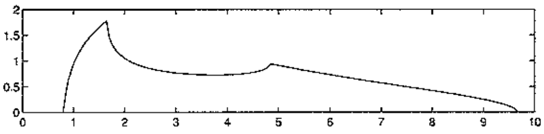
0
0.5
1
1.5
2
0
1
2
3
4
5
6
7
8
9
10

Application of a linearized Euler analysis to fan noise prediction

Dr Ed Envia
NASA

Application of a Linearized Euler Analysis to Fan Noise Prediction

Ed Envia
NASA Glenn Research Center

❑ Rotor-Stator Interaction Tone Noise

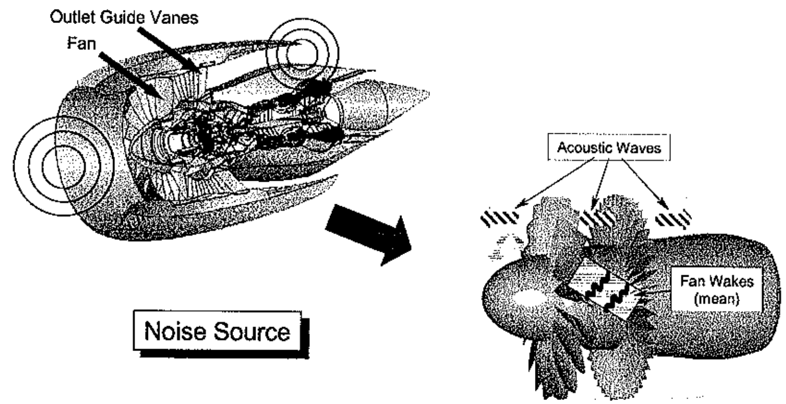

Noise Source

❑ Modeling Strategies

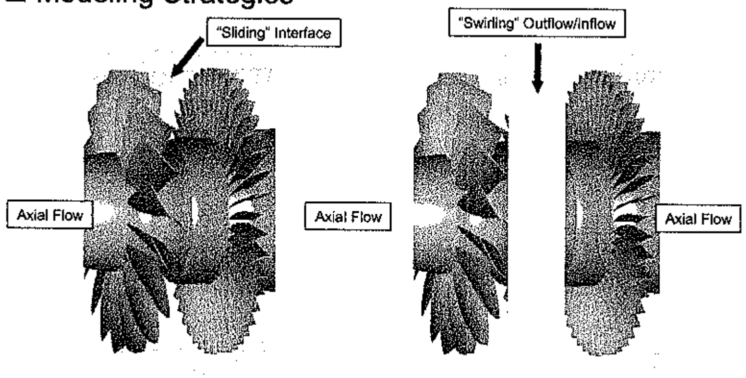

Coupled Blade-Row Computation (Time-Domain)

Isolated Blade-Row Computation (Time- or Frequency-Domain

❑ Approach

- Fan Wake Description: Steady RANS
  - Extract wake harmonic content at OGV leading edge
- OGV Acoustic Response: Linearized Unsteady Euler
  - TURBO (inviscid steady mean flow)
  - LINFLUX* (unsteady perturbations, acoustics)

* Verdon et al. (see NASA/CR-2001-210713)

❑ Technical Challenges

- Turbulence Model, Realistic Wake Diffusion (Grid Orientation)
- Non-Reflecting Boundary Conditions for Non-uniform Inflow/Outflow
- Stringent Computational Accuracy Requirements†

† Acoustic Pressure Perturbations ~0.2% of Background Flow (140 dB = 0.03 psi)

❑ Benchmarking: 2D Cascade

- Flat Plate Cascade Test Problem
- Comparison with Analytic Solutions (on pressure basis)

❑ Validation: Realistic 3D Configurations

- Representative Rotor-Stator Geometries
- Comparison with Duct Mode Measurements (on power basis)

❑ Benchmark: 2D Flat-Plate Cascade (M = 0.65)*

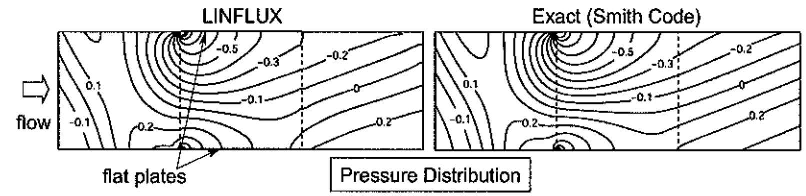

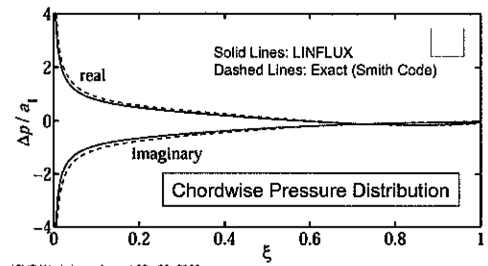

* Prasad & Verdon (see IJA, Vol 1, No. 2

❑ Validation: Advanced Ducted Propulsor (ADP)

- 18 Blades, 45 Vanes
- Design Tip Speed ~ 840 fps
- Comparisons for 2xBPF Tone Levels at 95% Design Tip Speed

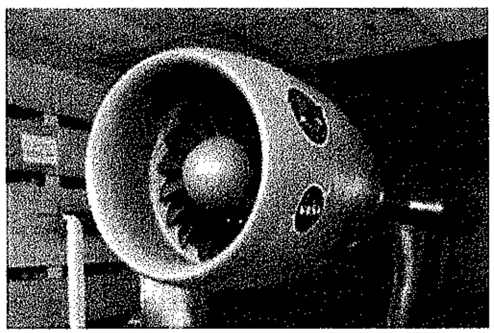

❑ Setup

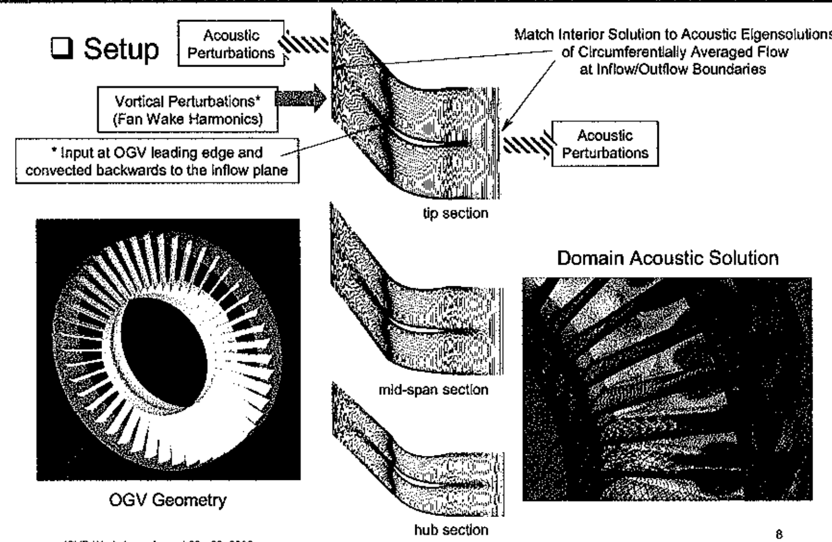

Results: Upstream* of OGV

* No unsteady blade row coupling effects or rotor transmission losses included in the theoretical predictions.

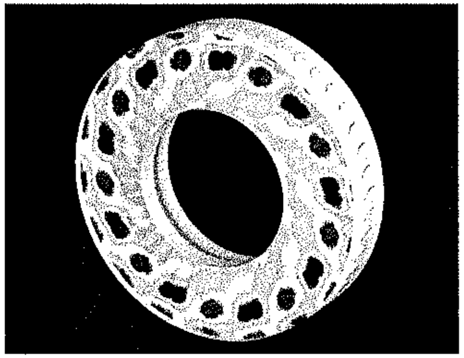

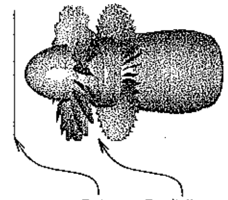

2xBPF Tone Levels		
Mode: (m,n)	Power (dB)	
(-9,0)	109.4	85.2
(-9,1)	110.6	88.9
(-9,2)	114.0	97.3
(-9,3)	101.4	88.7
(-9,4)	---	93.1
Total	116.7	99.7

Results: Downstream of OGV

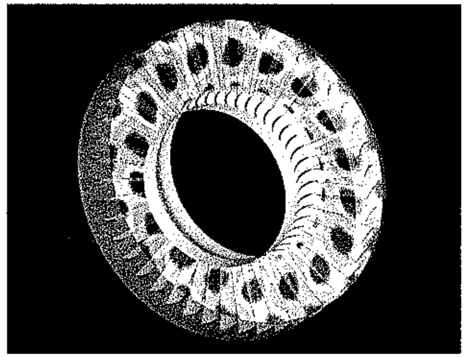

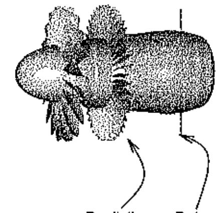

2xBPF Tone Levels		
Mode: (m,n)	Power (dB)	
(-9,0)	122.2	121.9
(-9,1)	121.0	121.2
(-9,2)	118.9	119.1
(-9,3)	110.7	108.9
Total	125.8	125.7

Results: Passage, Blade Row and Wall Pressure Distributions

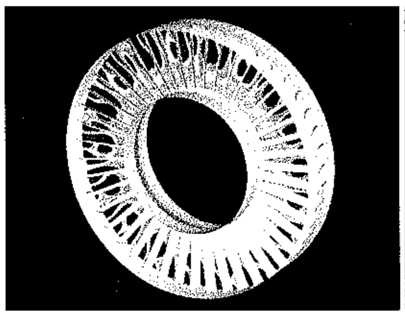

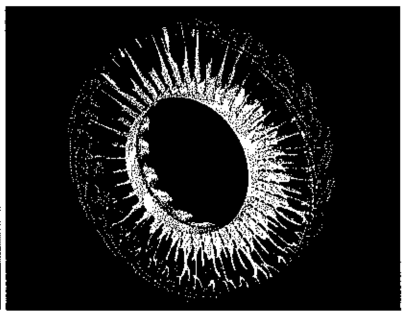

Validation: Source Diagnostic Test (SDT) Fan

- 22 Blades, 54/26 Vanes
- Design Tip Speed ~ 1200 fps
- Comparison for 1x and 2xBPF Tone Levels at 62% Design Tip Speed

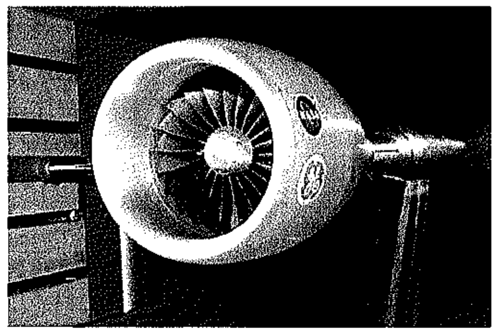

Cut-Off Stator (54-Vanes)

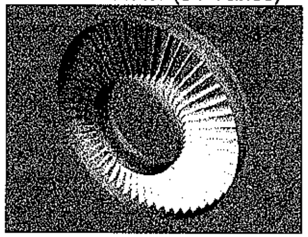

Cut-On Stator (26-Vanes)

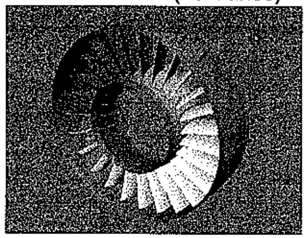

Downstream Tone Levels: Prediction Data

Cut-Off Stator (2xBPF)		Cut-On Stator (1xBPF)	
Mode: (m,n)	Power (dB)	Mode: (m,n)	Power (dB)
(-10,0)	113 114	(-4,0)	124* 127
(-10,1)	100 100	(-4,1)	120* 123
(-10,2)	101 106		
(-10,3)	102 101		
Total	114 115	Total	125* 128

* Meanflow Issues

54-Vane Configuration: Leaned OGV (Straight)

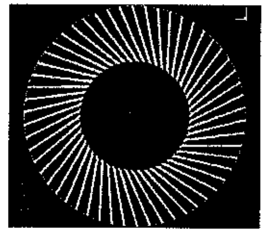

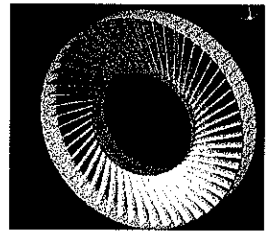

- Summary
  - Poor quality meanflow ("separated" at the hub)
  - Mixed noise reduction benefits predicted at 2xBPF (compared with radial OGV)
  - Expected ~8 dB power level reduction based on prediction from an analytical model

m,n	SPL	Power
(-10,0)	118 111	112 105
(-10,1)	106 116	100 109
Total	118 117	112 111

Radial OGV (Prediction)
Straight Lean OGV (Prediction)

1 dB Reduction Predicted

54-Vane Configuration: Leaned OGV (Composite)

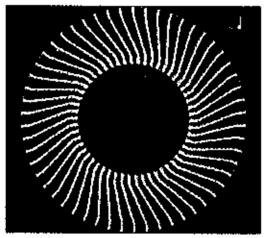

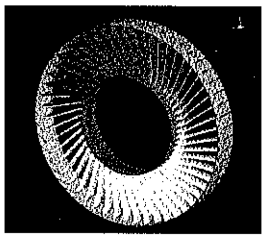

- Summary
  - Good quality meanflow
  - Sizable noise reduction benefits predicted at 2xBPF (compared with radial OGV)

m,n	SPL	Power
(-10,0)	118 111	112 105
(-10,1)	106 105	100 98
Total	118 112	112 106

Radial OGV (Prediction)
Composite Lean (Prediction)

6 dB Reduction Predicted

Conclusions & Issues

- Good quality noise solutions are feasible using linearized methods.
- Robust mean flow solutions are needed for good noise results.
- Inviscid mean flow calculations are problematic for unconventional geometries.
- Do linearized Navier-Stokes methods offer any advantage?
- If so, is rigorous linearization needed or can one do selective linearization?

Aerodynamics and acoustics of cascades in nonuniform flows

Professor Hafiz Atassi
Department of Aerospace & Mechanical Engineering
University of Notre Dame

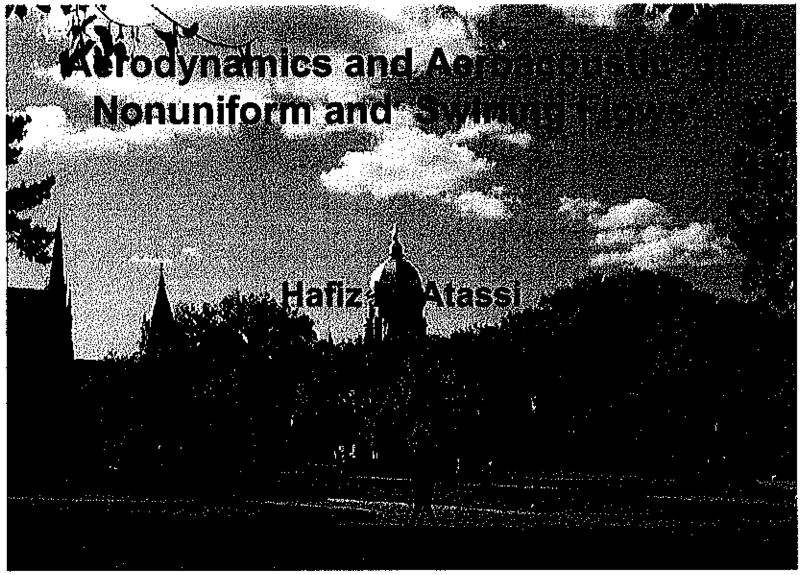

OVERVIEW OF PRESENTATION

- ❖ Issues Associated with Unsteady Nonuniform Flows.
- ❖ Fan Gust Problem: 3D High Frequency Nonuniform Swirling Flow
- ❖ Disturbances in Swirling Flows
- ❖ Normal Mode Analysis and Nonreflecting Boundary Conditions
- ❖ Stability of Swirling Flows
- ❖ High Frequency Formulation
- ❖ Conclusions

Generic Problem
Airfoil in Nonuniform Flow

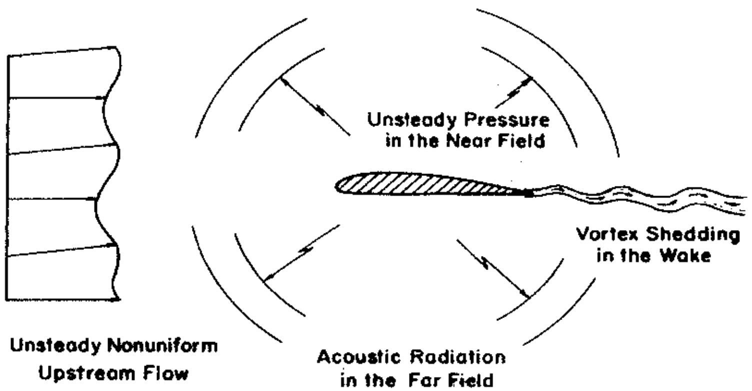

Aeroacoustics and Unsteady Aerodynamics

- ❖ Sound is the far-field signature of the unsteady flow.
- ❖ The aeroacoustic problem is similar to that of forced vibration but with emphasis on the far-field. It is a much more difficult computational problem whose outcome depends on preserving the far-field wave form with minimum dispersion and dissipation.
- ❖ Inflow/outflow nonreflecting boundary conditions must be derived to complete the mathematical formulation as a substitute for physical causality.

Disturbaces in Uniform Flows

Splitting Theorem:

The flow disturbances can be split into distinct potential(acoustic), vortical and entropic modes obeying three independent equation.

- The vortical velocity is solenoidal, purely convected and completely decoupled from the pressure fluctuations.
- The potential (acoustic) velocity is directly related to the pressure fluctuations.
- The entropy is purely convected and only affects the density through the equation of state.
- Coupling between the vortical and potential velocity occurs only along the body surface.
- Upstream conditions can be specified independently for various disturbances.

Equations for Linear Aerodynamics

- **Vortical Mode:** $\vec{u}_v = \vec{u}_\infty(\vec{x} - \vec{U}t)$
  - **Harmonic Component**

$$\vec{u}_g = \vec{a} e^{i(\vec{k}\cdot\vec{x} - \omega t)}$$

- **Potential Mode:**

$$\left(\frac{1}{c_0^2}\frac{D_0^2}{Dt^2} - \nabla^2\right)\phi = 0$$

- **Boundary Conditions:** impermeability along blade surface, Kutta condition at trailing edge, allow for wake shedding in response to gust.

Issues Associated with Nonuniform Flows

- The Kutta Condition.
- Linear vs Nonlinear Analysis: Uniform mean flow, RDT, Fully Nonlinear.
- Gust Description: Can we consider separately acoustic, vortical and entropic disturbances?
- What are the boundary conditions to be specified?
- What are the conditions for flow instability?
- What are transonic flow effects?
- Conservation relations for acoustic intensity and power?
- Turbulence modification.
- High Frequency.

Vortex Tavelling around an airfoil

Linear Theory

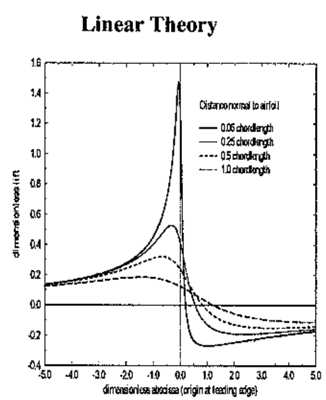

Comparison Between Theory and Computation.
Surface Pressure Induced By the Motion of a Vortex Near the Trailing-Edge

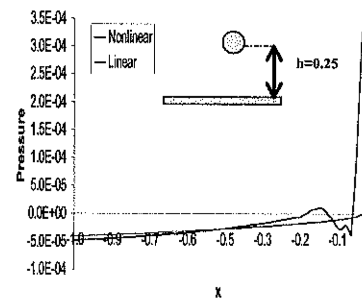

Vortex in a Strongly Nonuniform Flow at Low Mach Number

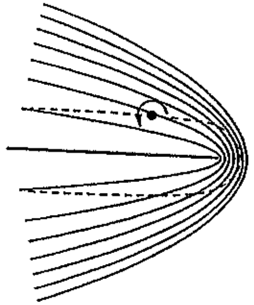

As the vortex travels near the trailing edge it is no longer convected by the mean flow. Its trajectory crosses the undisturbed mean flow. This increases the amount of fluid energy converted into acoustic energy. The acoustic power scales with M^3, much higher than that predicted by a dipole (M^6).

Cascade Flow with local Regions of Strong Interaction

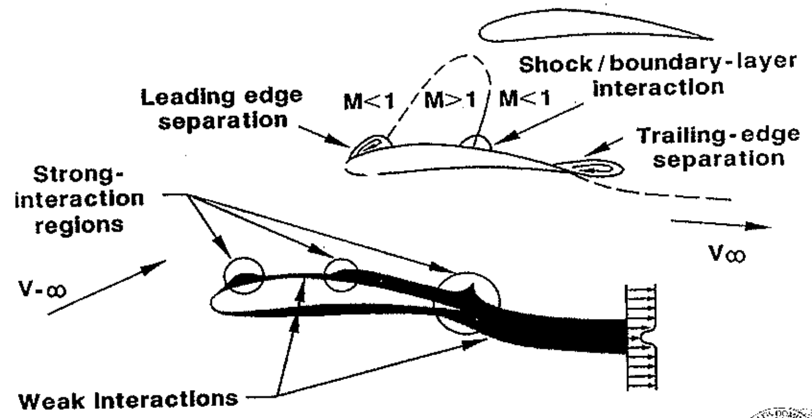

Cascade of Airfoils in a Three-Dimensional Gust Rapid Distortion Approximation

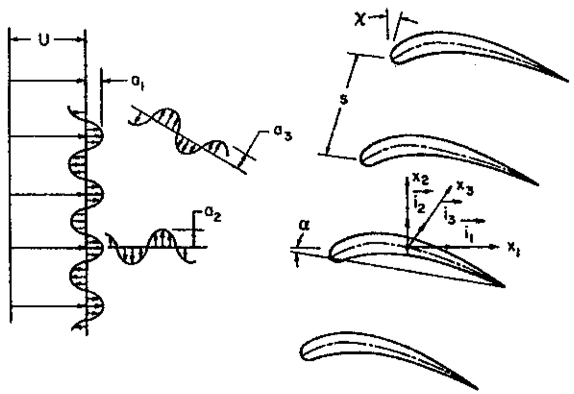

VORTEX STRETCHING AT THE STAGNATION POINT

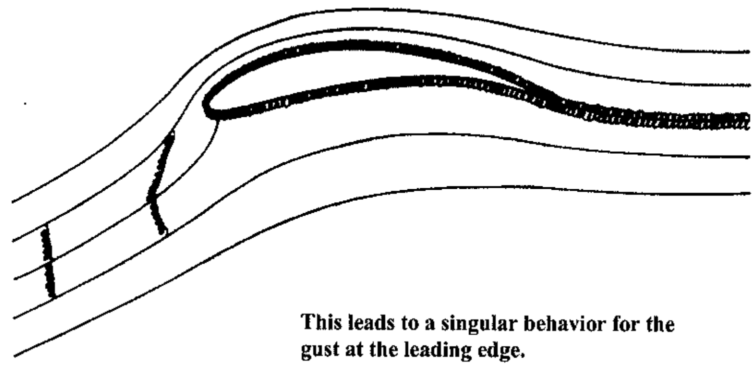

This leads to a singular behavior for the gust at the leading edge.

HIGH SPEED COMPRESSOR CASCADE

Surface Mach Number Distributions
—— Potential, – – –– Euler

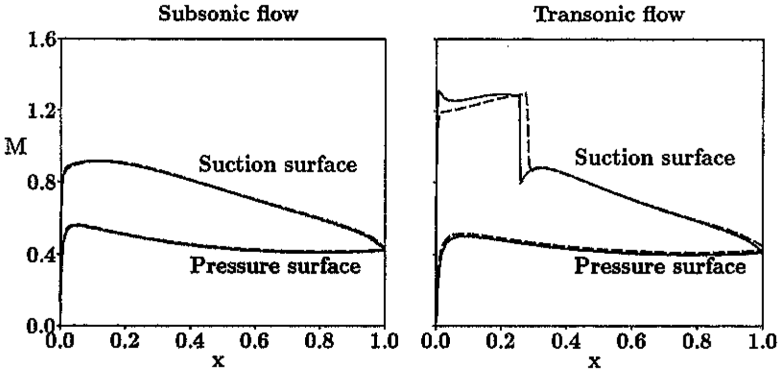

Cascade with modified NACA 0006 with a circular arc camber line, spacin=1, stagger=45°.

Comparison between Linear and Nonlinear Analyses for Subsonic Flows

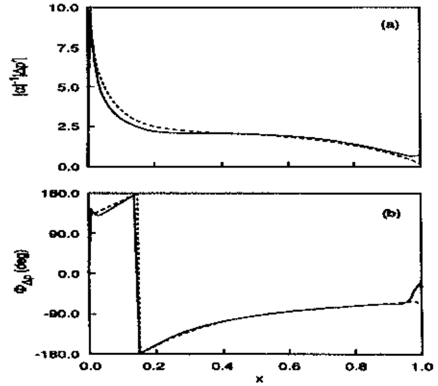

Magnitude (a) and Phase (b) of the first Harmonic Unsteady Pressure Difference Distribution for the subsonic Cascade Underhoing an In-Phase Torsional Oscillation of Amplitude a=2o at k1=0.5 about Midchord; M=0.7; _____ , Linear Analysis; ......, Nonlinear Analysis.

Comparison between Linear and Nonlinear Analyses for Transonic Flows

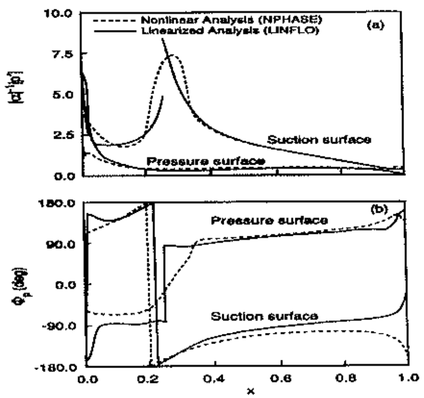

Magnitude (a) and Phase (b) of the first Harmonic Unsteady Pressure Difference Distribution for the Supersonic Cascade Undergoing an In-Phase Torsional Oscillation of Amplitude a=2° at k1=0.5 about Midchord; M=0.8.

Summary

- ❖ RDT unsteady analysis yields good results for subsonic flows.
- ❖ RDT unsteady analysis is adequate for transonic flows with local Mach number not exceeding 1.3.
- ❖ Strong nonlinear effects resulting from shock boundary layer interaction are significant as the local Mach number exceeds 1.3-1.4.

Response of a Loaded Linear Cascade to a Gust

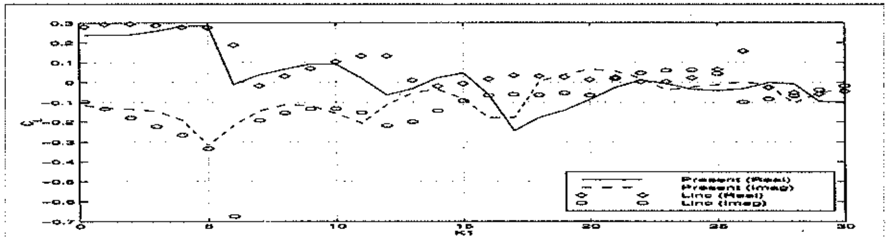

Figure 11: Real and imaginary parts of the unsteady lift versus the reduced frequency k_1 for a cascade of NACA 4406 blades ($\chi = 35°$, $\frac{s}{c} = 1.0$, $M_\infty = 0.3$, $k_2 = 0$)

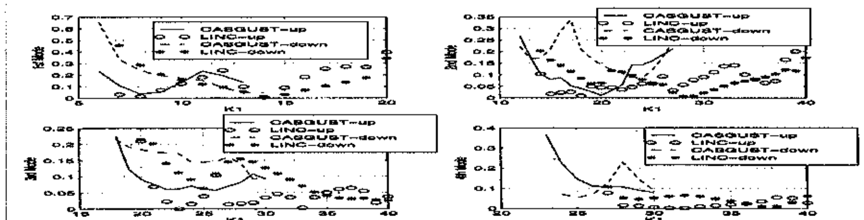

Figure 12: The first four modes of the sound radiated from a cascade of NACA 4406 blades ($\chi = 35°$, $\frac{s}{c} = 1.0$, $M_\infty = 0.3$, $k_2 = 0$)

Unsteady Pressure Field of a Loaded k_1=8.5

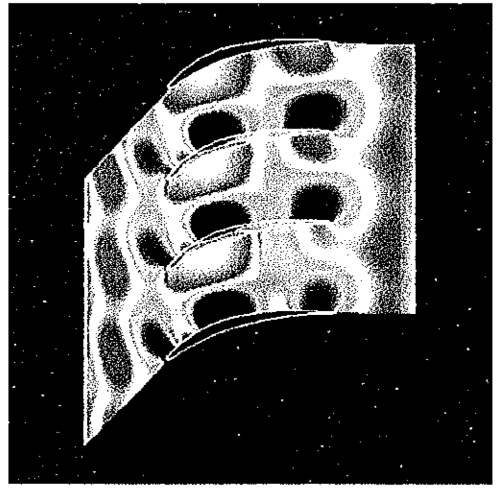

Acoustic Pressure for Second Mode in Response to a Transverse Gust, M=0.8, (a) upstream, (b) Downstream

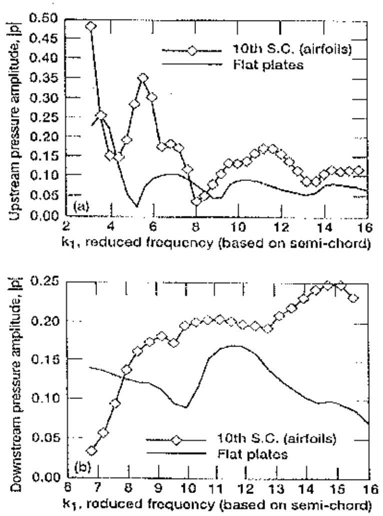

Summary of Results for A Loaded Cascade

- Cascade effects such as blade interference which depends on the spacing ratio, and stagger have strong influence on the aerodynamic and acoustic cascade response, particularly at low frequency.
- At high frequency the cascade response is dominated by the acoustic modes cut-on phenomena.
- For thin blades, the leading edge dominates the aerodynamic pressure and noise generation.
- For loaded blades at high Mach number, large unsteady pressure excitations spread along the blade surface with concentration near the zone of transonic velocity.
- Blade loading changes the upstream and downstream flows and thus affects the number and intensity of the scattered sound.

3D Effects
Swirling Flow in a Fan

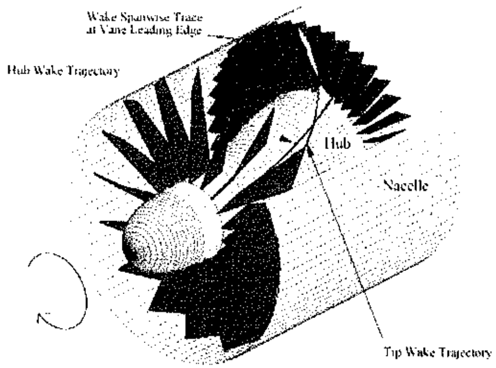

Scaling Analysis

- Multiple length scales:
  - Duct hub and tip Radii: Rah, Rat, Rotor/stator spacing: L
  - Chord length c, Blade spacing s=2pR/(B or V)
  - Turbulence Integral Scale = $\Lambda << c << R$
- Multiple Frequency Parameters:

$$\frac{\omega R}{c_0} = \frac{B \Omega R}{c_0} = BM_\theta >> 1 \qquad \frac{\omega \Lambda}{U_x} = \left(\frac{B\Lambda}{R}\right)\left(\frac{U_s}{U_x}\right) = O(1)$$

- Fast Variables: $\tilde{\vec{x}} = \frac{\vec{x}}{\Lambda}$
- Slow Variables: $\vec{x}^* = \frac{\vec{x}}{R}$

Blade passing frequency BPF=BΩ

Scaling Analysis

- Acoustic phenomena:
  - Acoustic frequency: nB Ω
  - Rossby number = $\frac{nB\,\Omega\,r_t}{c_0} >> 1$
- Convected Disturbances:
  - Convection Frequency ~ Shaft Frequency Ω
  - Rossby number = $\frac{\Omega r_t}{U_x} \approx O(1)$
  - Wakes are distorted as they convect at different velocity. Centrifugal accelerations create force imbalance which modifies amplitude and phase and may cause hydrodynamic instability.

Aerodynamic and Acoustic Blade Response

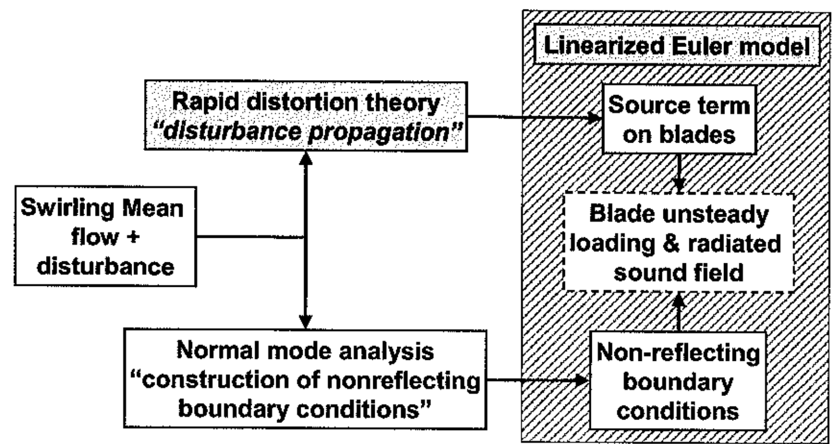

Mathematical Formulation

- Linearized Euler equations

$$\boxed{\vec{V}(\vec{x},t) = \vec{U}(\vec{x}) + \vec{u}(\vec{x},t)}$$

- Axisymmetric swirling mean flow

$$\boxed{\vec{U}(\vec{x}) = U_x(x,r)\vec{e}_x + U_s(x,r)\vec{e}_\theta}$$

- Mean flow is obtained from data or computation
- For analysis the swirl velocity is taken

$$\boxed{U_s = \Omega r + \frac{\Gamma}{r}}$$

- The stagnation enthalpy, entropy, velocity and vorticity are related by Crocco's equation

$$\boxed{\nabla H = T\nabla S + \mathbf{U}\times\zeta}$$

Normal Mode Analysis

Normal Mode Analysis

- A normal mode analysis of linearized Euler equations is carried out assuming solutions of the form

$$\boxed{f(r)e^{i(-\omega\, t + m_v\theta + k_{mn}x)}}$$

- Eigenvalue problem is not a Sturm-Liouville type and singular for vanishing

$$\Lambda_{mn} = \frac{D_0}{Dt} = -\omega + k_{mn}U_x + \frac{mU_s}{r}$$

- A combination of spectral and shooting methods is used in solving this problem
  - Spectral method produces spurious acoustic modes
  - Shooting method is used to eliminate the spurious modes and to increase the accuracy of the acoustic modes

Mode Spectrum
Spectral and Shooting Methods

M_x=0.55, M_Γ=0.24, M_Ω=0.21, ω=16, and m=-1

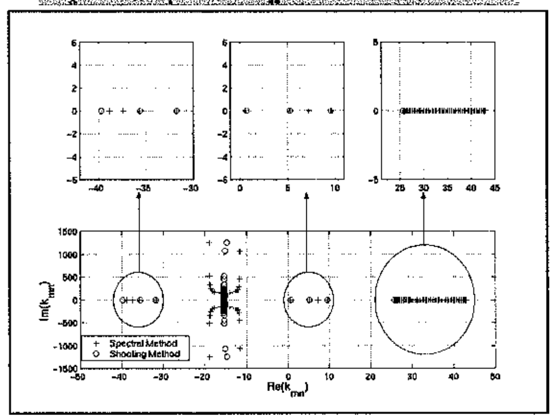

Pressure Content of Acoustic and Vortical Modes

M_x=0.5, M_Γ=0.2, M_Ω=0.2, ω=2π, and m=-1

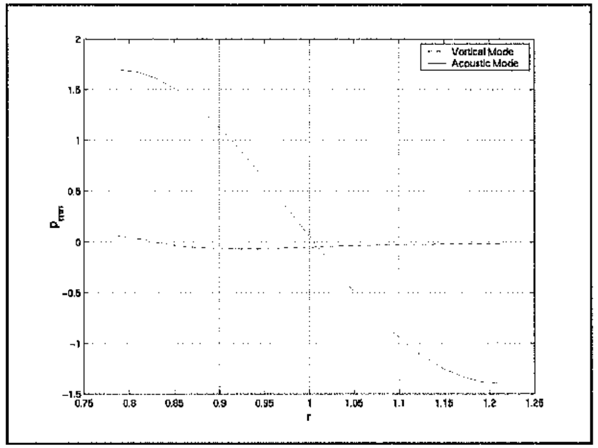

Effect of Swirl on Eigenmode Distribution

M_{xm}=0.56, M_Γ=0.25, M_Ω=0.21

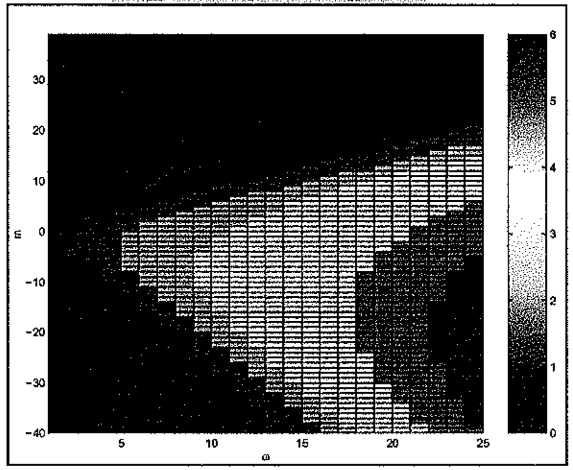

Nonreflecting Boundary Conditions

❖ Accurate nonreflecting boundary conditions are necessary for computational aeroacoustics

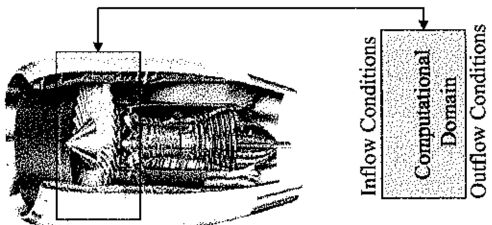

Quieting the skies: engine noise reduction for subsonic aircraft
Advanced subsonic technology program, NASA Lewis research center, Cleveland, Ohio

Formulation

❖ Presssure at the boundaries is expanded in terms of the acoustic eigenmodes.

$$p(\vec{x},t)=\int_{\omega}\sum_{\nu=-\infty}^{\infty}\sum_{n=0}^{\infty}c_{mn}p_{mn}(\omega,r)e^{i(-\omega t+m_\nu\theta+k_{mn}x)}d\omega$$

❖ Only outgoing modes are used in the expansion.
❖ Group velocity is used to determine outgoing modes.

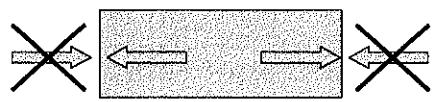

Causality

Nonreflecting Boundary Conditions (Cont.)

$$p(\vec{x},t) = \sum_{\nu=-M/2}^{M/2} \sum_{n=0}^{N} c_{mn}\, p_{mn}(r)\, e^{i(-\omega t + m_\nu \theta + k_{mn} x)} \Rightarrow [p] = [\Re][c]$$

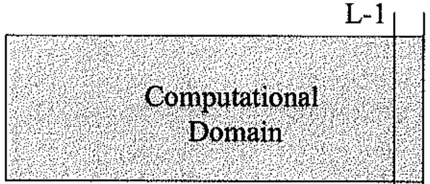

$$[p]_{L-1} = [\Re]_{L-1}[c] \qquad [p]_L = [\Re]_L[c]$$

$$[p]_L = [\Re]_L [\Re]_{L-1}^{-1} [p]_{L-1}$$

Summary of Normal Mode Analysis

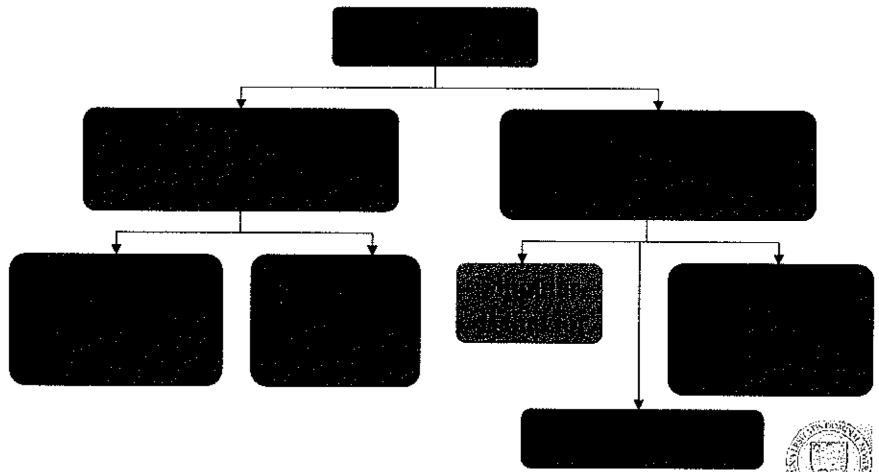

Stability of Swirling Flows

Rayleigh Criterion

- ❖ A necessary and sufficient condition for the stability of axisymmetric disturbances of incompressible rotating flows is:

$$\phi = \lambda^2 = \frac{1}{r^3 U_x^2} \frac{\partial (rU_\theta)^2}{\partial r} \geq 0$$

- ❖ This is *not* generally valid for non-axisymmetric disturbances and compressible flows. However, λ^2 is an important parameter for swirling flow stability analysis.

Inviscid Stability Analysis

❖ Analytical: Instability is possible.

❖ Numerical:

- Effect of λ^2
  - ❑ $\lambda^2 > 0$ Stable
  - ❑ $\lambda^2 \le 0$ Generally unstable
- Increasing m stabilizes the flow.
- Mean flow entropy gradient destabilizes the flow.

Mode Spectrum-Effect of λ^2

M_x=0.3676, ω=7.3529, m=1, r_h/r_t=0.6

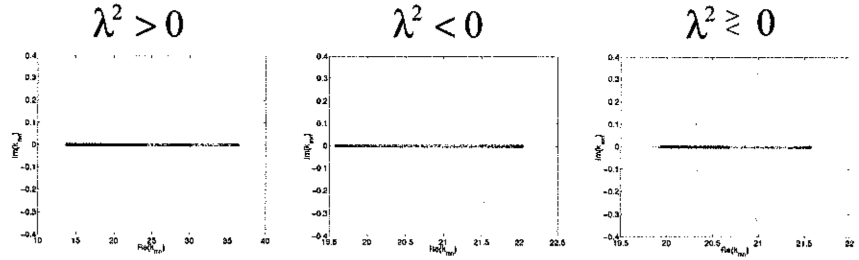

	$\lambda^2 > 0$	$\lambda^2 < 0$	$\lambda^2 \gtrless 0$
M_Γ	0.2206	-0.2206	-0.2206
M_Ω	0.2206	0.0735	0.2206

Other Factors Affecting Stability

❖ Accelerating flows

- Mean flow axial acceleration is stabilizing.
- Mean flow swirl axial variation may be destabilizing.

❖ Viscous effects

- Small scales are most affected by viscosity.
- For large modal number *m (equivalent to wave-number)*, viscous effects are large.

Vortical Disturbances

Wake Distortion by Swirl

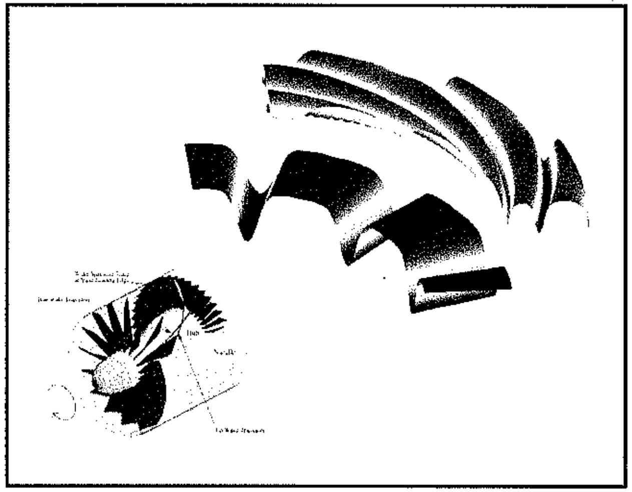

Effect of Swirl and Viscosity on Axial Wake Defect Evolution

$$U(x,r) = 85\, e_x + \frac{50}{r} e_\theta,\ Re_{effective} = 10{,}000$$

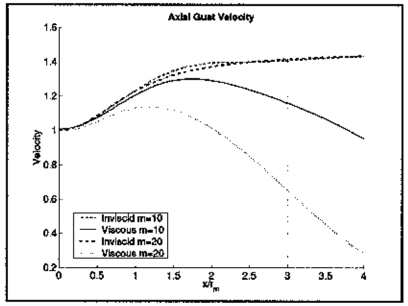

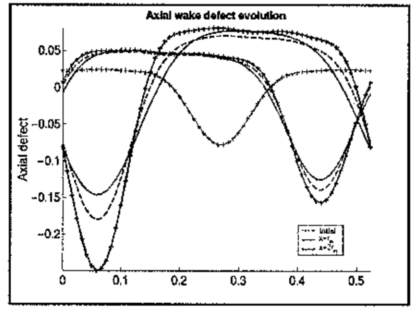

$$\text{Damping} \equiv \chi \approx O\left(\exp\left(-\frac{m^2}{Re_{effective}\, r^2} x\right)\right)$$

Effect of Free-Vortex Swirl on One-Dimensional Spectra for Turbulence Velocity

$r_t/t_h = 1.5$, $U_s^{(m)}/U_x = 1.0$

Radial Velocity

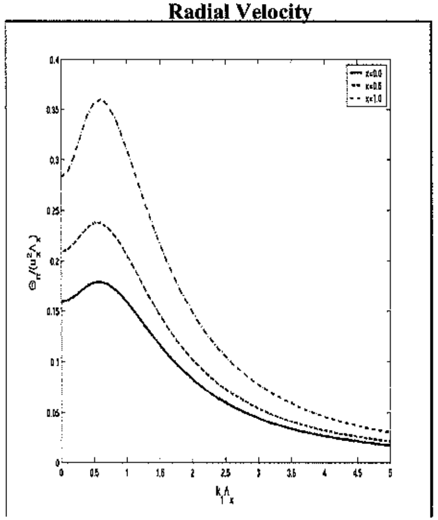

Cross Axial-Radial Velocity

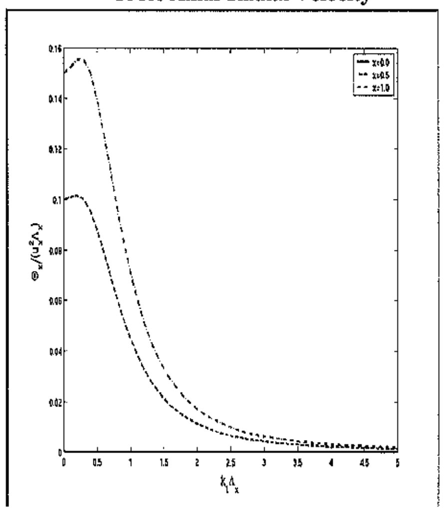

Formulation of the Blade Response Problem

- ❖ **Primitive Variable**
  - ❖ Pseudo-time, 2nd order accurate Lax-Wendroff scheme
  - ❖ Compact Fourth Order Scheme

4 or 5 equations to solve

No help from high frequency

- ❖ **Velocity Splitting**
  - ❖ Low frequency: 4 or 5 equations to solve
  - ❖ High Frequency: Coupling is weak between wave equation and convected equations

Mathematical Formulation
Splitting Velocity Approach

$$\boxed{\mathbf{u} = \mathbf{u}^R + \nabla\phi}$$

$$\boxed{p' = -\rho_o \frac{D_o\phi}{Dt} \quad \text{where} \quad \frac{D_o}{Dt} = \frac{\partial}{\partial t} + \mathbf{U}_o \cdot \nabla}$$

$$\frac{D_o}{Dt}\frac{1}{c_o^2}\frac{D_o\phi}{Dt} - \frac{1}{\rho_o}\nabla\cdot(\rho_o\nabla\phi) = \frac{1}{\rho_o}\nabla\cdot(\rho_o\vec{u}^R) - \frac{\partial s'/\partial t}{2c_p}$$

$$\frac{D_o\vec{u}^R}{Dt} + (\vec{u}^R\cdot\nabla)\vec{U} = -(\nabla\times\vec{U})\times\nabla\phi - \frac{D_o\phi}{Dt}\frac{\nabla s_o}{c_p}$$

$$\frac{D_o S'}{Dt} + (\vec{u}'\cdot\nabla)s_o = 0$$

Domain Decomposition
Inner and Outer Regions

Vorticity and pressure are weakly coupled over a large distance yielding significant effects. Solution is simplified by removing phase.	Vorticity and pressure are weakly coupled over a short distance with small Effects.
O(R)	O(c)

Conclusions

- The TE flow condition strongly affects the level of radiated sound.
- Blade loading effects are significant and more so at higher M and at high frequency affect the acoustics more than the aerodynamics. They also change the cuton/cutoff conditions.
- 3D resonance conditions are much smoother than predicted by 2D theories.
- Entropy has destabilizing effects on the flow.
- Swirl modifies the blade upwash and turbulence energy spectra. It also affects the duct impedance and number of cut-on modes. The spinning modes are not symmetric.

Aerodynamic and acoustic response of an annular cascade in swirling flows

Mr Basman Elhadidi
Department of Aerospace & Mechanical Engineering
University of Notre Dame

Aerodynamic and Acoustic Response of An Annular Cascade in Swirling Flows

Basman Elhadidi
University of Notre Dame,
Notre Dame, Indiana, 46556

Overview

- Modeling unsteady blade loading and sound generation in swirling flows
  - High frequency
  - High-bypass engines

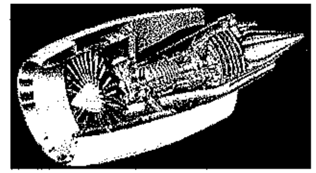

- Investigate effects of cascade geometry
  - Stagger, twist, lean, sweep and blade loading
- Investigate effect of swirling flow on up-wash modification
- Computationally efficient scheme for broadband calculations

Fan Noise Sources

- Inflow distortions
  - Boundary layers and ingested turbulence
- Fan wake interaction with vanes
  - Tonal noise
  - Broadband noise

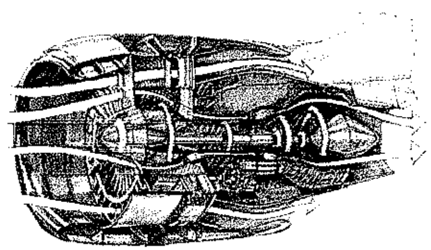

Aerodynamic Model

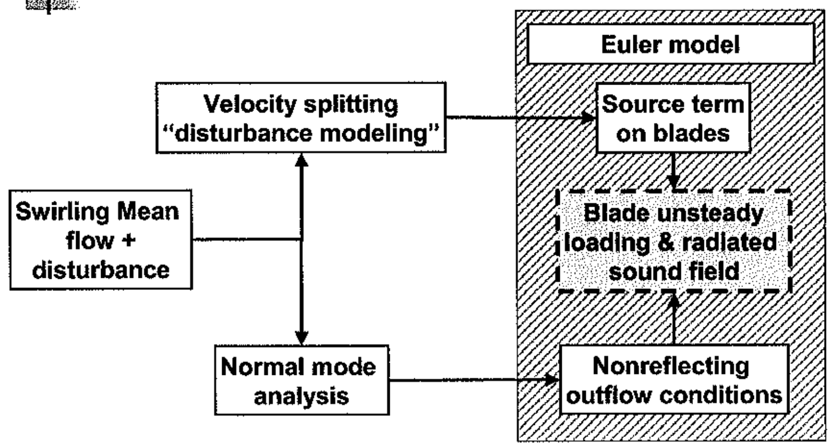

Frequency Domain Euler Models

Velocity Splitting - Primitive Variables	

▪ 3 hyperbolic equations
▪ 1 elliptic equation
  ▪ Solves for potential, minimum dispersion and dissipation
  ▪ Coupling decreases as frequency increases
▪ Computationally efficient
	▪ 4 hyperbolic equations
	  ▪ Some dispersion and dissipation errors
	  ▪ Equations remain coupled at all frequencies
	▪ Computationally expensive

Theoretical Model

- Linearize flow variables about a steady, non-heat conducting, isentropic, inviscid flow

$$\boxed{\begin{aligned} U(x,r,\theta,t) &= U_o(x,r,\theta)+u'(x,r,\theta,t) \\ p(x,r,\theta,t) &= p_o(x,r,\theta)+p(x,r,\theta,t) \end{aligned}}$$

- For simplicity, present results are for constant enthalpy and entropy with
  - Model 1 for unloaded blades: $\boxed{U_\theta(r)=\frac{\Gamma}{r}+\Omega r}$
  - Model 2: Quasi-three dimensional
- Splitting unsteady velocity

$$\boxed{\mathbf{u}'=\mathbf{u}^R+\nabla\phi}$$

Theoretical Model - Continue

- Linearized Euler

$$\boxed{\begin{aligned} &\frac{D_o\mathbf{u}^R}{Dt}+\left(\mathbf{u}^R\cdot\nabla\right)U=-(\nabla\times U)\times\nabla\phi \\ &\frac{D_o}{Dt}\frac{1}{c_o^2}\frac{D_o\phi}{Dt}-\frac{1}{\rho_o}\nabla\cdot(\rho_o\nabla\phi)=\frac{1}{\rho_o}\nabla\cdot\left(\rho_o\mathbf{u}^R\right) \end{aligned}}$$

- With

$$\boxed{p'=-\rho_o\frac{D_o\phi}{Dt} \quad \text{where} \quad \frac{D_o}{Dt}=\frac{\partial}{\partial t}+\mathbf{U}_o\cdot\nabla}$$

- High frequency analysis predicts weak coupling
- Normal mode analysis predicts two sets of solutions
  - Nearly convected : Little or no pressure
  - Nearly acoustic : Contains most of the pressure, are used to generate the non-reflecting outflow conditions
- Up-wash is determined from an initial-value analysis

Computational Domain

B (rotor blades)	16
V (stator blades)	24
C (chord)	2π/V
r_{tip}	1
L (length)	3c

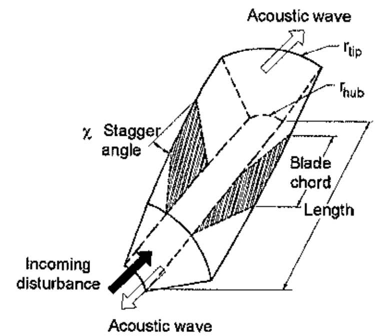

Initial Conditions

- Incident gust is represented as at x_o

$$\mathbf{u}(x_o, r, \theta, t) = \int_\omega \sum_{m'=-\infty}^{\infty} \sum_{n'=0}^{\infty} \mathbf{a}_{m'n'} e^{i\left(\alpha x_o + m'\theta - 2\pi m' \frac{r - r_{hub}}{r_{tip} - r_{hub}} - \omega t\right)} d\omega$$
$$\mathbf{a}_{m'n'} = \left(a_x^{(m'n')}, a_r^{(m'n')}, a_\theta^{(m'n')}\right)$$
$$\alpha = \frac{\omega - m' U_\theta / r}{U_x}$$

  - For high frequency, to leading order $\nabla \bullet \mathbf{u} = 0$
  - $a_{m'n'}$: gust in Fourier frequency domain. It is chosen such that the normal incident up-wash is unity at incidence
  - m' : pB , $\omega = pB\Omega$, Ω : Shaft speed, B : Rotor blades

Acoustic Pressure Intensity

- Solution at outflow is assumed as sum of outwardly modes, based on the group velocity

$$\phi = \sum_{m \in S_m} \sum_{n=1}^{N_r} c_{mn} \Phi_{mn}(r) e^{i(k_{mn} x + m\theta)}$$

- c_{mn} is defined as the acoustic pressure intensity

Uniform Flow
Unloaded Blades

Benchmark Test Problem
Uniform Flow – Full Annulus

r_{tip}/r_{hub}	1.0/0.5
$\omega^* = \omega r_m / c_o$	9.396
M_{tip}	0.783
M	0.5
Stagger	0°

Comparison with lifting surface (Schulten)

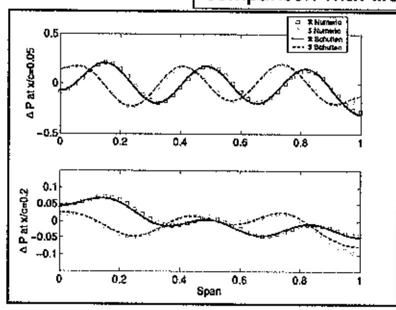

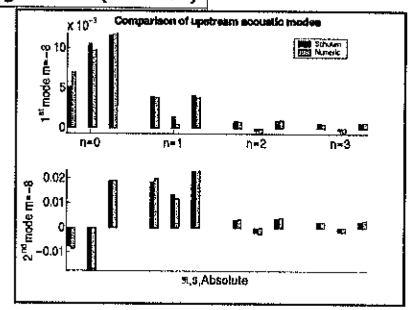

How Accurate is Strip – Analysis?

- Strip-analysis is <u>only</u> suitable for:
  - Low tip-hub ratios
  - Low frequency

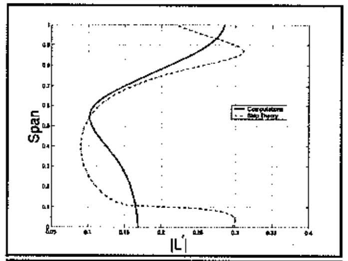

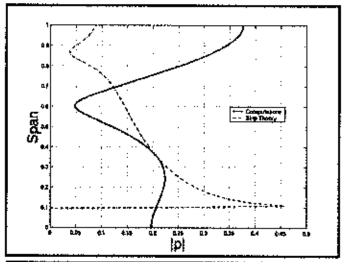

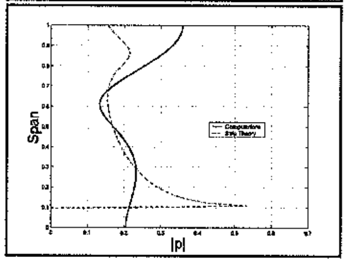

Results by Amr Ali

Swirling Flow
Unloaded Blades

Test Problem
Narrow Annulus Limit – Swirling Flow

r_{tip}/r_{hub}	1.0/0.98
ω	6.5π
M	0.5
Stagger	45°

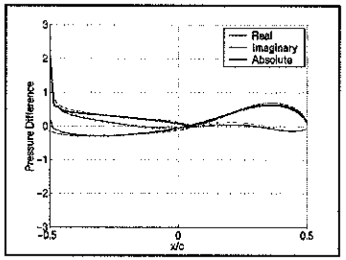

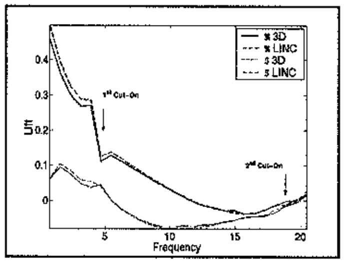

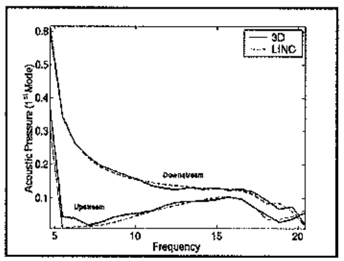

Test Problem
Full Annulus – Swirling Flow

- Comparison with a primitive variable code developed by Amr Ali
- Discrepancy in acoustic intensity of the order of 10% for first and second mode

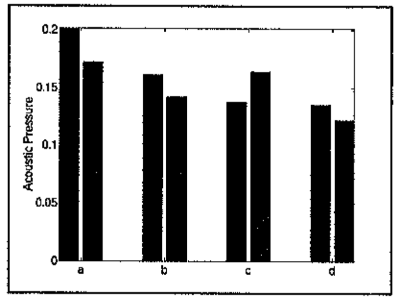

Case	a	b	c	d
	M_{xm}=0.41 M_θ=0.	M_{xm}=0.35 M_θ=0.2/r	M_{xm}=0.35 M_θ=0.2r	M_{xm}=0.35 M_θ=0.1r+0.1/r

Solver Characteristics – Full Annulus

$$\frac{D_o \mathbf{u}^R}{Dt} + (\mathbf{u}^R \cdot \nabla)\mathbf{U} = -(\nabla \times \mathbf{U}) \times \nabla\phi \quad \& \quad \frac{D_o}{Dt}\frac{1}{c_o^2}\frac{D_o\phi}{Dt} - \frac{1}{\rho_o}\nabla \cdot (\rho_o \nabla\phi) = \frac{1}{\rho_o}\nabla \cdot (\rho_o \mathbf{u}^R)$$

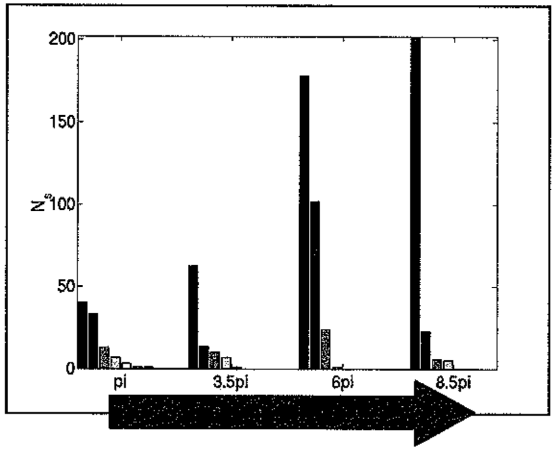

- N_s : number of iterations of iterative solver.
- N_c : number of coupling iterations between the wave and convection equation.

Solver Characteristics
Comparison of Successive Iterations

r_{tip}/r_{hub}	1.25/0.75
ω	3.5π
M_{xm}	0.36
M_θ	0.18r+0.18/r
Stagger	45°

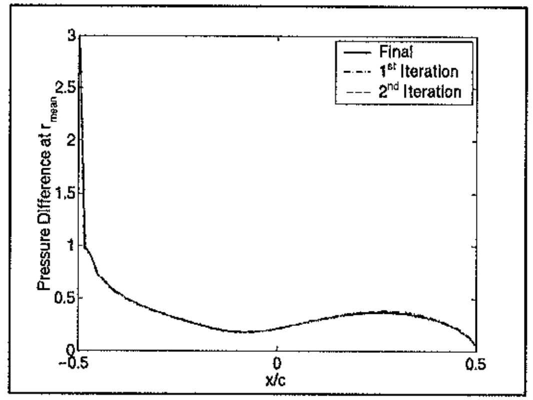

Effect of Blade Twist

r_{tip}/r_{hub}	1.25/0.75
ω	3.5π
M_{xm}	0.36
Stagger	45°

- Blade twist is crucial to avoid separation
- For present tip-hub ratio and initial conditions unsteady lift is higher
  - At hub for positive twist
  - At tip for negative twist (free vortex)

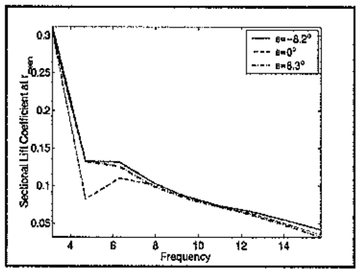

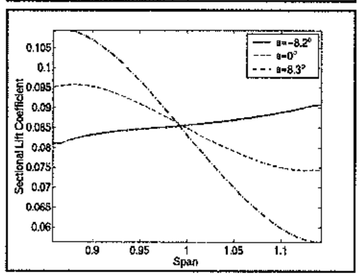

Effect of Blade Twist

- Blade twist effects are truly high frequency effects
  - First propagating mode is unaffected by blade twist
  - Second propagating mode is strongly affected by blade twist (higher frequency)

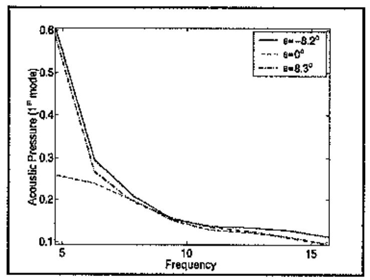

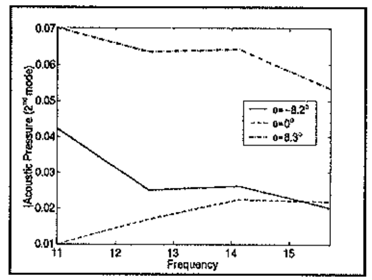

Three – Dimensional Incident Gust

- n′ increases spanwise phase variations
  - Reduces unsteady lift
  - 1st mode dominant for low frequency and n′=0
  - 2nd mode dominant for high frequency and n′=1

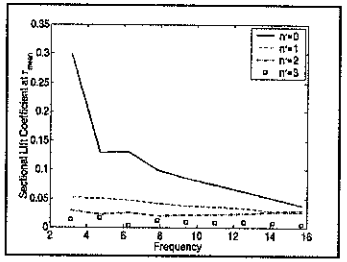

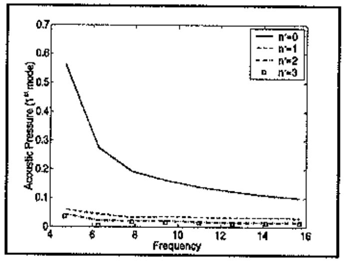

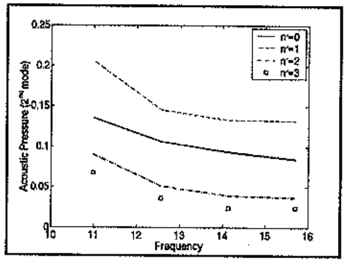

Swirl Up-wash Modification

- Gust up-wash is modified by swirl
- Domain decomposition is essential to model wake propagation over large distances
  - An asymptotic analysis is used to obtain the modified up-wash

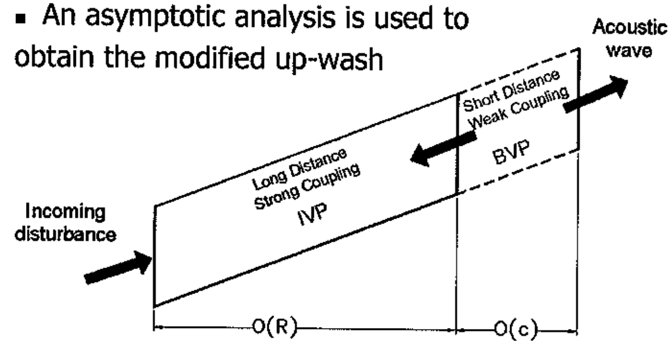

Swirl Up-wash Modification

- Swirl modifies the up-wash introducing spanwise phase variations and wake widening
- Similar effect to introducing n′
- This is an effect of swirl alone, not lean or sweep

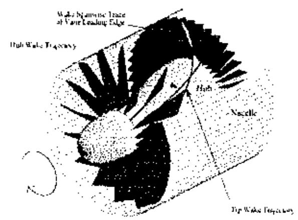

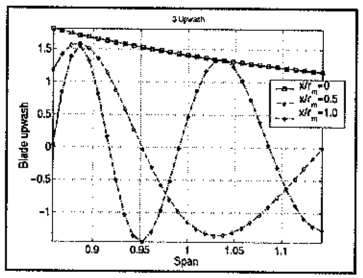

Swirl Up-Wash Modification

- Downstream sound intensity is greatly reduced
- Unsteady lift is reduced

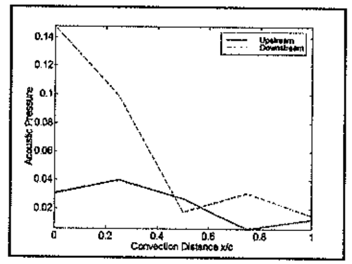

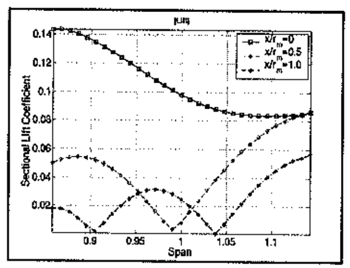

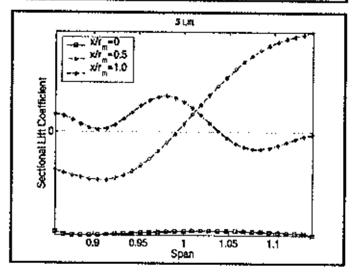

Swirling Flow
Loaded Blades

Test Problem
Narrow Annulus Limit – Swirling Flow

r_{tip}/r_{hub}	1.0/0.98
M_{∞}	0.3
Stagger	45°
Turning	11.76°

- Case of cambered thin blades to examine the effects of mean-flow turning and blade loading
- Comparison with 2D computational code CASGUST (Fang and Atassi)

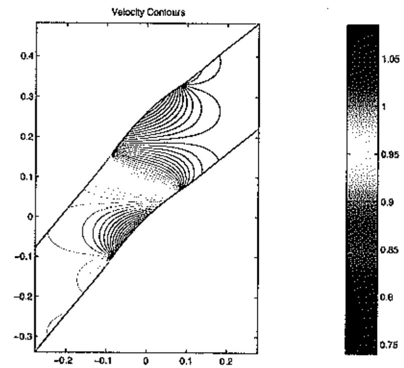

Pressure Difference

- Acoustic intensity is comparable with differences in the order of 10%
- Discrepancy between both numerical codes is considerable close to cut-on/cut-off conditions

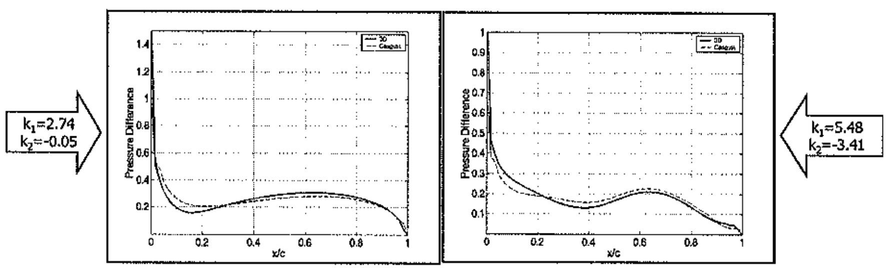

Narrow Annulus Limit
Effect of Blade Turning

- As turning increases, lift becomes smoother
  - Different cut-on/cut-off for upstream and downstream
- Acoustic pressure intensity of same order

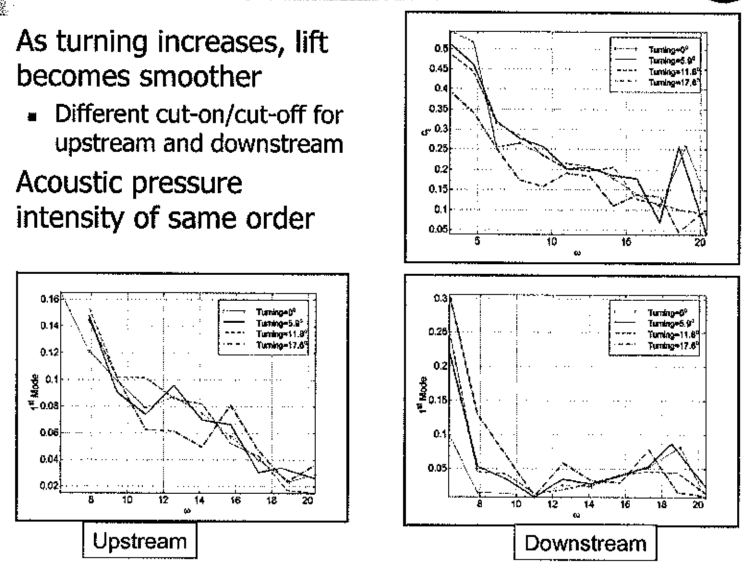

Full Annulus (Preliminary)

- Case of loaded three-dimensional blade with constant camber/chord

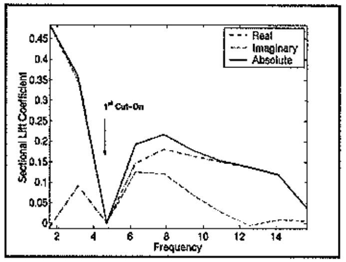

r_{tip}/r_{hub}	1.25/0.75
M_∞	0.3
Stagger (constant)	45°
Camber/Chord	0.05

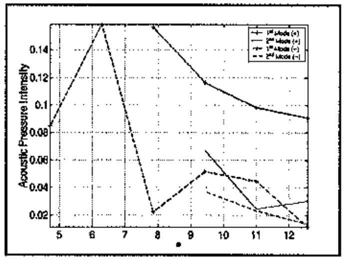

Modeling Errors and Simplification

- How Useful Are Flat Plate Models?
  - Real blades are loaded and turn the flow
    - Can we neglect the mean-flow gradients?
  - Flat plate models are used in most broadband models
    - Re-assessment for flat plate models is needed
- Three models of mean-flow are presented to assess simplifications introduced
  - Flat plates
  - Meridional flow (averaged flow)
  - Actual flow

Modeling Errors and Simplification: Mean-flow Distribution

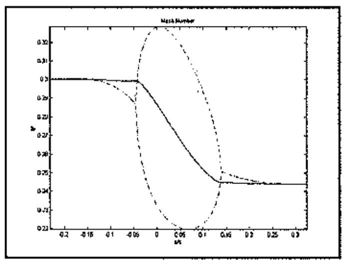

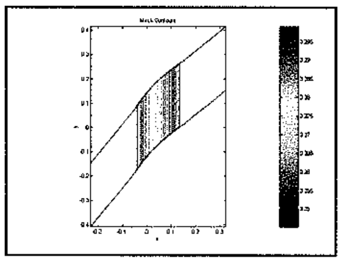

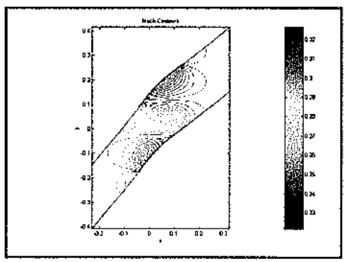

Modeling Errors and Simplification: Comparison of Results

- Flow turning models produce comparable unsteady lift and acoustic pressure intensities
- Flat plate models give erroneous acoustic pressure intensities

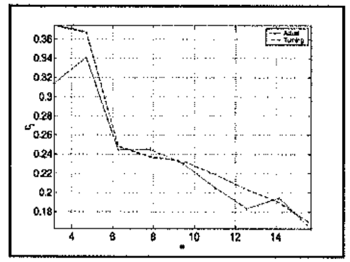

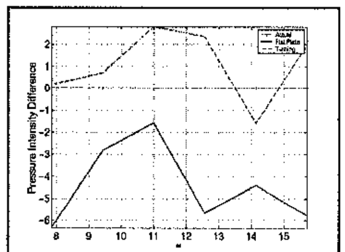

Downstream

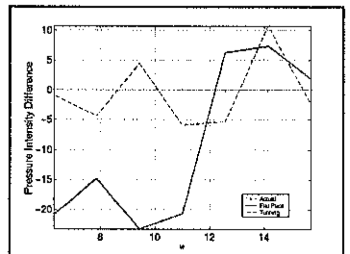

Upstream

Modeling Errors and Simplification: Unsteady Pressure Distribution

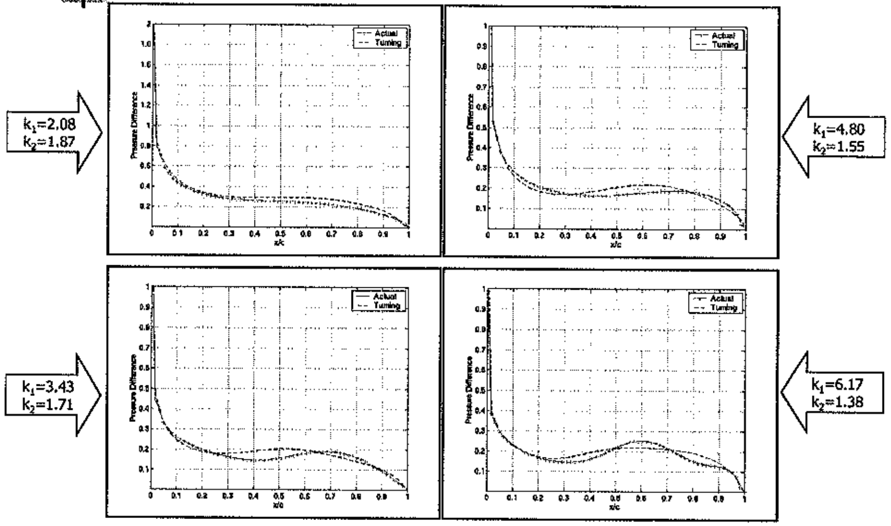

Application
Sound Reduction and Control

Sound Reduction and Control

- Rotor-stator noise can be reduced by:
  - Increasing phase variations of upstream wake
    - Introducing rotor and/or stator lean
    - Applying stator sweep
    - Increasing rotor-stator spacing
  - Accelerating mean flow
  - Applying active noise control and liners

Effect of Stator Lean

r_{tip}/r_{hub}	1.25/0.75
ω	3π
M	0.5
Stagger	0°

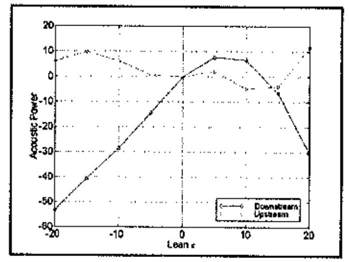

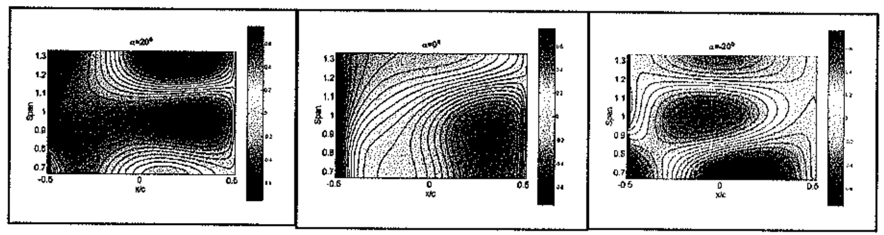

Effect of Stator Lean: Its Effectiveness

- Lean introduces spanwise phase variations which enhance the intensity of higher order modes
  - This may explain the increase of acoustic power
- Lean effectiveness depends on incident gust parameters

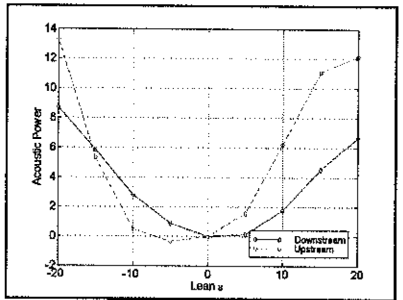

B=23, V=24, m=-1

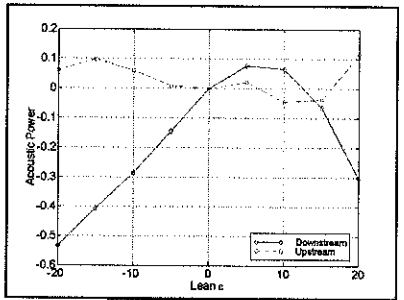

B=16, V=24, m=-8

Stator Sweep

r_{tip}/r_{hub}	1.25/0.75
ω	3π
M	0.5
Stagger	0°

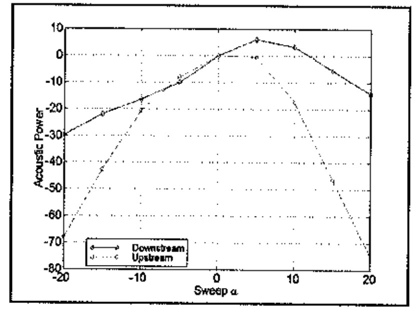

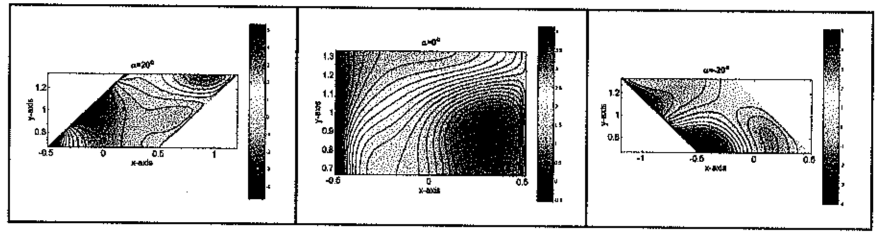

Conclusions

- An efficient model suitable of solving high frequency wake interaction has been developed, tested and validated.
- "Rule of thumb" in industry to use strip-theory is incorrect. Full three-dimensional calculations are essential at high frequency.
- Blade twist effects are dominant in high frequency.
- Incident spanwise variations (n') reduce the unsteady loading, however, higher order acoustic modes may be amplified.
- Swirl redistributes blade up-wash and can be used as an effective means for noise reduction.
- Blade lean may be used to reduce tonal noise, however, effectiveness may depend on rotor-stator configuration.
- Blade sweep is effective for noise reduction for large enough positive sweep.
- Current computations are of the order of minutes for small grids.

Future Work

- Code parallelization is underway:
  - To extend frequency range.
  - For use in broadband noise calculations.
  - Preliminary results indicate good scalability with increase of number of processors.

Feasibility of direct numerical simulation of model blade/gust interaction problems

Professor Neil Sandham

School of Engineering Sciences

University of Southampton

Feasibility of DNS/LES of model blade/gust problems

Neil Sandham,
Aero/Astro Southampton

- Previous DNS of leading- and trailing-edge model problems
- Vortex convection model problem
- Issues in blade/gust simulation

DNS code features

- High order (4^{th}, 6^{th}) differencing (non dissipative)
- Entropy splitting for nonlinear stability
- Characteristic inflow/outflow/far-field boundary conditions (optional buffer zones)
- Generalised co-ordinates (strong conservation form)
- Shock capturing option
- Multiblock, parallel code, optimised by Daresbury Laboratory (under UK Turbulence Consortium work programme) for Cray T3E, Origin 3000, Myrinet, HPC(x).

Computational Domain

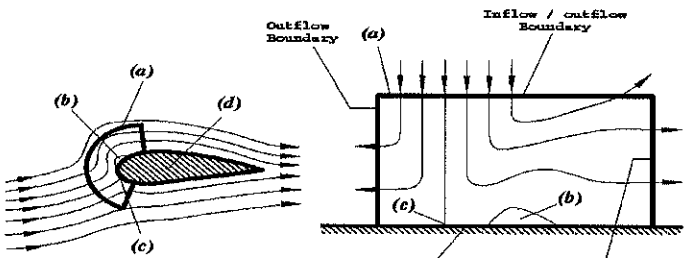

(a) Computational domain
(b) Separation bubble
(c) Stagnation point
(d) Aerofoil section

Statistics, Re=320,000

- Mean velocities
- Reynolds stresses
- BL characteristics

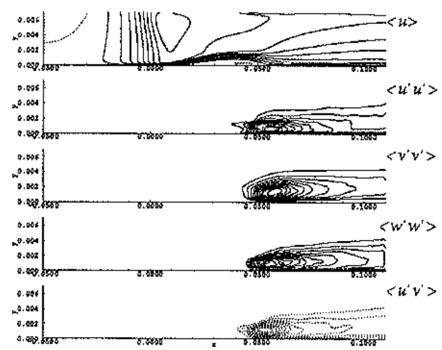

Trailing-edge flow simulation

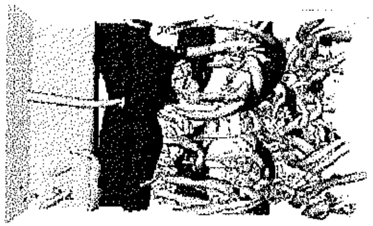

Plan view

- Cray T3E (early time)
- Up to 1024*512*128 grid points
- Turbulent inflow
- Convective outflow
- Spanwise-periodic
- Free-slip upper/lower

What do you want from a simulation?

A. Characterisation of the aerodynamic response to a gust

B. Simulation of the sound produced by a gust

Requirements will be more strenuous for B.

In instances with scale separation (large gust) and simple flow (predictable separation) A may be feasible by RANS

Suitable model problem(?)

- 2D aerofoil geometry
- Initial/upstream gust specification
- 3D time-accurate simulation

Issues with A: Aerodynamic response

- Grid resolution: $\Delta x^+ = 15$ $\Delta z^+ = 8$ $N = 10$ for $y^+ < 10$
- Transition modelling
- Spanwise box size
- Current DNS: Re=1-4×10^5 (depending on computer)
- Current LES: up to Re=10^6
- Re> 10^6 only with gross turbulence assumptions

Issues with B: Noise prediction

- As above, but add:
  - Cost of resolving sound waves away from blade (grid size)
  - Tuning of black-box boundary treatments (fringe and sponge zones)